Universitat Autònoma de Barcelona

Effect of Environmental Changes and Metal Stress on Phototrophic Microorganisms in Extreme Environments. Development of New Methodologies in High-Resolution Microscopy Techniques

Laia Millach Carrobé

UNIVERSITAT AUTÒNOMA DE BARCELONA

FACULTAT DE BIOCIÈNCIES
Departament de Genètica i Microbiologia

Effect of Environmental Changes and Metal Stress on Phototrophic Microorganisms in Extreme Environments

Development of New Methodologies in High-Resolution Microscopy Techniques

Laia Millach Carrobé

2017

UNIVERSITAT AUTÒNOMA DE BARCELONA

FACULTAT DE BIOCIÈNCIES
Departament de Genètica i Microbiologia

Effect of Environmental Changes and Metal Stress on Phototrophic Microorganisms in Extreme Environments

Development of New Methodologies in High-Resolution Microscopy Techniques

Tesis Doctoral presentada per obtenir el Grau de Doctor en Microbiologia per la Universitat Autònoma de Barcelona, per Laia Millach Carrobé.

Vist i plau dels Directors de la Tesi,

Dra. Isabel Esteve Martínez

Dr. Antonio Solé Cornellà

Bellaterra, Juliol del 2017

Als meus pares,
per fer-me costat sempre.

Life is a symbiotic and cooperative union
that lets those that work together triumph

Lynn Margulis (1938 – 2011)

Resum

Els efectes del canvi climàtic incideixen directament en les poblacions de microorganismes fotòtrofs dels tapissos microbians, produint alteracions en altres paràmetres ambientals com és l'increment de la temperatura, que pot provocar sequeres i fins i tot la desertització d'aquests ecosistemes, així com altres efectes en l'osmolaritat de les cèl·lules, degut a l'augment de la salinitat. Els microorganismes esmentats són molt abundants en els tapissos microbians, principalment els cianobacteris i les microalgues, que a més de ser els principals estabilitzadors d'aquests ecosistemes, al mateix temps es troben exposats a diferents condicions d'estrès.

La majoria dels estudis que es realitzen per valorar l'impacte que tenen sobre els microorganismes condicions ambientals tan variables utilitzen cultius axènics que provenen de microorganismes aïllats de l'ambient natural o bé de col·leccions de cultius; res més lluny de la realitat, ja que en els ambients naturals els microorganismes fotòtrofs estableixen associacions estables amb microorganismes heteròtrofs i, a vegades, amb altres fotòtrofs. A més, hi ha pocs estudis que analitzin, en aquestes condicions i a nivell individual, els efectes dels paràmetres ambientals o de la pol·lució per metalls en aquestes associacions.

La manca de metodologies que poden aplicar-se per esbrinar aquests efectes en un microorganisme en concret, quan està associat amb un altre de manera selectiva, *in vivo,* de manera ràpida i sense l'ús de cap tipus de tinció, és, per tant, un repte a la hora d'analitzar les possibilitats que tenen aquests microorganismes enfront a canvis tan dràstics. En aquest treball, s'ha intentat solucionar aquesta problemàtica mitjançant l'optimització de diferents tècniques que tenen com a base el microscopi làser confocal, considerant la principal característica dels cianobacteris i les microalgues, que és la d'emetre fluorescència natural. La clorofil·la *a* és el pigment majoritari d'aquests microorganismes i s'ha utilitzat amb anterioritat com a bioindicador, especialment en estudis realitzats en metalls per altres membre del grup.

Així mateix, una problemàtica important és esbrinar el paper que juguen aquests microorganismes en la resistència davant canvis sobtats de les condicions naturals o antropogèniques. En aquest sentit, també s'ha accentuat l'interès en les anomenades cèl·lules dorments i en l'estudi de cèl·lules viables i no viables. Per aquest motiu, en aquest treball s'ha posat a punt una nova metodologia que utilitza el microscopi làser confocal i dos làsers específics i que ha permès determinar el percentatge d'aquestes cèl·lules en mostres exposades a diferents condicions d'estrès. Els microscopis electrònics de rastreig i transmissió, ambdós acoblats a un detector d'energia dispersiva de raigs X, juntament amb el microscopi de transmissió de raig X del sincrotró ALBA, s'han aplicat en mostres sotmeses a varis factors d'estrès per avaluar els canvis morfològics en cèl·lules senceres i en seccions ultrafines, així com en estudis de captació de metalls extra- i intracel·lularment.

Els objectius del present treball s'han centrat en l'aplicació combinada de totes aquestes metodologies en dos consorcis de microorganismes: *Scenedesmus* sp. DE2009 i *Geitlerinema* sp. DE2011. L'efecte de la llum i la salinitat (com a paràmetres ambientals), així com l'impacte del plom, coure i crom (com a contaminants), s'ha estudiat àmpliament en cèl·lules individuals d'ambdós microorganismes. Finalment, aquesta tesi està estructurada en diferents capítols. El Capítol 3 correspon amb els articles publicats (un d'ells en revisió); així doncs, els resultats obtinguts de les investigacions realitzades s'exposen en les Seccions 3.1, 3.2 i 3.3 i es discuteixen globalment en el Capítol 4.

Resumen

Los efectos del cambio climático inciden directamente en las poblaciones de microorganismos fototróficos de los tapices microbianos, produciendo alteraciones en otros parámetros ambientales como es el incremento de la temperatura, que puede provocar sequías y hasta la desertización de estos ecosistemas, así como otros efectos en la osmolaridad de las células, debido al aumento de la salinidad. Dichos microorganismos son muy abundantes en los tapices microbianos, principalmente las cianobacterias y las microalgas, que además de ser los principales estabilizadores de estos ecosistemas, a veces se encuentran expuestos a diferentes condiciones de estrés.

La mayoría de los estudios, que se realizan para valorar los efectos que tienen sobre los microorganismos condiciones ambientales tan variables, utilizan cultivos axénicos que provienen de microorganismos aislados del ambiente natural o bien de colecciones de cultivos; nada más lejos de la realidad, ya que en los ambientes naturales los microorganismos fototróficos establecen asociaciones estables con microorganismos heterotróficos y, a veces, con otros fototróficos. Además, hay pocos estudios que analicen, en estas condiciones y a nivel individual, los efectos de los parámetros ambientales o de la contaminación por metales en estas asociaciones.

La falta de metodologías que pueden aplicarse para averiguar estos efectos en un microorganismo en concreto, cuando está asociado con otro de manera selectiva, *in vivo*, de manera rápida y sin el uso de ningún tipo de tinción, es, por tanto, un reto a la hora de analizar las posibilidades que tienen estos microorganismos frente a cambios tan drásticos. En este trabajo, se ha intentado solucionar dicha problemática mediante la optimización de distintas técnicas que tienen como base el microscopio láser confocal, considerando la característica principal de las cianobacterias y las microalgas, que es la de emitir fluorescencia natural. La clorofila *a* es el pigmento mayoritario de estos microorganismos y se ha utilizado con anterioridad como bioindicador, especialmente en estudios realizados en metales por otros miembros del grupo.

Asimismo, una problemática importante es valorar el papel que juegan estos microorganismos en la resistencia ante cambios repentinos de las condiciones naturales o antropogénicas. En este sentido, también se ha incrementado el interés por las denominadas células durmientes y en el estudio de células viables y no viables. Por este motivo, en este trabajo se ha puesto a punto una nueva metodología que utiliza el microscopio láser confocal y dos láseres específicos y que ha permitido determinar el porcentaje de estas células en muestras expuestas a diferentes condiciones de estrés. Los microscopios electrónicos de rastreo y transmisión, ambos acoplados a un detector de energía dispersiva de rayos X, junto con el microscopio de transmisión de rayos X del sincrotrón ALBA, se han aplicado en muestras expuestas a varios factores de estrés para evaluar los cambios morfológicos en células enteras y en secciones ultrafinas, así como para los estudios de captación de metales extra- e intracelularmente.

Los objetivos de este trabajo se han centrado en la aplicación combinada de todas estas metodologías en dos consorcios de microorganismos: *Scenedesmus* sp. DE2009 y *Geitlerinema* sp. DE2011. El efecto de la luz y la salinidad (como parámetros ambientales), así como el impacto de metales como plomo, cobre y cromo (como contaminantes), se ha estudiado ampliamente en células individuales de ambos microorganismos. Finalmente, esta tesis está estructurada en distintos capítulos. El Capítulo 3 corresponde con los artículos publicados (uno de ellos en revisión); así pues, los resultados obtenidos de las investigaciones realizadas se exponen en las Secciones 3.1, 3.2 y 3.3 y se discuten globalmente en el Capítulo 4.

Summary

The effects of climate change directly affect the populations of phototrophic microorganisms in microbial mats, causing alterations in other environmental parameters such as the increase in temperature. This in turn causes drought and sometimes the desertification of these ecosystems, as well as affecting the osmolarity of cells due to the increase in salinity. The microorganisms referred to are highly abundant in microbial mats; principally, they are cyanobacteria and microalgae, which, apart from being the main stabilisers of these ecosystems, are exposed to distinct stress conditions at the same time.

Most studies carried out to assess the impact on microorganisms of such variable environmental conditions use axenic cultures that come from microorganisms isolated from the natural environment or else from culture collections. Nothing could be further from reality, since—in natural environments—phototrophic microorganisms establish stable associations with heterotrophic bacteria and, at times, with other phototrophs. In addition, very few studies analyse (in these conditions and at individual level) the effects of environmental parameters or of metal pollution in these associations.

The lack of methodologies that can be applied to ascertain these effects in a specific microorganism, when this is selectively associated with another, *in vivo*, swiftly and without using any type of staining, is therefore a challenge in analysing the possibilities of these microorganisms when facing such drastic changes. In the current work, an attempt has been made to solve this problem by means of the optimisation of distinct techniques, based on confocal laser microscopy and centring on the main characteristic of cyanobacteria and microalgae, which is the emission of natural fluorescence. Chlorophyll *a* is the majority pigment in these microorganisms and has previously been used as a bioindicator, in studies carried out with metals by other members of the group.

Determining the role played by these microorganisms in the resistance to sudden changes in natural or anthropogenic conditions is a further, and important, issue. In addition, in this respect, the interest in dormant cells and in the study of viable and non-viable cells has increased. For this reason, a new methodology has been developed in this work; using a confocal laser microscope and two specific lasers, this has allowed us to ascertain the percentage of these cells in samples exposed to distinct stress conditions. The electronic scanning and transmission microscopes, both coupled to an X-ray dispersive energy detector, jointly with the transmission soft X-ray microscope from the ALBA synchrotron, have been used in samples prepared to evaluate morphological changes due to stress factors, both in complete cells and in ultrafine sections, as well as in studies of extra- and intracellular metal extraction.

The objectives of this work centre on the combined application of all these methodologies on two consortia of microorganisms: *Scenedesmus* sp. DE2009 and *Geitlerinema* sp. DE2011. The effect of light and salinity (as environmental parameters), in addition to the impact of lead, copper and chromium (as pollutants) was studied extensively in individual cells for both microorganisms. Finally, this thesis is organised into distinct chapters. The Chapter 3 correspond to the articles that have already been published (one of them currently under review); thus, the results obtained from the research carried out are therefore presented in Sections 3.1, 3.2 and 3.3 and are discussed globally in Chapter 4.

Abbreviations

Symbol	Meaning
3D	Three-Dimensional
AOTF	Acousto-Optic Tunable Filter
ANOVA	One-way Analysis of Variance
ART	Algebraic Reconstruction Technique
CHE	Confederación Hidrográfica del Ebro
Chl *a*	Chlorophyll *a*
CLSM	Confocal Laser Scanning Microscopy
CLSM-DL	Confocal Laser Scanning Microscopy and Dual Laser
CLSM-*λscan*	Confocal Laser Scanning Microscopy and *λscan* function
DMSO	Dimethyl sulfoxide
EDX	Energy Dispersive X-ray
EPS	Extracellular Polymeric Substances
IC_{50}	Inhibitory Concentration (50%)
LOEC	Lowest Observed Effect Concentration
MFI	Mean Fluorescence Intensity
MIF	Maximum Intensity Fluorescence
MMC	Minimum Metal Concentration
NaCl	Sodium Chloride
NPAF	Non-photosynthetic Autofluorescence signal
P	Probability value
PAF	Photosynthetic pigment Autofluorescence signal
PAM	Pulse Amplitude Modulation
PEA	Plant Efficiency Analyzer
PP	Polyphosphate inclusions
PSII	Photosystem II
ROI	Regions-Of-Interest
SEM	Scanning Electron Microscopy
TEM	Transmission Electron Microscopy
TXM	Transmission ray-X Microscopy

Tables and Figures

Structure of the Thesis

Chapter 1 – Introduction: In the first chapter is introduced an overview of extreme environments, microbial mats and their populations. The study is focused on the Ebro Delta microbial mats and mainly on cyanobacteria and microalgae, the dominant populations of these ecosystems. The problems presented by the study of these phototrophic microorganisms are also emphasized, since most of them form aggregates or consortia and do not grow on solid media or they do so with difficulty. It is for that, the importance of searching methodologies that can be applied *in vivo,* at single-cell level, with no handling of the sample and providing reliable results in short time consuming. Finally, the objectives of this thesis are develop and applied various methodologies to evaluate the effect of different stress factors on two selected phototrophic microorganisms: *Scenedesmus* sp. DE2009 and *Geitlerinema* sp. DE2011.

Chapter 2 – Material and Methods: In this chapter is described the sampling site of Ebro Delta microbial mats, the isolated microorganisms and their culture conditions, and all the methodologies applied in this work.

Chapter 3 – Results: This chapter is divided in three sections; each one corresponds to the articles published (one of them currently under review). In the first section is presented a new method to determine *in vivo* the physiological state and cellular viability of phototrophic microorganisms to environmental changes. In the second and third sections are evaluated the metal stress on two phototrophic microorganisms by means different high-resolution microscopy techniques.

Chapter 4 – General Discussion: In this chapter, the results obtained in this dissertation are widely discussed. The first part is a general discussion of the methods used and their benefits compared to other techniques. The second part of the discussion is a detailed analysis of the effect of light, salinity and metal stress on phototrophic microorganisms.

Chapter 5 – Conclusions and Future Prospects: In the last chapter is listed the conclusions obtained in this Thesis and the future prospects opened up by this work.

CONTENTS

Chapter 1 – Introduction

Those habitats that are subject to very stressful environmental conditions are considered as extreme living environments. Widely distributed all over the world, these ecosystems, and the microorganisms that live in them, have become models for the search for extra-terrestrial life, and are also considered as current models to explain the beginning of life on our planet (Horikoshi and Grant, 1998). For these reasons, they have been and are currently still being widely studied. In this context, alkalinity, acidity, hypersalinity, extreme cold, and extreme heat are considered as extreme environments. Extreme habitats are also those that are under high atmospheric pressure conditions (oceans and deep lakes), or radiation, and those that are persistently without oxygen or water (hot and cold deserts, and some endolithic habitats). Over the years, habitats altered by human activities and polluted with heavy metals or organic compounds (mines and oil spills) have been also considered as extreme environments. Information about different types of extreme habitats is summarized in Table 1.1.

Microbial mats are widely distributed around the world in different ecosystems, including extreme habitats, such as marine waters (Esteve et al., 1992; 1994; Otte et al., 1999), hydrothermal vents (Miranda et al., 2016), hot-springs (Roeselers et al., 2007), hypersaline ponds (Hoehler et al., 2001) and polar regions (Morgan-Kiss et al., 2006; Jungblut et al., 2011). These ecosystems, developed in water-sediment interfaces, are formed by multilayered benthic microbial populations, although fungi, protozoa and other eukaryotic microorganisms have also found forming complex communities. The microbiota of mats are distributed along vertical microgradients of different physical-chemical parameters and also depends of the metabolic products of each group of microorganisms release to the natural habitat, which in turns serve as energy, carbon and electron acceptor sources for other groups. Marine mats may grow to a few centimeters in thickness, of which only the top few millimeters are oxygenated. In wet microbial mats, the upper layers (green color) are dominated by oxygenic phototrophic bacteria and algae. Under these layers, orange and red colors due to the pigments of

anoxygenic phototrophic bacteria can clearly distinguish in a well developed mat. In the lowest layers anaerobic microorganisms such us methanogenic and sulfate reducing bacteria are dominant (Fig. 1.1).

Table 1.1. Extreme environments diversity.

Type of Extreme Environment	Physical Characteristic / Inhabitant	Examples of Habitats	Reference
Dry	Absence of water Desiccation *Endolith*	Hot deserts	*Azua-Bustos et al., 2012*
		Cold deserts	*de los Ríos et al., 2014*
		Rocks	*de la Torre et al., 2003*
Salty	High Salt [NaCl] > 3.5% *Halophile*	Hypersaline waters	*Paul et al., 2016*
		Salt flats	*Hayashida et al., 2017*
		Evaporite salt deposits - Crust	*Csotonyi et al., 2010*
Acid	pH < 4 *Acidophile*	Acid hot-springs	*Sakai et al., 2016*
		Acid waters	*García-Moyano et al., 2012*
Alkaline	pH > 9 *Alkaliphile*	Alkaline hot-springs	*Nakagawa* and *Fukui, 2002*
		Alkaline lakes	*Edwardson et al., 2014*
High Temperature	60 – 80 ºC *Thermophile* Temp. > 80 ºC *Hyperthermophile*	Hot-springs	*Portillo et al., 2009*
		Geothermal areas	*Slobodkin* and *Wiegel, 1997*
		Hydrothermal vents	*Kato et al., 2009*
Low Temperature	Temp. < 5 ºC *Psychrophile*	Cold waters	*Glaring et al., 2015*
		Polar regions	*de los Ríos et al., 2015*
		Glacial deposits	*Fernández-Martínez et al., 2016*
Radiation	High radiation (UV, IR, X-rays, γ-rays)	Radioactive materials	*Rivasseau et al., 2016*
		Radioactive thermal spring	*Weidler et al., 2007*
Under Pressure	Under high hydrostatic pressure *Barophile*	Deep lakes	*Deutzmann et al., 2014*
		Oceans	*Verma et al., 2017*

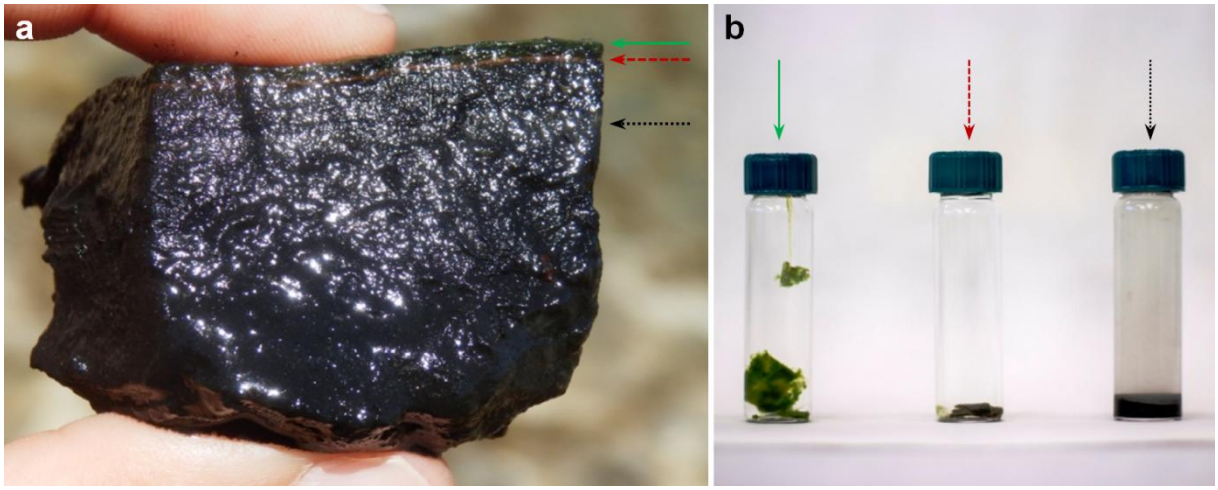

Fig. 1.1. Ebro Delta microbial mat structure **(a)**. Phototrophic oxygenic microorganisms, green layer (—); purple anoxygenic bacteria, red layer (----) and sulfate reducing bacteria and methanogenic, black layer (····) **(b)**.

For a long period of time, our research team has been studying the hypersaline Ebro Delta microbial mats, located at the outflow of the Ebro River (Spain). The Ebro River is 928 km long, flows from the north of the Iberian Peninsula into the Mediterranean Sea, and drains an area of approximately 85,000 km^2. Its basin is the most economically important area of northern of Spain. The Ebro Delta is the second most important wetland in Spain after the Guadalquivir River marshes, and the second one of the Mediterranean area, after the Camargue (France). The Ebro Delta is also considered the third largest delta in the Mediterranean, with a 320 km^2 triangular surface and it is located on the northeastern coastline of the Iberian Peninsula (0°35'E – 0°56'E; 40°33'N – 40°47'N) (Guerrero et al., 2002; Balasch and Ruiz, 1998). In 1983, some of the most outstanding natural areas of the delta were included in the Ebro Delta Natural Park (*Parc Natural del Delta de l'Ebre*) for their biological, geological, economic, and cultural significance (Mañosa et al., 2001). Of its total area, 78 km^2 corresponds to the Natural Park (25 %), 85 km^2 to orchards and fruits (25 %), and 160 km^2 to rice farming (50 %). Agriculture is currently one of the great economic foundations of the Delta, with a clear predominance of rice growing (more than 20,000 hectares, and the major part of this production is in Catalonia).

Fig. 1.2. Area orthophotographs of the Ebro Delta. Vuelo Americano Serie A (1945 -1946) **(a),** Vuelo Americano Serie B (1956-1957) **(b)**, LandSat Satellite (1984) **(c)** and Copernicus Satellite (2017) **(d)**. The arrows indicate: Illa de Buda and Cap de Tortosa (·····), Punta del Fangar (----) and Punta de la Banya (—).
Source: Institut Cartogràfic i Geològic de Catalunya.

The formation of the Ebro Delta began at the end of the last Ice Age about 50,000 years ago (Quaternary period). As a result, the sea level rose, flooding the mainland, and the continental shelf served as a base for sediment transported from the Ebro River. The Delta's geology has varied over the centuries, but its crucial formation period was established around the 17th century. Between 1957 and 2017, the aerial images show a clear shrinking of the delta, mainly due to two factors; natural phenomena, accentuated by the climate change, and the decrease in caudal flow of the River Ebro caused by the construction of dams from the 1960's (Mequinença, Flix and Riba-roja). The changes in the fluvial dynamics of the river have led to a change in the terrain in the river estuary, particularly in the Illa de Buda and the Cap de Tortosa, as well as in the protected areas of the Punta del Fangar or la Banya (Fig. 1.2). It is important to preserve these ecosystems, such as microbial mats, marshes, salt ponds, dunes, and sandy beaches, since they provide habitat for a large number of flora and fauna species forming part of the Ebro Delta.

Among the microorganism populations of the microbial mats of the delta, of special interest are the oxygenic photosynthetic bacteria that occupy the shallow green layer and especially the cyanobacteria, which together with the microalgae, are the dominant microorganisms of these ecosystems. Both groups are responsible for the elevated primary production produced by means of CO_2 fixation, and which contribute to the growth of the heterotrophic population that also uses the oxygen produced by these microorganisms as terminal electron acceptor. The cyanobacteria, especially the filamentous ones, usually from groups that are wrapped in exopolysaccharide layers, and play an important role in the stabilization of delta sediments.

In recent years, three phototrophic microorganisms have been isolated from the microbial mats of the Ebro Delta, all of them very abundant in these habitats, and identified as: *Microcoleus chthonoplastes* DE2006 (Diestra et al., 2005), *Scenedesmus* sp. DE2009 (Maldonado et al., 2010b) and *Geitlerinema* sp. DE2011 (Burgos et al., 2013). These photosynthetic microorganisms have the capacity to assimilate CO_2, with Chlorophyll *a* (Chl *a*) being their major photosynthetic pigment. On the one hand, *Microcoleus chthonoplastes* DE2006 and *Geitlerinema* sp. DE2011 are filamentous cyanobacteria that form individual long filaments, sometimes densely packed and surrounded by a mucopolysaccharide sheath. Cells from filaments vary in size from 3.13 to 3.75 μm and its chloroplasts are distributed evenly inside the cells. The cells are septate and do not contain gas vacuoles. On the other hand, *Scenedesmus* sp. DE2009 is an eukaryotic microorganism, a microalga with spherical cells, and a diameter of 7 – 9 μm, with its chloroplasts distributed peripherally within the cells.

These phototrophic microorganisms have relationships with other heterotrophic bacteria with which they form stable consortia, and in which mutualistic symbiosis are established, and in the majority of cases involve the production of organic material and protection against stress factors by the photosynthetic microorganisms (Fig. 1.3).

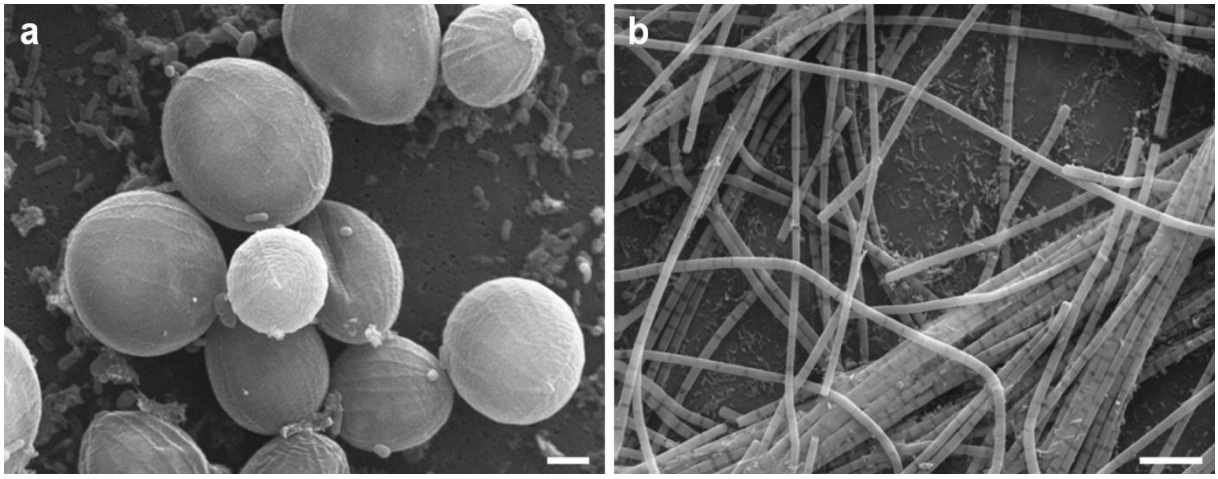

Fig. 1.3. SEM micrographs of *Scenedesmus* sp. DE2009 consortium **(a)** and *Geitlerinema* sp. DE2011 consortium **(b)**. Scale bars represent 1 *μ*m and 10 *μ*m, respectively.

In this last sense, some heterotrophic bacteria that form consortia are nitrogen-fixing, an ability that the identified phototrophic microorganisms do not have. Among these heterotrophic bacteria that form these consortia, *Paracoccus* sp. DE2007 (Diestra et al., 2007), *Micrococcus luteus* sp. DE2008 (Maldonado et al., 2010a) and *Ochrobactrum* sp. DE2010 (unpublished results) have also been found and isolated from Ebro Delta microbial mats.

The isolation and culture of phototrophic microorganisms is not easy, as they do not normally grow in solid media, or they do so with difficulty. On the other hand, the ease in which they form consortia or aggregates means that the classic environmental microbiology techniques cannot be applied for their study.

Other additional problems that have to be added to those already mentioned, is that in deltas and in particular the Ebro Delta, an increase in temperature is being produced in these ecosystems (probably due to the climate change). This is producing a strong evaporation of the marine waters that flood them, and thus a drying out of the microbial mats. These are evident with the appearance of crusts and a significant increase in salinity due to this drying out (Fig. 1.4).

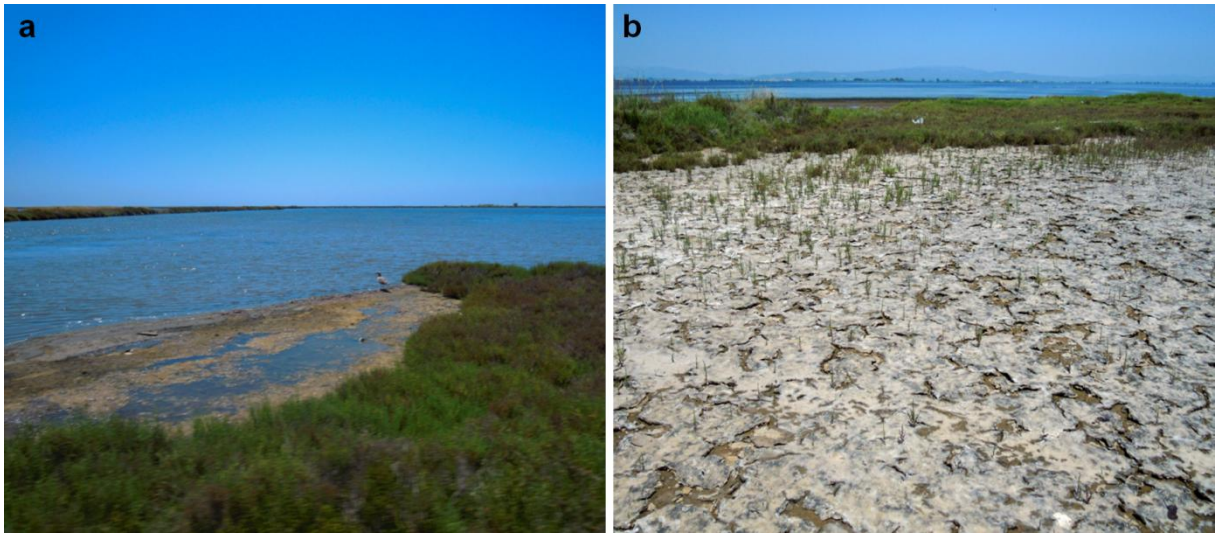

Fig. 1.4. Ebro Delta microbial mats covered by water **(a)** and forming crusts in the dry season **(b)**.

As a result of these disturbances, there are changes in the biodiversity and biomass in the microorganism populations (Garcia-Pichel et al., 2001; Lan et al., 2014). In addition, these populations develop strategies at an individual level, such as the formation of "dormant cells" in order to support the stress conditions (de los Ríos et al., 2004; Rajeev et al., 2013). This dormancy mechanism is frequently offered as a plausible explanation for the persistence of bacterial populations under suboptimal or harsh conditions (Stevenson, 1978; Dworkin and Shah, 2010).

Thus, it is important to study the details of the main physico-chemical parameters in order to be able to understand the impact that these environmental changes have on these phototrophic populations. Fig. 1.5 shows some of the sampling stations of the *Confederación Hidrográfica del Ebro* (CHE) along the Ebro River, from its source to its estuary. Table 1.2 indicates the range of values of the different physico-chemical parameters obtained at each one of them. The data used correspond to the measurements obtained over the last 10 years (May 2007 – May 2017, CHE).

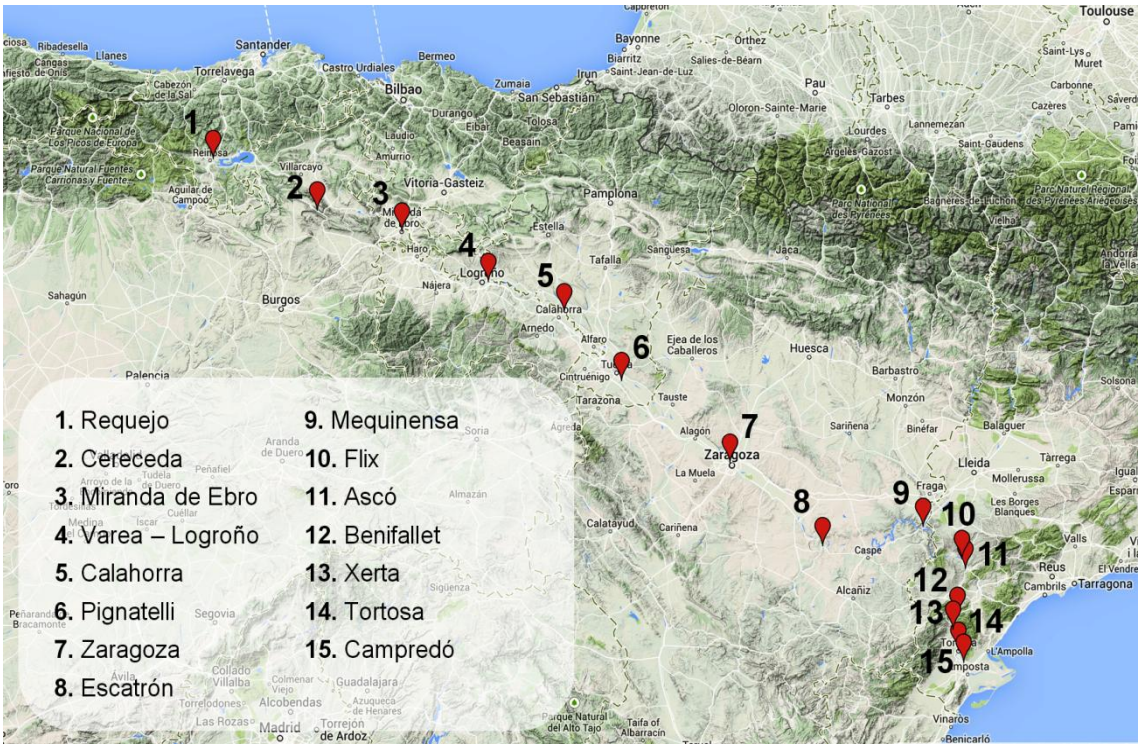

Figura 1.5. Location of sampling stations of *Confederación Hidrográfica del Ebro*.

Table 1.2. Range of values of the different physico-chemical parameters of the Ebro river obtained from the sampling stations of the *Confederación Hidrográfica del Ebro* shown in Figure 1.5. Source: CHE, 2007 - 2017.

Sampling Station	**Temp.** (ºC)	**pH**	**EC**[1] $_{20\ ºC}$ (μS cm^{-1})	**DO**[2] (mg O_2 L^{-1})	**Alkalinity** (mg CO_3Ca L^{-1})
Requejo	3.3 – 14.6	7.5 – 8.1	108 - 496	6.6 – 12.6	96 - 120
Cereceda	6.0 – 23.1	7.6 – 8.4	227 - 405	8.2 – 12.5	*ND*
Miranda de Ebro	5.8 – 23.5	7.2 – 8.3	285 - 874	5.2 – 12.6	99 - 182
Varea – Logroño	6.0 – 24.5	7.6 – 8.6	280 - 775	6.9 – 18.7	107 - 164
Calahorra	7.2 – 24.7	7.5 – 8.4	456 - 1134	7.1 – 12.4	*ND*
Pignatelli	6.8 – 26.9	7.7 – 8.4	459 - 1372	7.1 – 12.7	150 - 214
Zaragoza	6.3 – 25.8	7.8 – 8.4	547 - 2180	7.2 – 12.6	147 - 237
Escatrón	5.5 – 28.0	7.6 – 8.4	747 - 2363	6.9 – 14.5	170 - 235
Mequinensa	6.9 – 26.3	7.7 – 8.4	651 - 2073	6.1 – 14.1	156 - 218
Flix	7.6 – 25.3	7.7 – 8.4	591 - 1923	5.3 – 13.8	134 – 185
Ascó	8.4 – 27.5	7.8 – 8.4	566 - 1616	5.8 – 12.2	109 - 180
Benifallet	7.7 – 27.5	7.5 – 8.4	611 - 1722	6.8 – 12.4	158 - 203
Xerta	7.9 – 27.1	7.6 – 8.4	590 - 1709	5.6 – 11.9	148 - 174
Tortosa	6.8 – 27.8	7.8 – 8.5	656 - 1696	6.9 – 15.2	123 - 180
Campredó	9.2 – 28.5	7.9 – 8.5	551 - 1526	6.4 – 12.6	161 - 190

[1] **EC**: Electrical Conductivity
[2] **DO**: Dissolved Oxygen
ND: Not Determined

Finally, another stress effect is the abundance of contaminants that accumulate in river mouths and estuaries. Both the Ebro River and its Delta are currently subjected to anthropogenic pollution, mainly as a consequence of industrial and mining activities that discharge their waste into the river, as well as due to the agricultural crops (rice and fruits), which increase the amount of pesticides in the Delta. Another important source of pollution has been the use of lead (Pb) pellets in hunting waterfowl (Mateo et al.,

1997). Hence, the predominant pollutants in these habitats are: herbicides, fertilisers, pesticides, algicides, insecticides, hydrocarbons and metals (Mañosa et al., 2001; Nziguheba and Smolders, 2008).

Among the metals, lead (Pb^{2+}), copper (Cu^{2+}), and chromium (Cr^{3+}) were chosen to be tested in this study due to their different levels of toxicity. The mean concentrations of these three metals obtained in distinct sampling stations of the CHE are shown in Table 1.3.

Table 1.3. Mean concentrations of lead, chromium, and copper obtained along the some sampling stations of the *Confederación Hidrográfica del Ebro*. Source: CHE, 2007-2017.

Sampling Station	[Pb] ($\mu g\ L^{-1}$)	(μM)	[Cr] ($\mu g\ L^{-1}$)	(μM)	[Cu] ($\mu g\ L^{-1}$)	(μM)
Requejo	< 0.5	$<2.4\cdot10^{-3}$	< 2	$<3.9\cdot10^{-4}$	< 2	$<3.2\cdot10^{-2}$
Cereceda	< 2 – 5	$<9.7\cdot10^{-3}$ - $2.4\cdot10^{-2}$	< 2	$<3.9\cdot10^{-4}$	< 2	$<3.2\cdot10^{-2}$
Miranda de Ebro	< 0.5 – 10	$<2.4\cdot10^{-3}$ - $4.8\cdot10^{-2}$	< 1 – 5	$<1.9\cdot10^{-2}$ - $9.6\cdot10^{-2}$	< 2 – 10	$<3.2\cdot10^{-2}$ - $1.6\cdot10^{-1}$
Varea – Logroño	< 0.5 – 10	$<2.4\cdot10^{-3}$ - $4.8\cdot10^{-2}$	< 1 – 5	$<1.9\cdot10^{-2}$ - $9.6\cdot10^{-2}$	< 2 – 10	$<3.2\cdot10^{-2}$ - $1.6\cdot10^{-1}$
Calahorra	< 0.5 – 5	$<2.4\cdot10^{-3}$ - $2.4\cdot10^{-2}$	< 2	$<3.9\cdot10^{-4}$	< 2 – 3	$<3.2\cdot10^{-2}$ - $4.7\cdot10^{-2}$
Pignatelli	< 0.5 – 5	$<2.4\cdot10^{-3}$ - $2.4\cdot10^{-2}$	< 2	$<3.9\cdot10^{-4}$	< 2 – 4	$<3.2\cdot10^{-2}$ - $6.3\cdot10^{-2}$
Zaragoza	< 2 – 5	$<9.7\cdot10^{-3}$ - $2.4\cdot10^{-2}$	< 1 – 2	$<1.9\cdot10^{-2}$ - $3.9\cdot10^{-4}$	< 2 – 4	$<3.2\cdot10^{-2}$ - $6.3\cdot10^{-2}$
Escatrón	< 0.5 – 5	$<2.4\cdot10^{-3}$ - $2.4\cdot10^{-2}$	< 2	$<3.9\cdot10^{-4}$	< 2 – 3	$<3.2\cdot10^{-2}$ - $4.7\cdot10^{-2}$
Mequinensa	< 0.5 – 5	$<2.4\cdot10^{-3}$ - $2.4\cdot10^{-2}$	< 2	$<3.9\cdot10^{-4}$	< 2 – 3	$<3.2\cdot10^{-2}$ - $4.7\cdot10^{-2}$
Flix	< 0.5 – 5	$<2.4\cdot10^{-3}$ - $2.4\cdot10^{-2}$	< 2	$<3.9\cdot10^{-4}$	< 2	$<3.2\cdot10^{-2}$
Ascó	< 0.5 – 10	$<2.4\cdot10^{-3}$ - $4.8\cdot10^{-2}$	< 1 – 5	$<1.9\cdot10^{-2}$ - $9.6\cdot10^{-2}$	< 2 – 10	$<3.2\cdot10^{-2}$ - $1.6\cdot10^{-1}$
Benifallet	< 0.5 – 6	$<2.4\cdot10^{-3}$ - $2.9\cdot10^{-2}$	< 2	$<3.9\cdot10^{-4}$	< 2	$<3.2\cdot10^{-2}$
Xerta	< 0.5 – 10	$<2.4\cdot10^{-3}$ - $4.8\cdot10^{-2}$	< 2	$<3.9\cdot10^{-4}$	< 2 – 3	$<3.2\cdot10^{-2}$ - $4.7\cdot10^{-2}$
Tortosa	< 0.5 – 10	$<2.4\cdot10^{-3}$ - $4.8\cdot10^{-2}$	< 1 – 5	$<1.9\cdot10^{-2}$ - $9.6\cdot10^{-2}$	< 2 – 10	$<3.2\cdot10^{-2}$ - $1.6\cdot10^{-1}$
Campredó	< 0.5 – 1	$<2.4\cdot10^{-3}$ - $4.8\cdot10^{-3}$	< 2	$<3.9\cdot10^{-4}$	< 2 – 3	$<3.2\cdot10^{-2}$ - $4.7\cdot10^{-2}$

Metals such as zinc, copper, iron, magnesium, cobalt, and manganese are required by most living organisms for their normal cellular functions. Essential metals are often present at low concentrations in the environment, however, and must be imported into cells, often at the expense of energy. In contrast to essential metals, toxic metals such as cadmium, lead, and mercury can disrupt cellular functions by competing with essential metal for their metal-binding sites and/or by altering the redox state of cells (Hanikenne et al., 2005; Merchant et al., 2006).

Because of the toxicity and the ubiquity of metals in the environment, microorganisms have developed multiple ways of dealing with both essential and unwanted toxic metals. Immobilization of metals, mainly in cyanobacteria and microalgae cells, consists of two mechanisms: the biosorption and bioaccumulation. Biosorption (extracellular metal uptake) is one of the strategies used in biorepair processes to describe the passive accumulation of metals on the cell wall surface containing functional groups (carboxyl, hydroxyl, phosphate, amino, sulfhydryl) (Schiewer and Volesky, 2000). Bioaccumulation is defined as the intracellular accumulation of metals by microorganisms. It consists in the first place of biosorption in the cell surface followed by transport and accumulation either in intracellular compartments or directly in the cell cytoplasm.

One of the problems detected in metal bioaccumulation by phototropic microorganisms is that, due to their structural similarity to essential elements, non-essential metals can enter inside the cells via non-selective ion channels and damage cellular components either directly (by competing with native anions and blocking enzyme function) or indirectly (by producing reactive oxygen species). Both effects are highly damaging to chloroplasts, with the former allowing metal cations to directly destroy the structure and function of chloroplast membranes and the latter resulting in various forms of damage in all organelles, including the peroxidation of chloroplast membranes (Romero-Puertas et al., 2004). In addition, metal ions inhibit the uptake

and transportations of essential metals such as manganese (Mn), zinc (Zn) and iron (Fe) to maintain cell functioning (Hou et al., 2007).

Taking into account all the aforementioned problems, it is essential to seek and develop new methodologies that will enable differentiating the different types of microorganisms in the same sample and to characterize the physiological state and photosynthetic performance of microbial cells. Furthermore, it is necessary to provide valuable information on the viability and functioning of microbial communities in complex samples in response to distinct stress conditions and at single-cell level.

In recent years, our working group has optimized and develop different methods, including: Confocal Laser Scanning Microscopy (CLSM) (Solé et al., 2007; Burnat et al., 2010) and electron microscopy techniques, both scanning and transmission, coupled to an energy-dispersive X-ray system (EDX) (Burgos et al., 2012).

CLSM was applied to analyze the diversity and total cyanobacterial biomass profiles within different microbial mats (CLSM-IA) (Solé et al., 2009) and to determine the viability and biomass of heterotrophic microorganisms in different environmental conditions (FLU-CLSM-IA) (Puyen et al., 2012a; 2012b). Moreover, the *λscan* function in CLSM has been widely used to statistically analyze the changes in the fluorescence intensity of the Chl *a* used as a biomarker, against lead (Maldonado et al., 2011), copper (Seder-Colomina et al., 2013) and chromium (Puyen et al., 2017). These three metals are found in low concentrations in the Ebro River (Table 1.3), and are deposited in the mats, causing damage in the microbe communities.

In addition, Scanning Electron Microscopy (SEM) and Transmission Electron Microscopy (TEM) combined with EDX have also been used to determine the extra- and intra-cellular uptake of these metals in different microorganisms, which has been useful for their possible application in bioremediation (Puyen et al., 2012b; Coreño-

Alonso et al., 2014). Some of these methods have been optimized especially to determine the effect of different metals in cultures of microorganisms isolated from their natural habit, as well as in artificial laboratory ecosystems (microcosms), and on samples directly obtained from the natural environment (Esteve et al., 2013).

CLSM has shown to be a fast and efficient microscope for *in situ* observations made at a cellular level, without the manipulation of the samples and a spatial resolution of 200 nm. This is an outstanding optical microscopy technique, as it provides accurate and non-destructive optical sections, giving high-resolution images where out-of-focus views are eliminated. Furthermore, using this methodology, it is easy to differentiate morphotypes of phototrophic microorganisms living in mixed populations and establish its biomass at microscale level. On the other hand, a spectrofluorometric detector (*λscan* function) coupled to the microscope allows us to assess the effect of different parameters and pollutants at photosynthetic pigment level, and provides an *in vivo* analysis considering the state of the pigment performed in individual cells without staining protocols.

Electron microscopes utilize the same basic principles as light microscopes, but focus beams of energetic electrons rather than photons, to magnify an object and achieve a better resolution. SEM and TEM are two of the most versatile techniques for the examination and analysis of the microstructural characteristic of solid objects. For many years, SEM and TEM have been used for a wide range of scientific applications, such as for medical researches (Kalita et al., 2014), study and development of new materials (Campidelli et al., 2017; Su et al., 2017) and life science investigations (Wu, et al., 2013; González-Ramírez et al., 2016). In this last sense, for instance, Lawrence et al., 2003 examined by electron microscopy techniques the complex microbial communities and mapped the nature and distribution of macromolecular for understanding biofilm formation, among many other studies.

Finally, the characteristics of Transmission X-ray Microscopy (TXM) make it potentially ideal for localization and differentiation of biomolecules classes. This is possible due to the ability of soft X-rays to penetrate water, the presence of suitable core edges in the soft X-ray region, reduced radiation damage (compared to that caused by electron beam techniques) and a spatial resolution down to 50 nm, which is suitable for imaging bacteria (Otón et al., 2012; Pereiro and Chichón, 2014). One of the first microbiological investigations using a full-field transmission X-ray microscope with synchrotron radiation was carried out by Gilbert et al., (1999), demonstrating the potential of soft X rays for imaging early stage *Pseudomonas putida* biofilms. Nevertheless, very few studies have been published using this technology on phototrophic microorganisms (Leonardo et al., 2016).

The CLSM-*λscan* function has been optimized in this Thesis for a more detailed analysis of the physiological state of the pigments in response to different stress conditions. However, up until now it has not been possible to determine the viability of photosynthetic microorganisms *in vivo,* at cell level, with minimal manipulation of the samples and providing data of cellular percentage in short time consuming. It is for this reason that, in this dissertation has been set up of a new method using CLSM and a Dual Laser (CLSM-DL) that allows the simultaneous capturing of different and specific wavelengths within the spectrum by a *sequential scan.* This new method, once validated, has enabled the cellular viability to be determined in *Scenedesmus* sp. DE2009 against two environmental factors (salinity and light intensity), as well as against different metals, separately, and in their respective mixtures. Furthermore, a study has been made on the tolerance of the cyanobacterium *Geitlerinema* sp. DE2011 and the microalga *Scenedesmus* sp. DE2009 to chromium and the capacity to immobilize it in contaminated natural habitats. Ultimately, the toxic effect of the combination of different metals on the photosynthetic pigments of *Scenedesmus* sp. DE2009 was also studied.

The main objectives of the present work are shown below:

1. The optimization of the CLSM-*λscan* function in order to determine the physiological state of photosynthetic pigments at single cell level in complex environmental samples.

2. The development of a novel, fast and easy method using CLSM and two specific lasers (CLSM-DL) for differentiating living and dead microbial cells.

3. The application of various CLSM methodologies and different electron microscopic techniques to study the response of two phototrophic microorganisms to environmental changes and metal stress.

Chapter 2 – Material and Methods

In this chapter the sampling area and all the methodologies applied to study the response of different phototrophic microorganisms to several environmental parameters and metal stress are described.

2.1. Characterization of sampling site of the Ebro Delta microbial mats

The Ebro Delta has an area of about 350 km^2 and it has the characteristic delta shape with two lateral sand bars originated from the flow activity of the Ebro River. The Ebro Delta has a coastal Mediterranean climate, with mild temperatures ranging from 3 to 27 ºC and average annual rainfall of 500 mm, falling mostly during intermittent storms. The evaporation-precipitation balance is negative because losses of water due to evaporation are greater than water input by precipitation. The most important wind blows from NW, reaching speeds of about 50 km h^{-1}.

The salinity of the water in the microbial mats area is much higher than the sea salinity and ranges from 40 ‰ to 75 ‰. The temperature of water covering these mats range from 12°C to 30°C and pH from 7.5 to 9.0. Ebro Delta microbial mats develop 1 to 7 cm below the water surface (Esteve et al., 1992).

Microbial mats investigated in this study were placed in *La Banya* spit, close to *Trinity salt works*, in the south part of the sand bar called *Alfacs Penninsula* (Fig. 2.1).

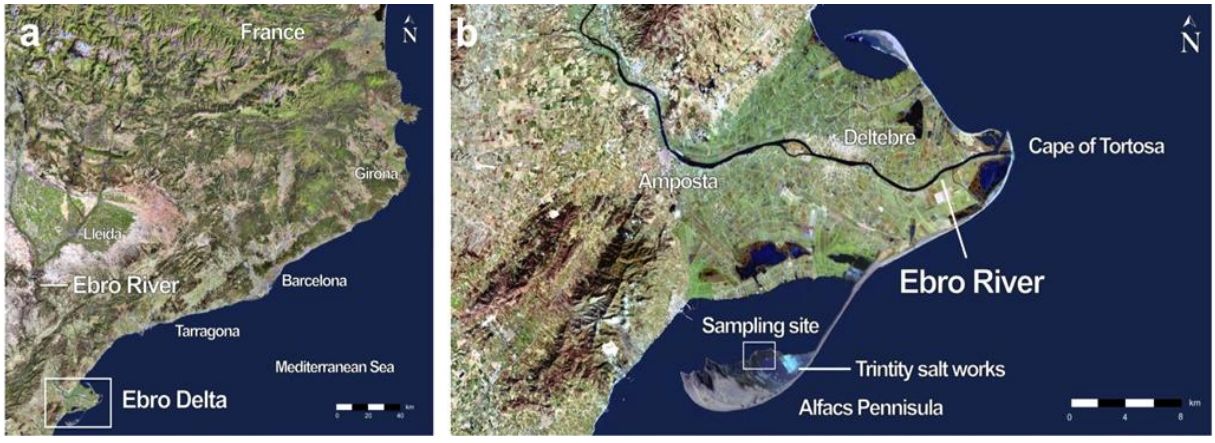

Fig. 2.1. Location of Ebro Delta **(a)** and microbial mats sampling site **(b)**.

2.2. Microcosms setup

Microcosms are artificial laboratory systems that are used to simulate and predict changes in natural environments under controlled conditions. Microbial mats samples were collected from the Ebro Delta on July 2013 and were taken carefully in 55 x 43 x 88 mm poly(methyl methacrylate) boxes preserving the structure of the microbial mat (Fig. 2.2a). Sediment samples were transferred to the laboratory protected from light and refrigerated at 4 ºC. Microcosms were maintained in the laboratory at room temperature, at natural light conditions and covered by water (Fig. 2.2b).

2.3. Isolation and identification of microorganisms from natural habitat

Two phototrophic microorganisms were selected for this study, both isolated from Ebro Delta microbial mats and identified as *Scenedesmus* sp. DE2009, a microalga (Fig. 2.2c) (Maldonado et al., 2010b), and *Geitlerinema* sp. DE2011, a cyanobacterium (Fig. 2.2d) (Burgos et al., 2013), by molecular biology methods: DNA extraction, PCR amplification of 16S rRNA or 18S rRNA genes, sequencing and phylogenetic analysis.

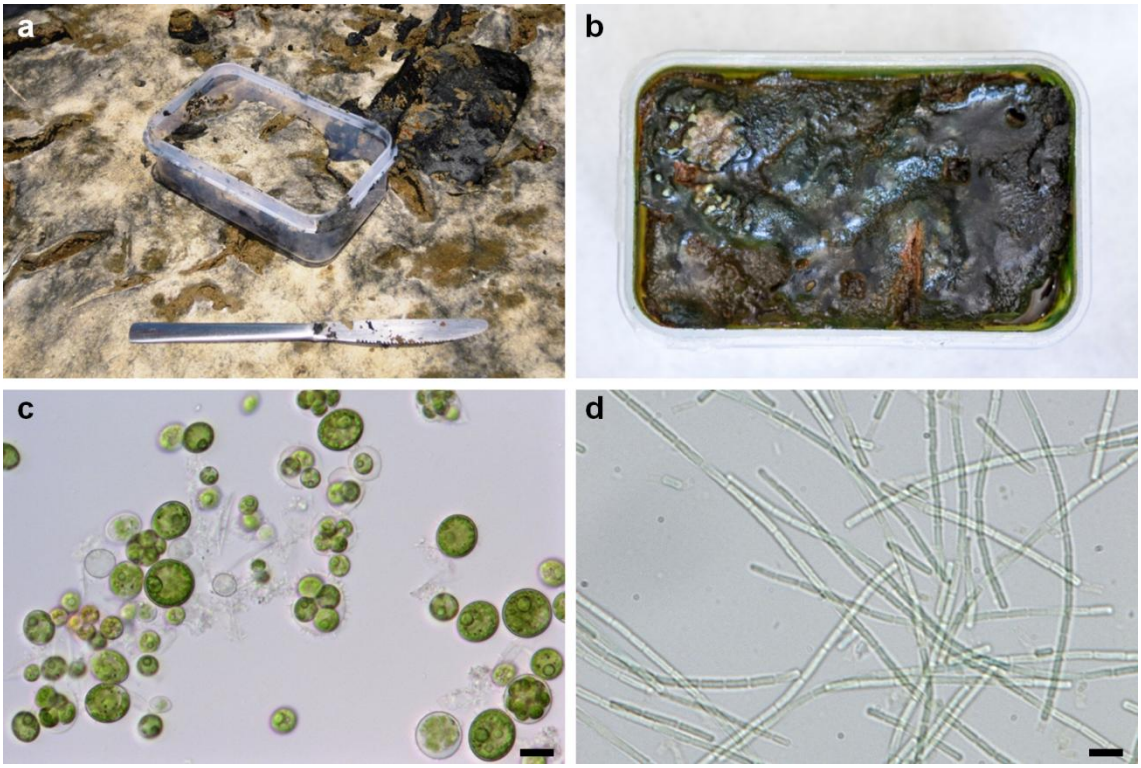

Fig. 2.2. Ebro Delta microbial mats **(a)**, microcosm's setup **(b)**, photomicrographs of the isolated *Scenedesmus* sp. DE2009 **(c)** and *Geitlerinema* sp. DE2011 **(d)**. Scale bars represent 5 *μ*m.

2.4. Microorganisms and culture conditions

2.4.1. *Scenedesmus* sp. DE2009

The microalga *Scenedesmus* sp. DE2009 was grown in liquid mineral Pfennig medium (Pfennig and Trüpper, 1992) in 100 mL flasks with a salinity of 2.65 g NaCl L^{-1} (Fig. 2.3). Cultures were exposed at the optimal growth temperature (27 °C) in a growth chamber (Climas Grow 180, ClimasLab, Barcelona) under continuous illumination with a light intensity of 6 µE m^{-2} s^{-1}, provided by cold white fluorescence lights.

Fig. 2.3. *Scenedesmus* sp. DE2009 liquid culture.

2.4.2. *Geitlerinema* sp. DE2011

The cyanobacterium *Geitlerinema* sp. DE2011 was cultivated in Pfennig mineral medium (Pfennig and Trüper, 1992) in 100 mL flasks with a salinity of 2.65 g NaCl L^{-1} (Fig. 2.4). Cultures were maintained at 27 ºC in a growth chamber and under continuous light conditions of 3.5 µE m^{-2} s^{-1}, provided by cold white fluorescence lights (Philips TL-D 18W-865).

Fig. 2.4. *Geitlerinema* sp. DE2011 liquid culture.

2.5. Preparation of stock solutions

2.5.1. Metal pollutants

The stock solutions of chromium, lead and copper were prepared by dissolving $Cr(NO_3)_3$ (Sigma-Aldrich, Bellefonte, PA, US), $Pb(NO_3)_2$ and $CuSO_4$, (Merck KGaA, Darmstadt, Germany) in deionized Milli-Q water and sterilized by filtration in Millex-GP 0.22 µm filters (Millipore, USA). The distinct working concentrations were obtained by serial dilution and these solutions were stored in the dark at 4 ºC. All experiments were carried out in duplicates for a period of 9 days. Control experiments for each test were performed in the absence of metal.

Scenedesmus sp. DE2009

On the one hand, the concentrations used to analyze the sensitivity of the microalga DE2009 to Cr^{3+} were: 0.25, 0.50, 0.75, 1, 5, 10, 15 and 25 µM (Fig. 2.5). Additionally, to determine the effect of Cr^{3+} on biomass and cellular viability, experiments at different concentrations: 0.75, 25, 100, 200 and 500 µM were performed. Finally, to assess the ability to accumulate Cr^{3+} external and/or internally, cultures were contaminated at concentrations of 1, 5, 10, 25, 50, 100 and 200 µM.

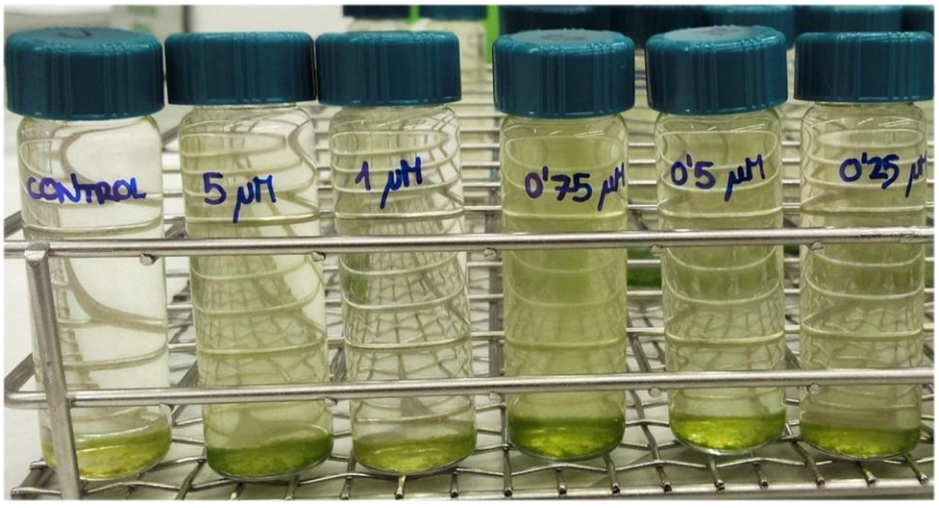

Fig. 2.5. Cultures of *Scenedesmus* sp. DE2009 polluted with different concentrations of Cr^{3+}.

On the other hand, *Scenedesmus* sp. DE2009 cultures were contaminated at fixed doses of 0.1 µM Pb^{2+}, 0.1 µM Cu^{2+} and 0.75 µM Cr^{3+} to assess how the presence of multiple metals both individually and in combination may alter photosynthetic pigments and viability. Moreover, single-metal concentrations of Pb^{2+} (1 µM to 25 mM), Cu^{2+} (1 µM to 25 mM) and Cr^{3+} (7.5 µM to 25 mM) and their ternary combination (1 µM Pb^{2+} – 1 µM Cu^{2+} – 7.5 µM Cr^{3+} to 1 mM Pb^{2+} – 1 mM Cu^{2+} – 7.5 mM Cr^{3+}) were prepared for the concentration-effect curves to assess the inhibition of the biomarker (Chl *a*) at cell level and determine the IC_{50} (the median inhibitory concentration that causes a 50 % effect with respect to a non-treated control).

Finally, cultures of microalga sp. DE2009 were polluted with Pb^{2+} and Cr^{3+} at concentrations of 1 mM and 2 mM for both metals to relate the cellular ultrastructural changes with the toxicity of the metal.

Geitlerinema sp. DE2011

The concentrations used to estimate the tolerance of this cyanobacterium to Cr^{3+} were: 0.025, 0.050, 0.1, 0.25, 0.50, 0.75, 1 and 5 µM; and to determine the ability to immobilize Cr^{3+} external and/or internally were: 1, 5, 10, 25, 50, 100 and 200 µM for a period of 9 days.

2.5.2. Light intensities

Various experiments were made to assess the effect of light on *Scenedesmus* sp. DE2009 consortium. For this end, the cultures were exposed to distinct light intensities: 2, 4, 6, 8, 10 and 12 μE m^{-2} s^{-1} (Fig. 2.6). These conditions were controlled accurately throughout all the experiments measuring every day the light intensity with a Luxometer C.A. 811 (Chauvin Arnoux, Metrix Paris, France). All experiments were performed for an exposure time of 7 and 30 days.

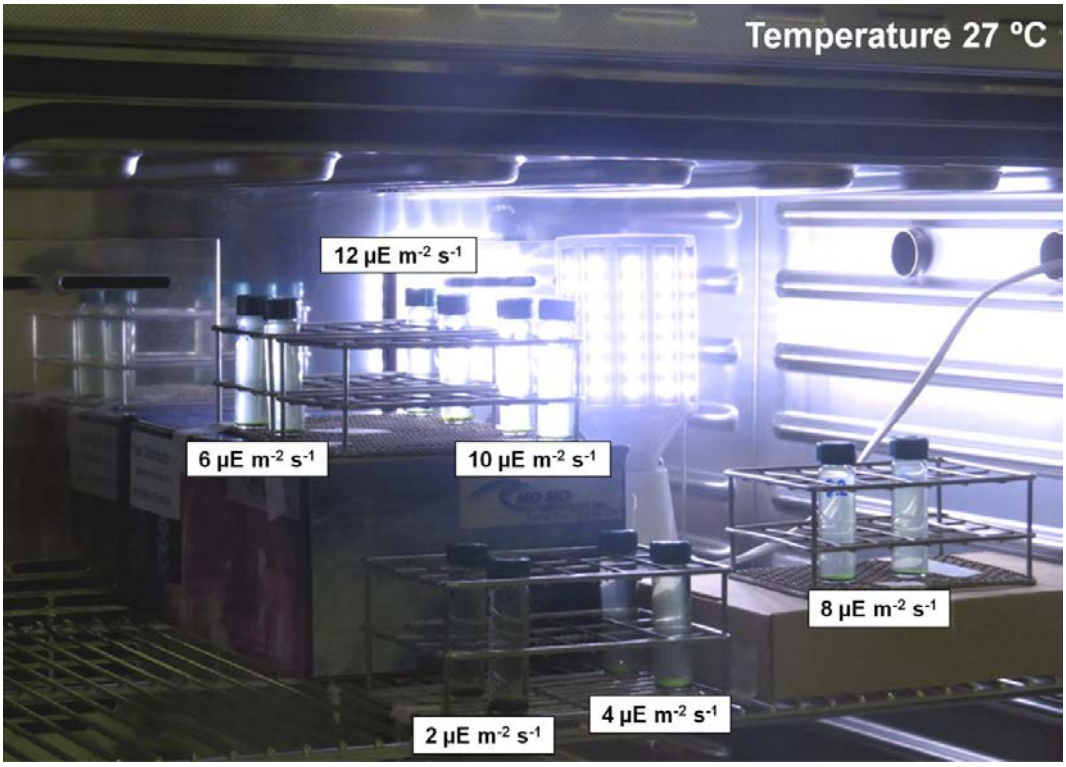

Fig. 2.6. Experimental design for the optimal light intensity evaluation.

2.5.3. Salinity doses

The salinity doses used to evaluate the impact of salt on *Scenedesmus* sp. DE2009 were 10, 35, 75 and 100 g NaCl L^{-1}. These concentrations were selected considering the changes in salinity detected in flood and dry (crust formation) periods in Ebro Delta sampling site. All experiments were performed for an exposure time of 7 and 30 days.

2.6. *In vivo* chlorophyll fluorescence methods

In this section are described the chlorophyll fluorescence methods used in this work to determine the effect of metal stress conditions on phototrophic microorganisms, as well as to evaluate the physiological state and cell viability of *Scenedesmus* sp. DE2009 in response to light and salinity treatments.

2.6.1. Pigment analysis by CLSM-*λscan* function

The *λscan* function of *Leica LAS AF* software (Leica Microsystems CMS GmbH) using a Leica TCS-SP5 CLSM (Leica Microsystems Heidelberg, GmbH, Mannheim, Germany) coupled to a spectrofluorometric detector was used in order to assess the sensitivity of phototrophic microorganism in response to distinct stress conditions.

This technique provides information on the state of the photosynthetic pigments of phototrophic microorganisms and determines the complete spectral distribution of the fluorescence signals emitted (autofluorescence) in a selected range of wavelengths. Each image sequence was obtained by scanning the same *xy* optical section throughout the visible spectrum. Images were acquired at the *z* position at which the fluorescence was maximal, and acquisition settings were constant throughout each experiment. The sample excitation was carried out with an Argon Laser at 488 nm (λ_{exe} 488) with a λstep size of 3 nm for an emission wavelength between 550 and 748 nm (Fig. 2.7)

In order to measure the Mean Fluorescence Intensity (MFI) of the *xyλ* data sets, the software *Leica LAS AF* was used. Images were visualized using the pseudocolour palette 4, where warm colours represent the high intensities and cold colours represent the low intensities of fluorescence. The regions-of-interest (ROIs) function was used to measure the spectral signature. For each sample, a set of 70 ROIs of 1 μm^2 distributed in the thylakoid area were defined for each metal concentration.

The pigment analysis by CLSM-*λscan* function allowed us to evaluate the physiological state of the phototrophic microorganisms at single-cell level, considering changes in the spectrum of Chl *a* used as a biomarker. For this purpose, the state of pigments was considered by means of the Maximum Intensity Fluorescence (MIF) signal detected at: 661 nm (Chl *a*) for *Geitlerinema* sp. DE2011 and 685 nm (Chl *a*) for *Scenedesmus* sp. DE2009.

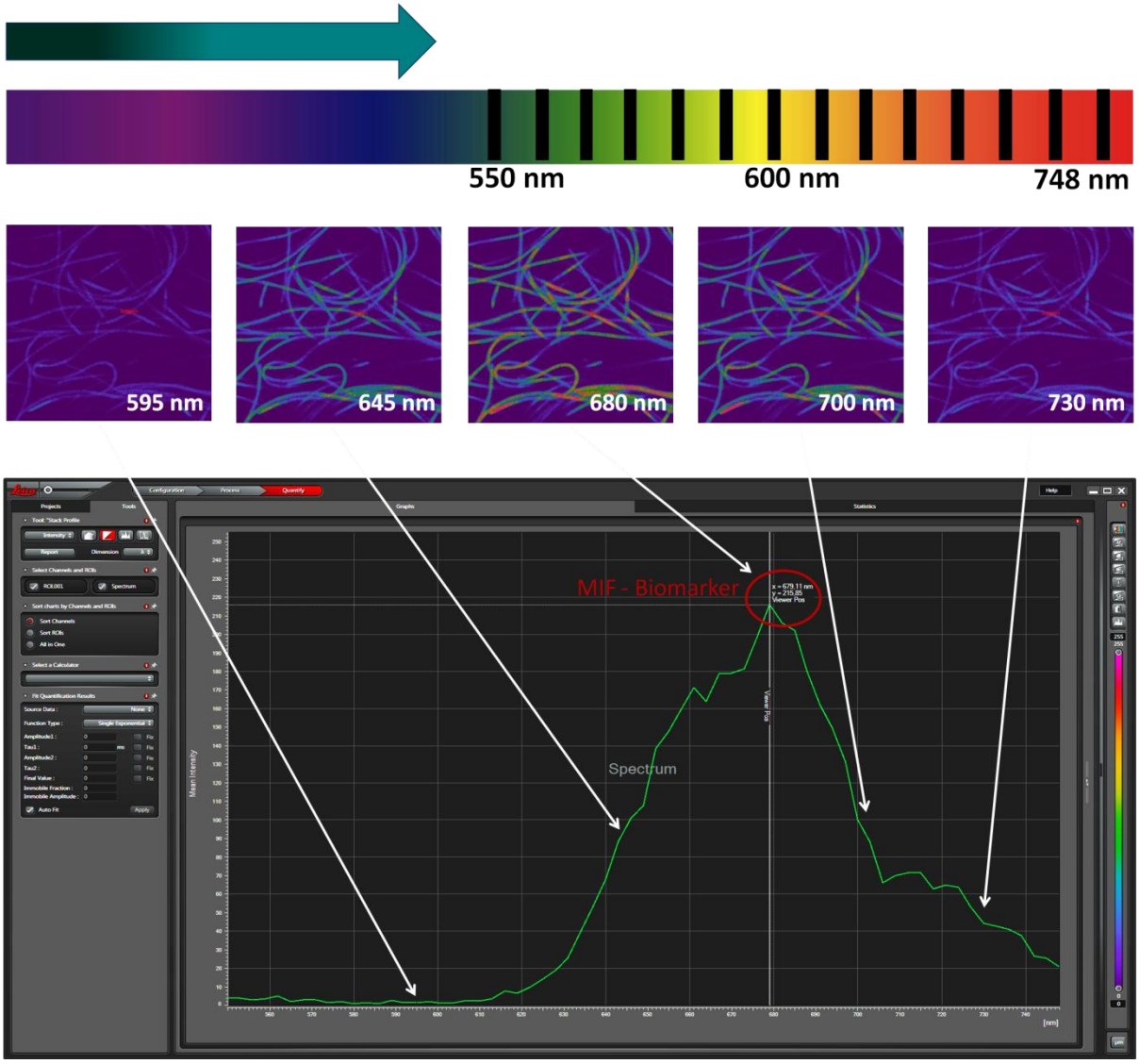

Fig. 2.7. Schema of CLSM-*λscan* method.

The CLSM-*λscan* method was applied to assess the tolerance and the *in vivo* effect of metals on *Scenedesmus* sp. DE2009 and *Geitlerinema* sp. DE2011 cultures in order to calculate the Minimum Metal Concentration (MMC) (when compared with the control) that significantly ($P < 0.05$) affects pigment fluorescence emission.

Besides, various concentrations of metals were prepared for the dose-response curves to evaluate the effectiveness of a metal in inhibiting the Chlorophyll *a* fluorescence (biomarker) at cell level, until pigment fluorescence intensity signal was not detected. This was done to determine the IC_{50}: the inhibitor concentration that provokes a response half way between the maximal (Top) and the minimal (Bottom) responses. The downward sloping dose curves follow a symmetrical sigmoidal shape and the IC_{50} data were calculated using a three parameter logistic model (GraphPad Prism, version 6 for Windows, La Jolla, CA, USA).

Spectral autofluorescence analysis optimization

The fluorescence emitted by the photosynthetic pigments and other nonspecific molecules of *Scenedesmus* sp. DE2009 was characterized, identified and evaluated by means of *λscan* function of CLSM. For the first time, three types of fluorescence signatures were detected when microalga cells were excited with a 405 nm UV laser diode: (1) photosynthetic pigments autofluorescence signal (PAF) emitted in the red range of the spectrum, (2) non-photosynthetic autofluorescence signal (NPAF) emitted within the green range, and (3) a mixture of both autofluorescence signals. In this sense, CLSM-*λscan* method was optimized to differentiate plainly between red and green autofluorescence signals.

This technique shows the complete spectral distribution of the fluorescence signals emitted by photosynthetic pigments of phototrophic microorganisms. Each image sequence was obtained by scanning the same *xy* optical section throughout the

visible spectrum using an x63 (1.4-numerical-aperture) oil immersion objective. Images were acquired at the *z* position at which the fluorescence was maximal and acquisition settings were constant throughout the experiment. Photosynthetic pigments excitation was carried out with an UV Laser at 405 nm and an Acousto-Optic Tunable Filter (AOTF) of 5 % for PAF and 15 % for NPAF. Both types of autofluorescence emissions were captured with a hybrid detector, in 10 nm bandwidth increments, with a λ step size of 3 nm and in the range from 420 to 750 nm. Statistically changes in the spectrum of Chl *a* at 684 nm, used as a biomarker, was considered to evaluate the state of pigments by means of the Maximum Intensity Fluorescence (MIF).

On the other hand, the MFI was obtained through the average fluorescence intensity for each wavelength within the studied range. For that, a set of 70 ROIs of 1 μm^2 for PAF and 20 ROIs for NPAF were selected in the thylakoid area of *Scenedesmus* sp. DE2009 to analyze the spectral signature and the peak emission range at cell level.

2.6.2. CLSM-DL method for cell viability assay

In this work, it is described a novel, fast and *in vivo* method using CLSM and a Dual Laser (CLSM-DL) to identify and quantify viable and non-viable cells of phototrophic microorganisms without the need of either staining or additional use of image treating software. This technique allows us to differentiate clearly two types of autofluorescence signals at cell level, observed previously in the CLSM-*λscan* studies. The CLSM-DL method has been tested in *Scenedesmus* sp. DE2009 consortium for differentiating dead and living microalga cells in response to distinct stress conditions.

For that reason, to capture both fluorescence signatures, separated and combined, a simultaneous *sequential scan* in two channels was carried out from each same *xyz* optical section using an x63 (1.4-numerical-aperture) oil immersion objective with a 1-Airy-unit confocal pinhole. On the one hand, PAF (living cells) was recorded in the red

channel (625 to 785 nm fluorescence emission) exciting the samples with a 561 nm laser diode and an AOTF of 20 %. On the other hand, NPAF (dead cells) was viewed in the green channel (500 to 585 nm fluorescence emission) using a 405 nm UV laser and an AOTF of 15 %. Both types of autofluorescence signals were captured with a hybrid detector. A set of 20 red and 20 green CLSM images (1024 x 1024 pixels) was obtained from all cultures analyzed. To determine the number of living (red signal) and dead cells (green signal) per condition, cell counts and statistical analysis were calculated.

2.6.3. 3D-CLSM reconstructions

In order to characterize the distribution of both autofluorescence signals (PAF and NPAF) on *Scenedesmus* sp. DE2009 whole cells, different z-series were acquired at the same CLSM conditions described in Section 2.6.2.

A z-series is a sequence of optical sections collected at different levels perpendicular to the optical axis (the z-axis) within a specimen. Z-series were collected by coordinating step-by-step changes in the fine focus of the microscope with sequential image acquisition at each step. The steps in focus were accomplished by a computer-controlled stepping motor that changes focus by small increments, in this case, of 250 nm along the z-axis. The images extracted from z-series were acquired in 512 x 512 pixels with an 1-Airy-unit confocal pinhole. Each stack of images was scanned from up to down in 70 optical sections in the *xy* planes, whose value corresponded to a thickness of 17.50 μm.

Following acquisition of the z-series, the files were exported into a computer three-dimensional (3D) reconstruction program for processing confocal images. Various projections were generated by the *Leica LAS AF* software and the *IMARIS* software package (version 7.2.1, Bitplane AG, Zürich, Switzerland) for 3D-reconstructions of *Scenedesmus* sp. DE2009 cells.

2.7. CLSM staining methods

In previous works, fluorochromes were used to determine biomass and viability of *Scenedesmus* sp. DE2009 cells polluted with Cr^{3+} (Section 3.2). Besides, the SYTOX Green nucleic acid stain was used to validate the new CLSM-DL method applied in the researches performed in Section 3.1 and 3.3.

2.7.1. FLU-CLSM-IA modified method

This technique was applied to estimate the microalga DE2009 biomass and cellular viability to various chromium concentrations, following a modification of the FLU-CLSM-IA method described by Puyen et al., (2012a). This methodology combines the use of a specific fluorochrome (FLU), the CLSM microscope, and free image-processing analysis software *ImageJ v.1.48s* (IA).

In this study, *Scenedesmus* sp. DE2009 autofluorescence (emission at 616-695 nm) and SYTOX Green Nucleic Acid Stain fluorescence (emission at 520–580 nm; Invitrogen, Life Technologies) were used simultaneously as markers for living and dead cells, respectively, in a simple dual-fluorescence viability assay. Both, the red and green fluorescence signals, were captured separately in a *sequential scan* process in two channels from each same *xyz* optical section using an x63 (1.4-numerical-aperture) oil immersion objective with an 1.5-Airy-unit confocal pinhole. On the first channel, samples were excited with a diode 561 nm (λ_{exe} 561) and an AOTF of 10 %. The emission of fluorescence was recorded at the red channel between 570 and 750 nm. On the second channel, samples were excited with an Argon Laser at 488 nm (λ_{exe} 488) and an AOTF of 10 %. The emission of fluorescence was captured at the green channel between 500 and 550 nm. In order to differentiate between viable and non-viable microalga cells, a set of 20 red and 20 green CLSM images (1024 x 1024 pixels) were

acquired from every culture of *Scenedesmus* sp. DE2009 to determine the biomass and cell viability at each Cr-concentration.

Subsequently, the CLSM images were transformed to binary images (black/white) applying fluorescence threshold values of 30 (red pixels) and 35 (green pixels) by means the *ImageJ v1.48s* software. To minimize the background detected in every pair of images a smoothing filter was used. Finally, to obtain bio-volume values, the Voxel Counter plug-in was applied to these filtered images (Rasband, 2014). This specific application calculates the ratio between the thresholded voxels (red and green fluorescent voxel counts) to all voxels from every binary image analyzed. The bio-volume value (Volume Fraction) was finally multiplied by a conversion factor of 310 fgC μm^3 to convert it to biomass (Fry et al., 1990).

2.7.2. SYTOX Green nucleic acid stain

SYTOX Green nucleic acid stain was applied to study the response of *Scenedesmus* sp. DE2009 to high salinity, considering this parameter as inductor of damage in the cells, and also to compare whether NPAF correspond to *Scenedesmus* sp. DE2009 dead cells. For that, samples were incubated at 6 $\mu E\ m^{-2}\ s^{-1}$ and 100 g NaCl L^{-1} for 7 days. Later, one aliquot was used as a control (without fluorochrome) and the other one was stained using a specific-fluorescence SYTOX Green dye (Molecular Probes Inc., Eugene, OR, USA). The original fluorescent probe containing 5 mM stock solution in Dimethyl Sulfoxide (DMSO) was diluted in deionized Milli-Q water for a final dye concentration of 5 µM and added to the cell suspension of microalga. The mixture was incubated for 30 minutes at room temperature in the dark and then observed by CLSM-DL method. No washing was required before or after SYTOX Green staining.

2.8. Electron microscopy techniques

In this section are described the electron microscopy techniques used in this work for determining whether *Geitlerinema* sp. DE2011 and *Scenedesmus* sp. DE2009 could immobilize chromium externally and/or internally, and to analyze changes in the morphology and ultrastructure of living and dead *Scenedemus* sp. DE2009 cells.

2.8.1. Scanning Electron Microscopy

The Scanning Electron Microscopy (SEM) technique was used in order to observe the external morphology and the EPS formation on phototrophic microorganisms.

For SEM analysis, cultures of those microorganisms were filtrated in Nucleopore™ polycarbonate membranes (Whatman, Ltd.) and then were fixed in 2.5 % glutaraldehyde diluted in Millonig phosphate buffer (Millonig, 1967) (0.1 M pH 4) at 4 °C for 2 hours and washed several times in the same buffer at 4 °C to remove the excess of fixative, dehydrated in increasing concentrations (30, 50, 70, 90 and 100 %) of ethanol and dried by critical-point (CPD 030 Critical Point Drier, BAL-TEC GmbH D – 58579 Schalksmühle). Finally, samples were mounted on aluminium metal stubs using an electrically-conductive double-sided adhesive tape and then coated with a 5 μm gold-palladium layer (K550 Sputter Coater, Emitech, Ashford, UK) for better image contrast. A Zeiss EVO®MA 10 scanning electron microscope (Carl Zeiss NTS GmbH, Oberkochen, Germany) was used to generate the images.

2.8.2. Transmission Electron Microscopy

The Transmission Electron Microscopy (TEM) technique was used in order to observe the ultrastructure of phototrophic microorganisms.

For TEM analysis, samples were fixed in 2.5 % glutaraldehyde diluted in Millonig's buffer phosphate (Millonig, 1967) (0.1 M pH 4) at 4 °C for 2 hours and washed several times in the same buffer at 4 °C to remove the excess of fixative. Then, samples were post-fixed in 1 % osmium tetroxide (OsO_4) at 4 °C for 2 hours, washed in the same buffer and centrifuged in order to obtain a pellet. They were then dehydrated in a graded series of acetone (50, 70, 90, 95 and 100 %) and embedded in Spurr's resin. Once the samples were included in the resin, ultrathin sections (70 nm), obtained with a Leica EM UC6 Ultramicrotome (Leica Microsystems, GmbH, Heidelberg, Germany), were mounted on carbon-coated titanium grids and stained with uranyl acetate and lead citrate according to the method described by Reynolds et al., (1963). Samples were viewed in a Hitachi H-7000 transmission electron microscope (Hitachi, Tokyo, Japan).

2.8.3. Energy dispersive X-ray microanalysis

Energy Dispersive X-ray (EDX) is a technique used for the elemental analysis of a sample. The technique is based on the analysis of X-rays emitted by matter in response to collisions with charged particles. To stimulate the emission of X-rays, a high energy beam of charged particles such as electrons, protons or an X-ray beam is focused in the area of the study sample. This charged particle collides with internal shell of the element and then an electron from an outer shell moves into empty shell. Since there are a series of jumps from higher to smaller shells, at this time X-rays are generated. This phenomenon is due to the fundamental principle that every element has a unique atomic structure that allows X-rays that are characteristic of the atomic structure of an element to be identified only from each other. The number and energy of emitted X-

rays in a sample can be detected and measured semiquantitatively by an energy dispersive spectrometer.

This detector, which may be coupled to both a SEM and a TEM, is connected to a computer with the software *INCA v.4.13* (Oxford Instruments, Bucks, England) that generates graphics with different peaks corresponding to each of the chemical elements present in the analyzed area. The great advantage of this approach is that the area to be analyzed can be selected by the user and the analysis of a sample area takes usually 60 s.

SEM-EDX

With the aim of determining whether *Geitlerinema* sp. DE2011 and *Scenedesmus* sp. DE2009 could accumulate chromium extracellularly, SEM coupled to EDX was used. For EDX microanalysis, cells were homogenously distributed and filtered on polycarbonate membrane filters. These filters were fixed, dehydrated and dried by critical-point drying and then coated with gold. An EDX spectrophotometer Link Isis-200 (Oxford Instruments, Bucks, England) coupled to the microscope operating at 20 kV was used for the analysis of the samples. Finally, EDX-SEM spectra from individual cells were obtained.

TEM-EDX

In order to assess whether *Geitlerinema* sp. DE2011 and *Scenedesmus* sp. DE2009 were able to sequester chromium intracellularly in the cytoplasm or in the polyphosphate (PP) inclussions, TEM coupled to EDX was used. For EDX microanalysis, sections of 200 nm thick were also stained with uranyl acetate and mounted on carbon-coated titanium grids. Samples were analyzed with an EDX spectrophotometer Link Isis-200 (Oxford Instruments, Bucks, England) coupled to a Jeol Jem-2011 transmission microscope (Jeol Ltd., Tokyo, Japan) operating at 200 kV. Finally, EDX-TEM spectra from individual cells were obtained.

2.8.4 Transmission soft X-ray Microscopy

Polluted and non-polluted cultures of *Scenedesmus* sp. DE2009 with chromium and lead were prepared for structural comparison using cryo-transmission soft X-ray tomography. Measurements were performed at the Transmission soft X-ray Microscope (TXM) of the MISTRAL beamline at ALBA synchrotron (Barcelona, Spain) (Sorrentino et al., 2015).

Cryo soft X-ray tomography is an emerging X-ray microscopy technique for three-dimensional visualization of cryo-preserved samples. This technique can provide structural information at the level of a whole cell without sectioning and staining at spatial resolution down to 50 nm (half-pitch) (Otón et al., 2012). The penetration power of soft X-rays in the water window energy range, between the inner-shell absorption edges of carbon (284 eV) and oxygen (543 eV), allows penetrating water layers up to 10 μm thickness, while carbon-rich structures, strongly absorbent, are visualised with good and natural absorption contrast. Samples cryo-fixation is the only step required in soft x-ray tomography.

In order to be observed and analyzed in the TXM, 4 μL of *Scenedesmus* sp. DE2009 cultures were deposited onto Quantifoil R 1.2/1.3 grids for 10 minutes. Later, the excess of samples was eliminated by blotting during 3 seconds and grids were plunge-frozen in liquid ethane using a Leica EM CPC (Leica Microsystems Heidelberg, Mannheim, Germany). The samples were vitrified for preventing radiation damage while collecting the data in the TXM. The plunge-freeze technique is suited for samples with thickness up to 10 μm. Before the experiment, vitrified samples were checked using a visible light microscope equipped with a cryo-correlative microscopy stage CMS196 (Linkam Scientific Instruments, Tadworth, UK). This checking procedure increased the efficiency of data collection at the synchrotron in two ways. First, it allowed creating a map of the grid for an easy location of relevant cells when the grid was loaded into the

TXM vacuum chamber. Second, it allowed discarding those grids with an inappropriate number of cells, ice thickness or carbon foil preservation.

Once inside the TXM the relevant microalga cells to be imaged with X-rays were localized again using an inline visible light fluorescence microscope with the TXM. A series of transmission contrast projections were collected for each *Scenedesmus* sp. DE2009 selected cells by rotating the specimen over a tilting range of -70º and +70º and with an angular step of 1º. The recorded tomographic projections were manually aligned using *eTomo IMOD v4.7.15* software (Kremer et al., 1996). Once aligned, the transmission projections were converted to absorbance projection and reconstructed using the Algebraic Reconstruction Techniques (ART) algorithm (Gordon et al., 1970) implemented in *TomoJ* plug-in (Messaoudii et al., 2007) of *ImageJ v1.48s* software. Finally, the experimental image projections were deconvolved using the Wiener filter (Otón et al., 2016), obtaining an increase of image quality in the final reconstructed tomograms.

2.9. Statistical analysis

Statistical tests were performed by one-way analysis of variance (ANOVA) and Tukey and Bonferroni's comparison *post hoc* tests. For all analyzes, a 95 % confidence interval was used. Differences were considered significant at $P < 0.05$. The statistics were carried out using *IBM SPSS Statistics* software (version 20.0 for Windows 7), *GraphPad Prism v.6* (GraphPad Software, La Jolla, CA, US) and *Microsoft Excel* (Microsoft, Redman, WA, US). Data were represented as the average ± standard deviation, unless otherwise stated.

Chapter 3 – Results

In the **Chapter 3**, the results are presented from the research carried out in this Thesis. The chapter is organised into three sections that correspond to articles that have already been published (Section 3.1 and 3.2) and the last one of them currently under review (Section 3.3).

The published articles are also shown in **Annex I.**

Section 3.1 Millach, L., Obiol, A., Solé, A., Esteve, I. (2017) **A novel method to analyze *in vivo* the physiological state and cell viability of phototrophic microorganisms by confocal laser scanning microscopy using a dual laser.**

Published in *Journal of Microscopy.*

Section 3.2 Millach, L., Solé, A., Esteve, I. (2015) **Role of *Geitlerinema* sp. DE2011 and *Scenedesmus* sp. DE2009 as bioindicators and immobilizers of chromium in a contaminated natural environment.**

Published in *Biomed Research International.*

Section 3.3 Millach, L., Solé, A., Esteve, I. (2017) **Combined CLSM techniques for rapid assessment of the effect and cell viability of phototrophic microorganisms under metal stress.**

Submitted to *Aquatic Toxicology.*

A Novel Method to Analyze *in Vivo* the Physiological State and Cell Viability of Phototrophic Microorganisms by Confocal Laser Scanning Microscopy Using a Dual Laser

Laia Millach, Aleix Obiol, Antonio Solé, and Isabel Esteve

Departament de Genètica i Microbiologia, Facultat de Biociències, Universitat Autònoma de Barcelona, Bellaterra, 08193, Barcelona, Spain.

SUMMARY

Phototrophic microorganisms are very abundant in extreme environments, where are subjected to frequent and strong changes in environmental parameters. Nevertheless, little is known about the physiological effects of these changing environmental conditions on viability of these microorganisms, which are difficult to grow in solid media and have the tendency to form aggregates. For that reason, it is essential to develop methodologies that provide data in short time consuming, *in vivo* and with minimal manipulating the samples, in response to distinct stress conditions.

In this paper, we present a novel method using Confocal Laser Scanning Microscopy and a Dual Laser (CLSM-DL) for determining the cell viability of phototrophic microorganisms without the need of either staining or additional use of image treating software. In order to differentiate viable and non-viable *Scenedesmus* sp. DE2009 cells, a *sequential scan* in two different channels was carried out from each same

xyz optical section. On the one hand, photosynthetic pigments fluorescence signal (living cells) was recorded at the red channel (625- to 785- nm fluorescence emission) exciting the samples with a 561-nm laser diode, and an Acousto-Optic Tunable Filter (AOTF) of 20 %. On the other hand, non-photosynthetic autofluorescence signal (dead cells) was recorded at the green channel (500- to 585- nm fluorescence emission) using a 405-nm UV laser, an AOTF of 15 %. Both types of fluorescence signatures were captured with a hybrid detector.

The validation of the CLSM-DL method was performed with SYTOX Green fluorochrome and electron microscopic techniques, and it was also applied for studying the response of distinct light intensities, salinity doses and exposure times on a consortium of *Scenedesmus* sp. DE2009.

INTRODUCTION

Oxygenic and anoxygenic photosynthetic microorganisms are very abundant in microbial mats. These ecosystems are widely distributed around the world, including extreme environments, where are subjected to periodic and strong changes in environmental parameters (Green et al., 2008, Antibus et al., 2012, de los Ríos et al., 2015, Cuadrado et al., 2015, Hoffmann et al., 2015).

Over a considerable period of time, our group has been studying microbial mats, hypersaline ecosystems located in the Ebro Delta, Tarragona, Spain (Esteve et al., 1994, Guerrero et al., 2002, Solé et al., 2009, Millach et al., 2015). These mats are developed in water-sediment interfaces and, are formed by multilayered benthic microbial communities that are distributed along vertical micro-gradients of different physicochemical parameters. Cyanobacteria and microalgae, located mainly in the upper green layers, play an important role in primary production in these mats, where they stabilize deltaic sediments over large areas. Among them, *Scenedesmus* sp. DE2009 has been isolated (Maldonado et al., 2010b) and identified by molecular biology methods (Burgos et al., 2013). This microorganism is very abundant in Ebro Delta microbial mats and their cells are spherical, with a diameter of 7 – 9 μm, and their chloroplasts are distributed laterally in the cell.

However, it is important to highlight that most phototrophic microorganisms isolated from natural habitats do not grow in solid laboratory cultures; additionally, they have a tendency to form aggregates. In this current work, therefore, *Scenedesmus* sp. DE2009 was selected as a model because it grows with difficulty in a solid medium and forms a consortium with heterotrophic bacteria.

Various studies have been made to analyze changes in microbial diversity in stress conditions such us desiccation and high salinity by means molecular techniques (Garcia-Pichel et al., 2001, Rajeev et al., 2013, Lan et al., 2014), nevertheless, less is

known about the impact on cell viability that changes in different environmental conditions may cause, mainly in the microorganisms that colonize extreme habitats, and particularly in those that usually show increased survival in stress conditions. Among diverse stressing factors, high light intensity and dry conditions, which in turn increase salinity, are very important parameters that should be considered in ecosystems subjected to long periods of annual drought.

For this reason, it is essential to develop methodologies that characterize the physiological state of microbial cells and provide valuable information about the viability and functioning of microbial communities. Plate counting is one of the most fundamental microbiological techniques in determining the number of viable cells in a sample (Buck, 1979). However, as we have already mentioned, most isolated microorganisms from natural environments do not grow in solid media.

The analysis of pigment excitation/absorption spectra (Roldán et al., 2004) and quantification of the chlorophyll content are frequently used to quantify and identify microorganisms (Gregor and Maršálek, 2004; Wagenen et al., 2014). The Pulse-Amplitude-Modulation (PAM) fluorometry can also be used for ultrasensitive fluorescence measurements in distinct layers of photosynthetically active material (Schreiber, 1998). This technique is non-invasive and has frequently been used to estimate the photosynthetic efficiency within oxygenic organisms (Genty et al., 1989, Perkins et al., 2002). For that, *in vivo* chlorophyll fluorescence methods have for a long time been used for non-destructive estimation of biomass and growth rates (Büchel and Wilhelm, 1993; Huot and Babin, 2011) and for the detection and quantification of changes induced in the photosynthetic apparatus (Mehta et al., 2010). Nevertheless, all these methods are suitable for pigment analysis or photophysiology studies, but cannot be applied to distinguish between viable and non-viable cells.

Finally, other alternative and common viability assays are fluorescent staining like DNA-specific SYTOX Green dye (Sato et al., 2004) or other fluorochromes (Pouneva, 1997), and flow cytometry (Al-Rubeai et al., 1997, Dorsey et al., 1989, Veldhuis et al., 2001); but in both methods staining is required and, in the second one is difficult to apply in filamentous cyanobacteria and in microorganisms that tend to form aggregates.

In this article, a novel, simple, non-intrusive, rapid and *in vivo* method was developed for determining the cell viability of phototrophic microorganisms without the need of prior staining by Confocal Laser Scanning Microscopy. This method is based on a *sequential scan* using a Dual Laser (CLSM-DL) that allows the capturing of different and specific wavelengths within the spectrum at the same time. High-resolution images are obtained that can help to clearly distinguish living cells from dead ones, overlapping and separately, and without the need of a subsequent analysis of the generated images.

The objectives of this work are (i) to set up a fast and easy CLSM-DL method for differentiating living and dead microbial cells; (ii) to validate the method by means of other microscopy techniques and (iii) to justify its applicability to the study of *Scenedesmus* sp. DE2009 response to light and salinity treatment.

MATERIAL AND METHODS

Strain and culture conditions

The microalga *Scenedesmus* sp. DE2009 was isolated from Ebro Delta microbial mats (0°35'E - 0°56'E; 40°33'N - 40°47'N), Tarragona, Spain. This microorganism was grown in liquid mineral Pfennig medium (Pfennig and Trüpper, 1992) in 100 mL flasks with a salinity condition of 2.65 g NaCl L^{-1}. Cultures were exposed and maintained at the optimal growth temperature at 27 °C in a growth chamber (Climas Grow 180, ClimasLab, Barcelona) under continuous illumination with a light intensity of 6 μE m^{-2} s^{-1}, provided by cold white fluorescence lights (Philips TL-D 18W-865). These cultures were used as control in all the experiments performed.

Experimental conditions

Various experiments were made applying the CLSM-DL and complemented with CLSM-*λscan* function to assess the effect of light and salinity at single-cell level on *Scenedesmus* sp. DE2009 consortium. For this end, the cultures were exposed to distinct light intensities (2, 4, 6, 8, 10 and 12 μE m^{-2} s^{-1}). These conditions were controlled accurately throughout all the experiments measuring every day the light intensity with a Luxmeter C.A. 811 (Chauvin Arnoux, Metrix Paris, France).

On the other hand, different salinity doses (10 g L^{-1}, 35 g L^{-1}, 75 g L^{-1} and 100 g L^{-1}) were selected considering changes in salinity detected in flood and dry (crust formation) periods in Ebro Delta sampling site. Furthermore, all experiments were performed for short periods (7 days) and long-term (30 days) under the same growth conditions mentioned in Section 2.1.

Pigment analysis by CLSM-*λscan* function

Scenedesmus sp. DE2009 cultures were evaluated *in vivo* to determine the emission spectra of microalga pigments by *λscan* function of Leica LAS AF Software using a Leica TCS-SP5 CLSM (Leica Microsystems Heidelberg GmbH, Mannheim, Germany). This technique, based on a fluorescence method, shows the complete spectral distribution of the fluorescence signals emitted by photosynthetic pigments of phototrophic microorganisms. Statistically changes in the spectrum of Chlorophyll *a* (Chl *a* = 684 nm), used as a biomarker, was considered to evaluate the state of pigments by means of the Maximum Intensity Fluorescence (MIF).

In this paper, CLSM-*λscan* method was optimized to differentiate plainly between red and green fluorescence signals. In this sense, each image sequence was obtained by scanning the same *xy* optical section throughout the visible spectrum using an x63 (1.4-numerical-aperture) oil immersion objective. Images were acquired at the *z* position at which the fluorescence was maximal and acquisition settings were constant throughout the experiment. Photosynthetic pigments excitation was carried out with an UV Laser at 405 nm and an AOTF of 5 % for PAF and 15 % for NPAF. Both types of fluorescence emissions were captured with a hybrid detector, in 10 nm bandwidth increments, with a λ step size of 3 nm and in the range from 420 nm to 750 nm.

On the other hand, the MFI was obtained through the average fluorescence intensity for each wavelength within the studied range. For that, a set of 70 ROIs of 1 μm^2 for PAF and 20 ROIs for NPAF were selected in the thylakoid area of *Scenedesmus* sp. DE2009 to analyze the spectral signature at cell level and the peak emission range.

CLSM-DL method for viability assay

The CLSM-DL method has been tested in *Scenedesmus* sp. DE2009 consortium for differentiating dead and living microalga cells. For that reason, to capture both fluorescence signatures, separated and combined, a *sequential scan* in two channels was carried out from each same *xyz* optical section. On the one hand, PAF was recorded in the red channel (625- to 785- nm fluorescence emission) exciting the samples with a 561-nm laser diode and an AOTF of 20 %. On the other hand, NPAF was viewed in the green channel (500- to 585- nm fluorescence emission) using a 405-nm UV laser, an AOTF of 15 %. Both types of fluorescence signals were captured with a hybrid detector. A set of 20 red and 20 green CLSM images (1024 x 1024 pixels) was obtained from all cultures analyzed. To determine the number of living (red signal) and dead cells (green signal) per condition, cell count and statistical analysis were calculated.

Furthermore, in order to characterize the distribution of both fluorescence signatures on *Scenedesmus* sp. DE2009 cells, a series of optical sections (CLSM stack) were acquired, at the same conditions described above. The 17.25 μm thick stack was scanned from up to down in 69 optical sections, in *x-y* planes every 0.25 μm along the optical axis with a 1-Airy-unit confocal pinhole. Various projections were generated by the Leica LAS AF software and the IMARIS software package (version 7.2.1, Bitplane AG, Zürich, Switzerland) for 3D-reconstructions of *Scenedesmus* sp. DE2009 cells.

SYTOX Green Nucleic Acid Stain

To validate the CLSM-DL method and quantify *Scenedesmus* sp. DE2009 dead cells, the samples were incubated at 6 μE m^{-2} s^{-1} and 100 g NaCl L^{-1} for 7 days. Later, one aliquot was used as a control (without fluorochrome) and the other one was stained using a specific-fluorescence SYTOX Green dye (Molecular Probes Inc., Eugene, OR, USA). The original fluorescent probe containing 5 mM stock solution in DMSO was diluted in deionized Milli-Q water for a final dye concentration of 5 μM and added to

the cell suspension of microalga. The mixture was incubated for 30 minutes at room temperature in the dark and then observed by CLSM-DL method. No washing was required before or after SYTOX Green staining.

Electron Microscopy Techniques

Electron microscopy techniques were used to analyze changes on the morphology and ultrastructure of living and dead *Scenedesmus* sp. DE2009 cells. The samples were incubated at 6 μE m^{-2} s^{-1} and 100 g NaCl L^{-1} for 7 days. For SEM analysis, cultures were filtrated in Nucleopore™ polycarbonate membranes (Whatman, Ltd.) and then were fixed in 2.5 % glutaraldehyde diluted in Milloning phosphate buffer (0.1 M pH 4) at 4 °C for 2 hours. Later, samples were washed in the same buffer, dehydrated in increasing concentrations of ethanol and dried by critical-point (CPD 030 Critical Point Drier, BAL-TEC GmbH D – 58579 Schalksmühle). Finally, samples were coated with a 5 μm gold-palladium layer (K550 Sputter Coater, Emitech, Ashford, UK) for better image contrast. A Zeiss EVO®MA 10 SEM (Carl Zeiss NTS GmbH, Oberkochen, Germany) was used to observe the samples.

For TEM analysis, cultures were fixed in 2.5 % glutaraldehyde diluted in Milloning phosphate buffer. Samples were post-fixed in 1% OsO_4 at 4 °C for 2 hours and washed in the same buffer. They were then dehydrated in a graded series of acetone and embedded in Spurr's resin. Ultrathin sections (70 nm), obtained with a Leica EM UC6 Ultramicrotome (Leica Microsystems, GmbH, Heidelberg, Germany), were mounted on carbon-coated copper grids and stained with uranyl acetate and lead citrate. Samples were viewed in a JEM-1400 TEM (JEOL, USA).

Statistical analysis

Statistical analyzes were performed by ANOVA and Tukey and Bonferroni's comparison *post hoc* tests. Differences were considered significant at $p < 0.05$. The analyzes were performed using IBM SPSS Statistics software (version 20.0 for Windows).

RESULTS AND DISCUSSION

Autofluorescence emission spectra of *Scenedesmus* sp. DE2009 cells

Previously, the fluorescence emitted by the photosynthetic pigments and other nonspecific molecules of *Scenedesmus* sp. DE2009 was characterized, identified and evaluated by means of *λscan* function of CLSM. Three types of fluorescence signatures were detected when microalga cells were excited with a 405 nm UV laser diode: (1) PAF emitted in the red range, (2) NPAF emitted within the green range, and (3) a mixture of both autofluorescence signals.

The emission profiles correspond to individual cells of *Scenedesmus* sp. DE2009 showing only PAF signal are represented in Fig. 3.1.1a. The PAF spectra recorded indicated a high intensity emission peak at 684 nm, produced by Chl *a* (Fig. 3.1.1b). The results obtained by CLSM-*λscan* function demonstrated that the differences were not statistically significant ($P < 0.05$) among 6, 8 and 10 μE m^{-2} s^{-1}. An *xyz* optical section corresponding to PAF detected in the microalga growing at 12 μE m^{-2} s^{-1} is shown in Fig. 3.1.1c.

In the same conditions, some cells of *Scenedesmus* sp. DE2009 emitted only NPAF. The spectra recorded in these cells showed irregular curves, with a maximum fluorescence intensity at the range of 460-530 nm (Fig. 3.1.1d). This type of green emission was confirmed by CLSM images (Fig. 3.1.1e). Generally, NPAF was distributed evenly across the cell cytoplasm and cells showed a disorganization of the thylakoids and a lack of pigment. These cellular differences were observed by bright-field microscopy (Fig. 3.1.1f).

Finally, a few cells also emitted both autofluorescence signals: PAF and NPAF. In this case, the emission spectra recorded showed two distinct fluorescence intensities: (i) a low-intensity uneven peak at 684 nm (Chl *a*) and (ii) a wide and irregular fluorescence

intensity in the green region (Fig. 3.1.1g). These cells were considered an intermediate physiological state between viable and non-viable (Fig. 3.1.1e, 3.1.1f and 3.1.1h), since the Chl *a* peak still emitted fluorescence, but their cell integrity was damaged.

To evaluate the optimal light intensity for the growth of *Scenedesmus* sp. DE2009 during a long period of time, an analogous experiment was carried out under the same light conditions for 30 days (Fig. 3.1.2). The *λscan* plots corresponding to PAF emission showed differences in the MIF in response to varying light intensities (Fig. 3.1.2a). In this case, the highest MIFs correspond to 6 and 8 μE m^{-2} s^{-1} and no statistically significant differences ($P < 0.05$) were found between them, using the Tukey and Bonferroni comparison test. A decrease in the MIF was observed in the rest of the light intensities tested for a month. An *xyz* optical section from PAF detected in cultures of *Scenedesmus* sp. DE2009 growing at 8 μE m^{-2} s^{-1} is shown in Fig. 3.1.2b.

Finally, when comparing the MIF results obtained at 7 and 30 days, no statistically significant differences ($P < 0.05$) were found between 6 and 8 μE m^{-2} s^{-1}. These results suggest that the optimum light intensity for the growth of *Scenedesmus* sp. DE2009 is in this range, since the exposure time does not alter the MIFs.

Set up of CLSM-DL method

In this work, it is described a novel, fast and *in vivo* method to identify and quantify viable and non-viable *Scenedesmus* sp. DE2009 cells without manipulation of the samples. This technique allows us to differentiate clearly two types of fluorescence signatures at cell level observed previously in the CLSM-*λscan* studies. A simultaneous scan of the same *xyz* optical section is showed for PAF corresponding to living cells (Fig. 3.1.3a), for NPAF representing dead cells (Fig. 3.1.3b) and an overlap of both autofluorescence signal (Fig. 3.1.3c). The percentages of living and dead cells were calculated from these CLSM images.

For determining the *in vivo* effect of light on cellular viability of *Scenedesmus* sp. DE2009 by means of CLSM-DL, two experiments at different light intensities were performed. Changes in microalga viability growing for 7 days are represented in Fig. 3.1.3d. These results showed low significant differences ($P < 0.05$) in all the light intensities tested, which indicated a slight effect of light. However, there were no significant differences ($P < 0.05$) among 6, 8 and 10 μE m^{-2} s^{-1}, which also represent the highest values of viable cells in this experiment: 93.52%, 93.11% and 93.18%, respectively. A similar experiment was performed in cultures growing for 30 days (Fig. 3.1.3e). In this case, it is important to highlight that, even at 10 μE m^{-2} s^{-1} (67.48 %) and 12 μE m^{-2} s^{-1} (58.81%), a high percentage of viable cells was also remained. These results confirm the high viability level was maintained in all the light intensities assayed.

Finally, a reduction of cell viability at 10 μE m^{-2} s^{-1} (25.69 %) and 12 μE m^{-2} s^{-1} (29.80 %) was observed for light exposure experiments between 7 and 30 days using the Tukey and Bonferroni comparison test. However, no statistically significant differences ($p < 0.05$) were only found at 6 μE m^{-2} s^{-1}, which also corresponds to the highest percentage of living cells. Hence, it was considered important to fix the light parameter at 6 μE m^{-2} s^{-1} in salinity experiments. In the same way, our results in light experiments agree with those obtained in other microalgae studies at low light intensities. In this case, Ferreira et al., 2016 demonstrated an increase in chlorophyll content at 16.91 ± 0.45 μmol photons m^{-2} s^{-1} to capture light in a more efficient manner in *Scenedesmus dimorphus* (UTEX 1237); and Pal et al., 2013 indicated that 1000-1500 lux (6-9 μE m^{-2} s^{-1}) were the best light intensities in order to produce maximum yield in *Chaetoceros muelleri* (CS-178).

Validation of the CLSM-DL method

First, to validate the CLSM-DL method, SYTOX Green nucleic acid stain and electron microscopic techniques were applied to study the response of this microorganism to the highest salinity condition (100 g NaCl L^{-1}), considering this parameter as inductor of damage in the cells. The objective was to compare whether NPAF corresponded to *Scenedesmus* sp. DE2009 dead cells. Second, the CLSM-DL method was applied for assessing the effect of salinity at different doses over a long period of time on photosynthetic pigments and cell viability.

Analysis of the correlation between NPAF and dead cells

Samples were stained using a specific-fluorescence SYTOX Green nucleic acid fluorochrome. The results demonstrated that the differences were not statistically significant ($F = 1.367$) ($P > 0.05$) between the cells stained by SYTOX Green (45.79 %) and NPAF cells (50.95 %). Hence, a very good correlation was established between the cells stained by SYTOX Green (Fig. 3.1.4a) and cells emitting NPAF (Fig. 3.1.4b), being the second one a more accurate technique, since heterotrophic bacteria showed no fluorescent signal.

In addition, electron microscopy techniques (SEM and TEM) were also used to analyze the changes in morphology and cellular ultrastructure in cells that emitted in NPAF. This was done to check if these cells had clear symptoms of degradation, which would confirm the non-viability of the microalga. Changes in cell morphology can be clearly observed between healthy cells (Fig. 3.1.5a) and collapsed cells, which present invagination of the cell wall, a reduction of cell volume and an irregular morphology (Fig. 3.1.5b). Moreover, various pleomorphic cells, a rupture of the cell wall and intracytoplasmic membrane, and a retraction of the cytoplasm were viewed in the same growth conditions in ultrathin sections (Fig. 3.1.5c and 3.1.5d). According Kroemer et

al., (1995) and Naganuma (1996), the loss of membrane integrity is a late stage of the automortality process resulting in the total disintegration of the alga cell.

Effect of salt stress

The results related to PAF demonstrated that MIFs peaks (Chl *a*) decreased, mainly between 35 g L^{-1} and 75 g L^{-1}, while the concentrations of salinity increased from control culture to 100 g NaCl L^{-1}. In some cases, a displacement of the Chl *a* peak towards 684 nm (at 35 g L^{-1}) and 681 nm (at 75 g L^{-1} and 100 g L^{-1}) was produced. On the contrary, the *λscan* plots corresponding to NPAF showed irregulars curves with an evident plateau from 460 nm to 530 nm and a positive correlation between NPAF intensity and all the salinity doses (Fig. 3.1.6a).

The second experiment was performed at the same conditions mentioned above, but maintaining *Scenedesmus* sp. DE2009 cultures for 30 days. The Chl *a* peak at distinct salinities followed the same pattern as the obtained in the previous experiment, but in this case, the MIF peak was drastically reduced from 10 g NaCl L^{-1}. The NPAF also followed the same pattern as in the previous experiment (Fig. 3.1.6b).

However, in both experiments, the salt impact on photosynthetic pigments varied significantly according to the salinity doses assayed. Highly statistically significant differences on MIF ($P < 0.05$) were observed between control and all the NaCl concentrations tested, both at 7 days and at 30 days. The result also indicated that, in short periods of time (7 days) the differences were not statistically significant between the highest concentrations: 75 g L^{-1} and 100 g L^{-1}, while for long periods (30 days) the differences were significant and the MIF peak was not detected at the maximum concentration tested at 100 g L^{-1}. These results demonstrate that, at these high concentrations, there is a clear effect of salinity on *Scenedesmus* sp. DE2009 and this effect also increases with time.

Likewise, a viability assay applying the CLSM-DL method was carried to investigate the cell viability in response to varying salinities. The same *xyz* optical section is showed for PAF corresponding to living cells (Fig. 3.1.7a), for NPAF representing dead cells (Fig. 3.1.7b) and an overlap of both autofluorescence signals (Fig. 3.1.7c). The conversion of this data into relative frequency made it possible to observe that the percentage of viable cells decreased when the salinity doses increased.

Changes in viability for 7 days are shown in Figure 3.1.7d. These values showed high significant differences ($P < 0.05$) between the control and all the salinities tested, which indicate a negative effect of salt on the cellular viability of the microalga. However, at low salinity concentrations (10 g L^{-1} and 35 g L^{-1}) viable cells remained in high levels (81.73 % and 74.12 %, respectively). On the contrary, no statistically significant differences ($P < 0.05$) were found between the highest salinity doses (75 g L^{-1} and 100 g L^{-1}), and although the percentage of living cells decreased (57.39 % and 52.54 %, respectively), it remained still fairly high.

For 30 days of salinity exposure, high statistically significant differences ($P < 0.05$) were also found between the control and all the salinities tested, nevertheless the trend was different (Fig. 3.1.7e). In this case, viable cells decreased drastically from 10 g L^{-1} (79.24 %) to 100 g L^{-1} (8.27 %), corresponding to a reduction of 70.9 %, being the exposure time a very important variable to consider on cell viability. These results indicated that the salinity had a great influence on the percentage of living and dead Scenedesmus sp. DE2009 cells; although a small proportion of the community was still active.

Another important advantage to the application of the CLSM-DL method is that it allows characterising the distribution of distinct fluorescent signals within the microalga cells through 3D reconstructions. In Figure 3.1.8, it was observed that PAF and NPAF were distributed externally on *Scenedesmus* sp. DE2009 cells, which correspond to a

non-degraded and degraded pigment, respectively (Fig. 3.1.8a). Some of cells also presented NPAF externally and PAF internally, which correspond to an intermediate state of pigment degradation, probably due to a displacement and relocation of thylakoids within the cells (Fig. 3.1.8b and 3.1.1g).

3D easy projections also confirmed that the healthy cells (PAF) are very abundant in control cultures (Fig. 3.1.8c), whilst damaged cells (NPAF) are dominant in cultures exposed at the highest salinity (Fig. 3.1.8d). Other authors considered autofluorescence intensity as an indicator of integrity of the photosynthetic apparatus (Billi et al., 2011), whilst green autofluorescence was considered by Tang and Dobbs (2007) a common feature in diverse organisms and that its presence was independent of the cells physiological status. Nevertheless, we disagree with this last hypothesis, since NPAF was detected only in a few cells in control cultures. Moreover, a direct correlation was found between NPAF and non-viable cells, as demonstrated in light and salinity experiments.

Finally, in accordance with all the advantages described, the CLSM-DL method can be applied to assessing viability in other photosynthetic microorganism, whether these form aggregates or as individual cells. In addition, this method could be especially useful in characterising the physiological state of individual cells within microbial communities in extreme environments, in which dead and living cells coexist.

CONCLUSIONS

In conclusion, the newly developed CLSM-DL method can be providing data in short time consuming, *in vivo* and at cellular level without the need of either staining or additional use of image treating software. This technique can be useful to distinguish cultivable and non-cultivable phototrophic microorganisms, including those that form consortia with heterotrophic bacteria, since it rules out any interference with these microorganisms. The CLSM-DL method combined with the CLSM-*λscan* function confirms that there is a strong and good correlation of both the cells' physiological state and the performance of photosynthetic pigments with the percentages of individual living cells.

ACKNOWLEDGEMENTS

We express our thanks to the staff of the *Servei de Microscòpia* for technical assistance with the confocal and electron microscopes and the *Servei de Llengües,* both at the Universitat Autònoma de Barcelona. We also thank Eneko Mitxelena for his support on images digital processing and Marc Alamany, who provided valuable comments on the manuscript. Finally, we acknowledge Cristina Sosa for her help in this work.

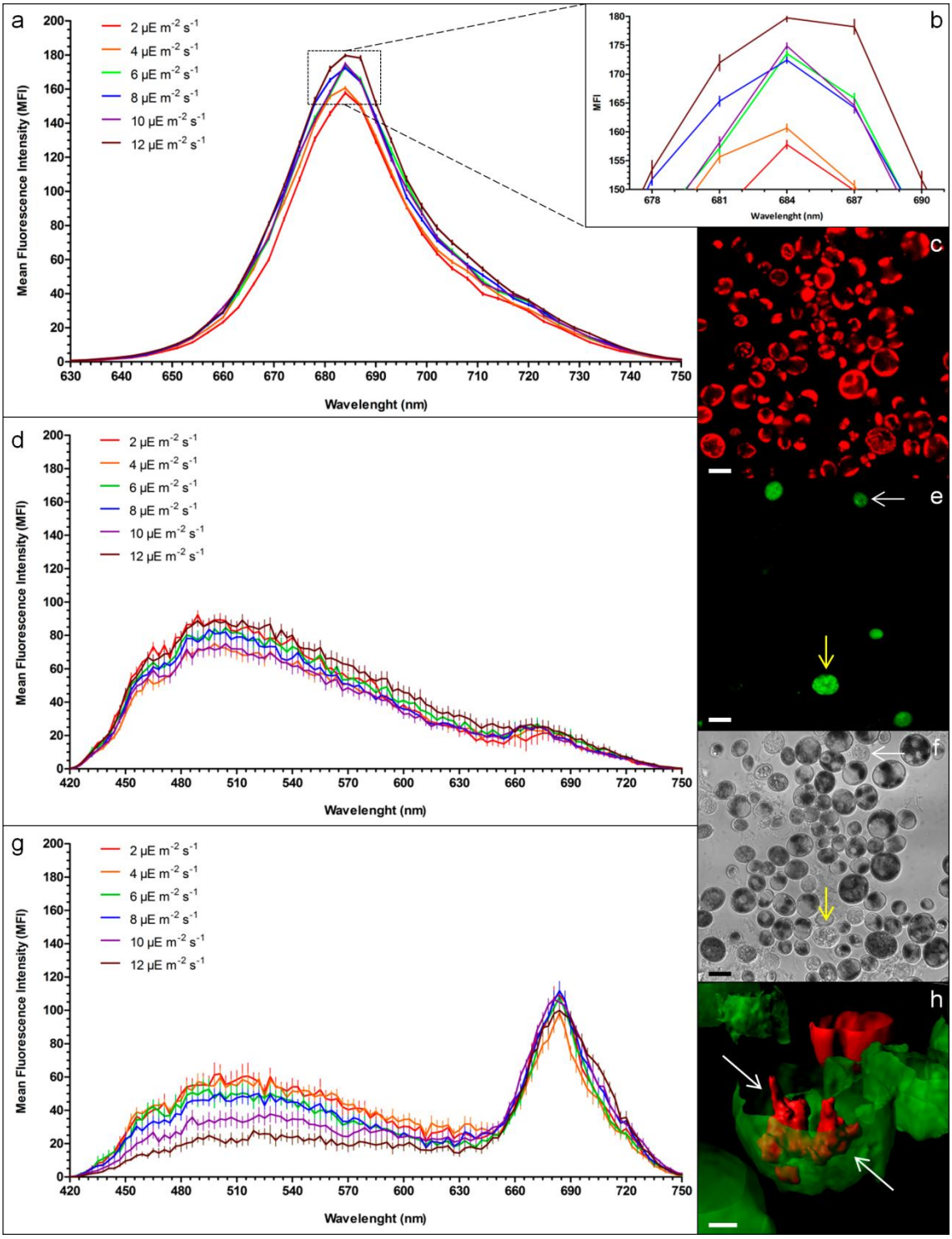

Figure 3.1.1. *λscan* plots of *Scenedesmus* sp. DE2009 cultures grown at different light intensities for 7 days. Spectral profiles corresponding to cells emitting PAF **(a)**. Detail of the emission peak at 684 nm for chlorophyll *a*, used as biomarker **(b)**. Spectral profiles corresponding to cells emitting NPAF (yellow arrows) **(d)**. Spectral profiles corresponding to an intermediate physiological stage of the cells (white arrows) **(g)**. 2D plots represent the MFI data ± SE: emission wavelength, *x* axis; MFI, *y* axis. CLSM images from the same *xyz* optical section of *Scenedesmus* sp. DE2009 grown at 12 μE m^{-2} s^{-1}: PAF emission **(c)**, NPAF emission **(e)** and bright-field micrograph **(f)**. Scale bars represent 10 μm. 3D reconstruction of *Scenedesmus* sp. cells **(h)**. Scale bar represents 2.5 μm.

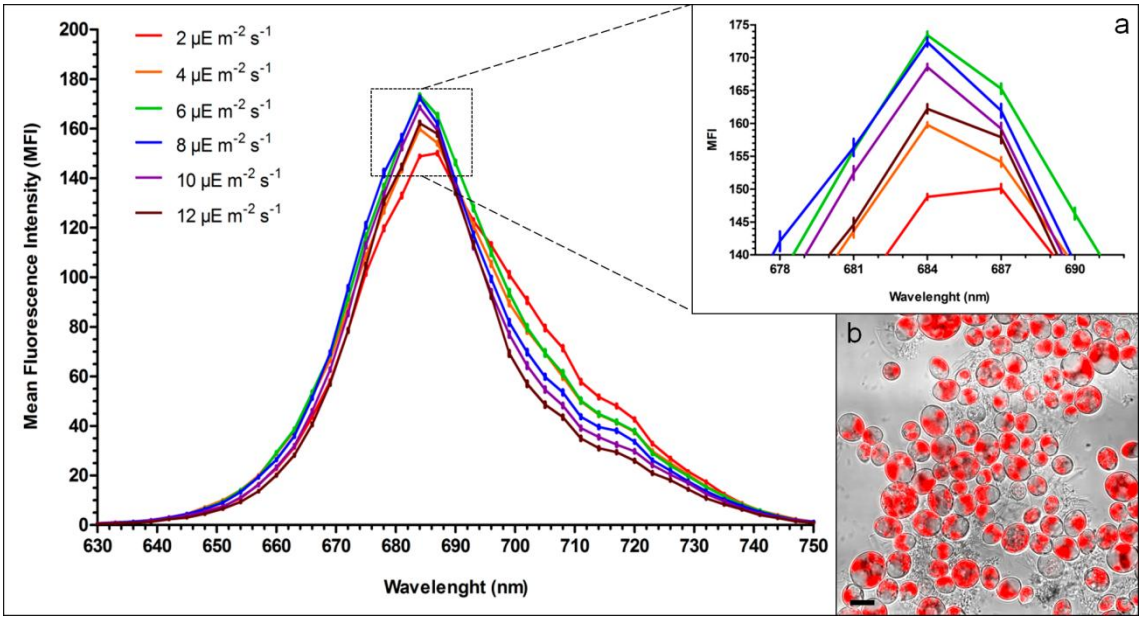

Figure 3.1.2. *λscan* plots of *Scenedesmus* sp. DE2009 cultures grown at different light intensities for 30 days. Spectral profiles corresponding to cells emitting PAF. Detail of the emission peak at 684 nm for chlorophyll *a*, used as biomarker **(a)**. 2D plots represent the MFI data ± SE: emission wavelength, *x* axis; MFI, *y* axis. Summa projection of PAF emission and bright-field microscopy of microalga sp. DE2009 grown at 8 μE m^{-2} s^{-1} **(b)**. Scale bars represent 10 μm.

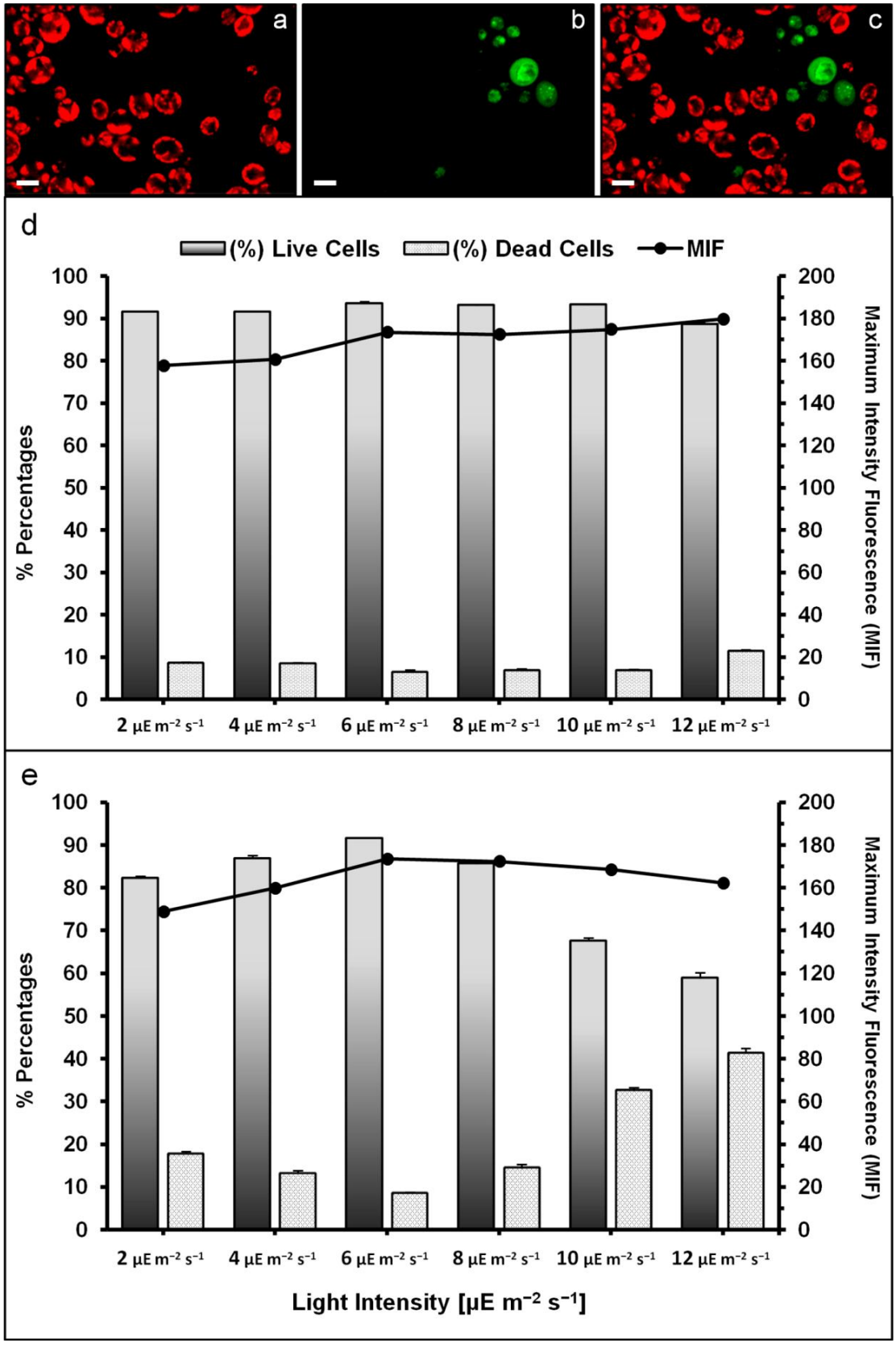

Figure 3.1.3. CLSM images from the same *xyz* optical section of *Scenedesmus* sp. DE2009 grown at 6 μE m^{-2} s^{-1}: PAF **(a)**, NPAF **(b)** and summa projection of both autofluorescence signals **(c)** Scale bars represent 10 μm. MIF and relative abundance of living and dead *Scenedesmus* sp. DE2009 cells at distinct light intensities (expressed as a percentage) for 7 days **(d)** and 30 days **(e)**. The bars indicate the standard error of the mean.

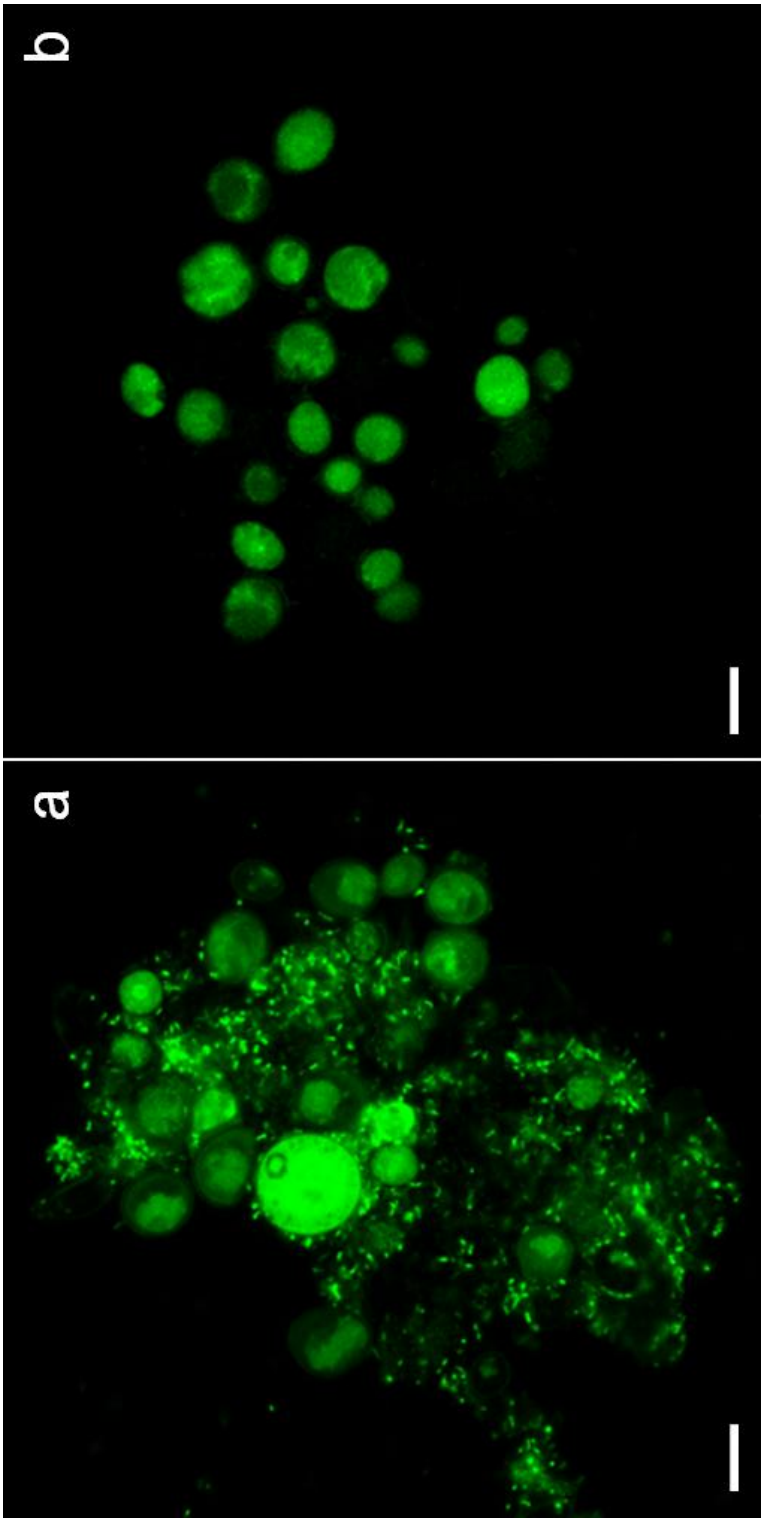

Figure 3.1.4. CLSM images of *Scenedesmus* sp. DE2009 grown at 6 μE m^{-2} s^{-1} and 100 g NaCl L^{-1} for 7 days. Cells stained by SYTOX Green nucleic acid fluorochrome **(a)** and cells emitting NPAF by CLSM-DL **(b)**. Scale bars represent 10 μm.

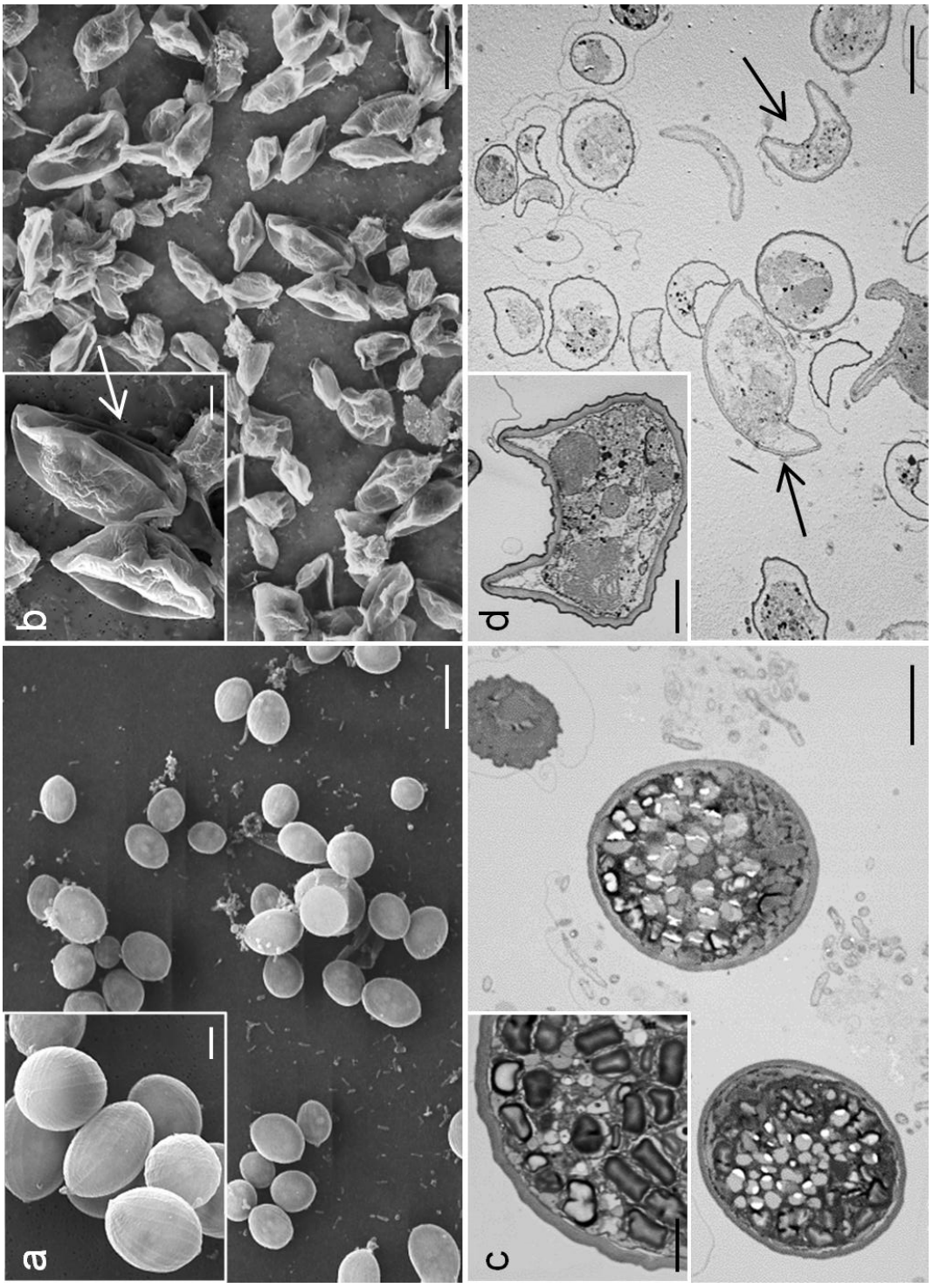

Figure 3.1.5. SEM micrographs of *Scenedesmus* sp. DE2009 grown at 6 μE m^{-2} s^{-1} for 7 days in control cultures **(a)** and in cultures grown at 100 g NaCl L^{-1} **(b)** (white arrow). Scale bars represent 10 μm (general) and 2 μm (close up images). Ultrathin sections of the same microorganism in control cultures **(c)** and in cultures grown at 100 g NaCl L^{-1} **(d)** (black arrows). Scale bars represent 5 μm (general) and 2 μm (close up images).

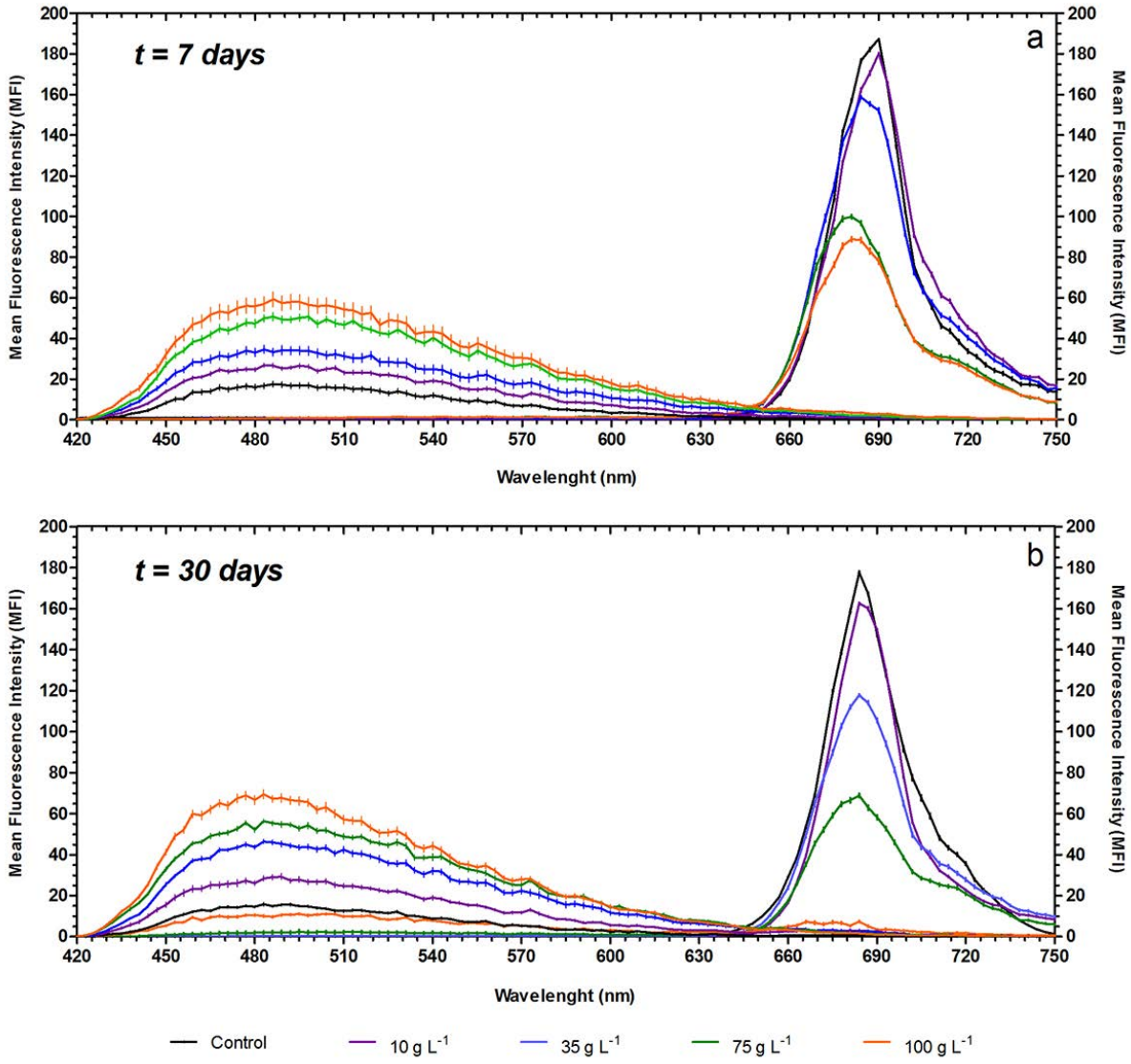

Figure 3.1.6. *λscan* plots of *Scenedesmus* sp. DE2009 cultures grown at different salinity doses during 7 days **(a)** and 30 days **(b)** Overlay of the spectral profiles corresponding to cells emitting PAF (living cells) and NPAF (dead cells). 2D plots represent the MFI data ± SE: emission wavelength, *x* axis; MFI, *y* axis.

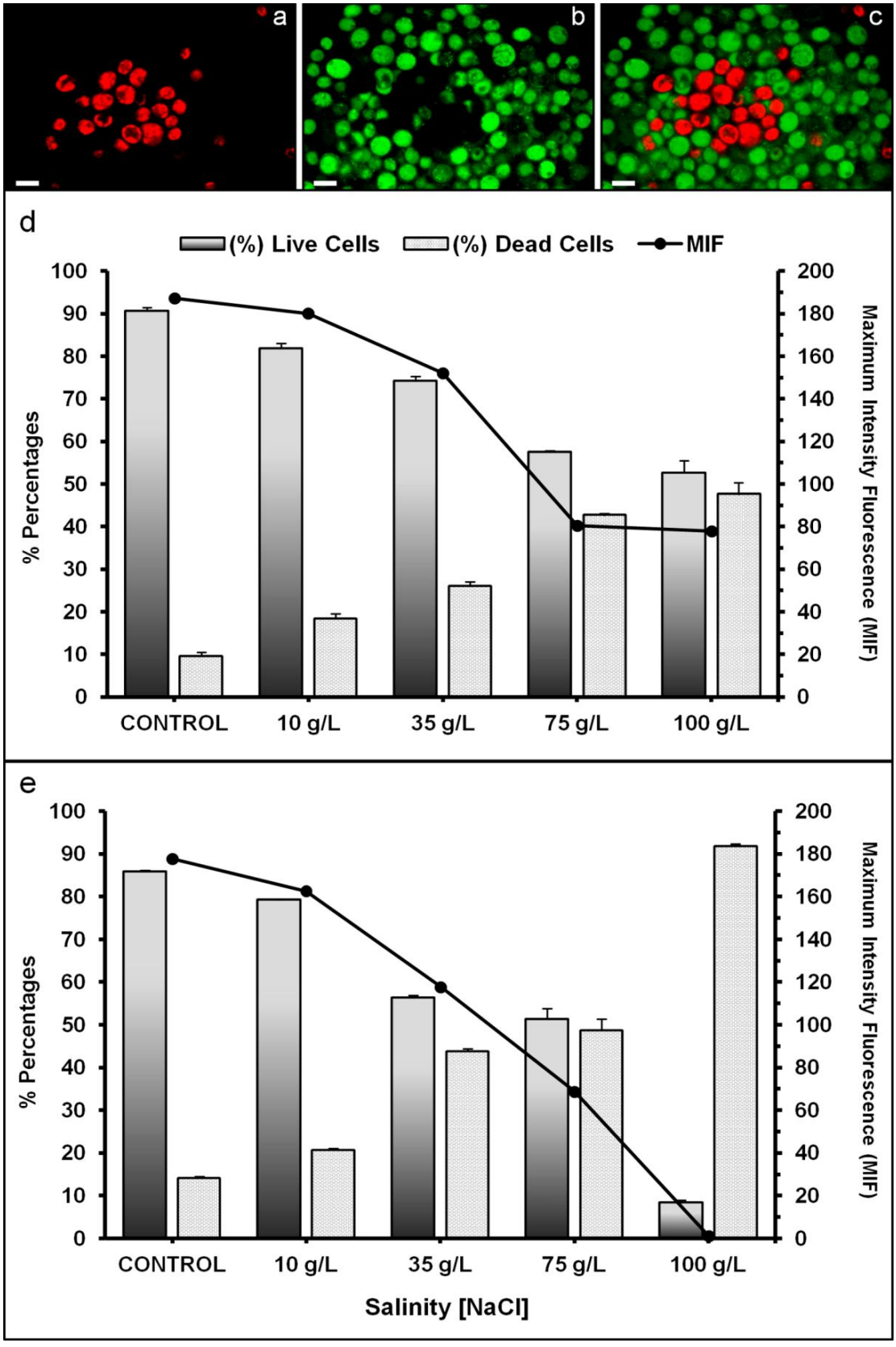

Figure 3.1.7. CLSM images from the same *xyz* optical section of *Scenedesmus* sp. DE2009 grown at 100 g NaCl L^{-1}: PAF **(a)**, NPAF **(b)** and summa projection of both autofluorescence signals **(c)** Scale bars represent 10 μm. MIF and relative abundance of living and dead *Scenedesmus* sp. DE2009 cells at distinct salinity doses (expressed as a percentage) for 7 days **(d)** and 30 days **(e)**. The bars indicate the standard error of mean.

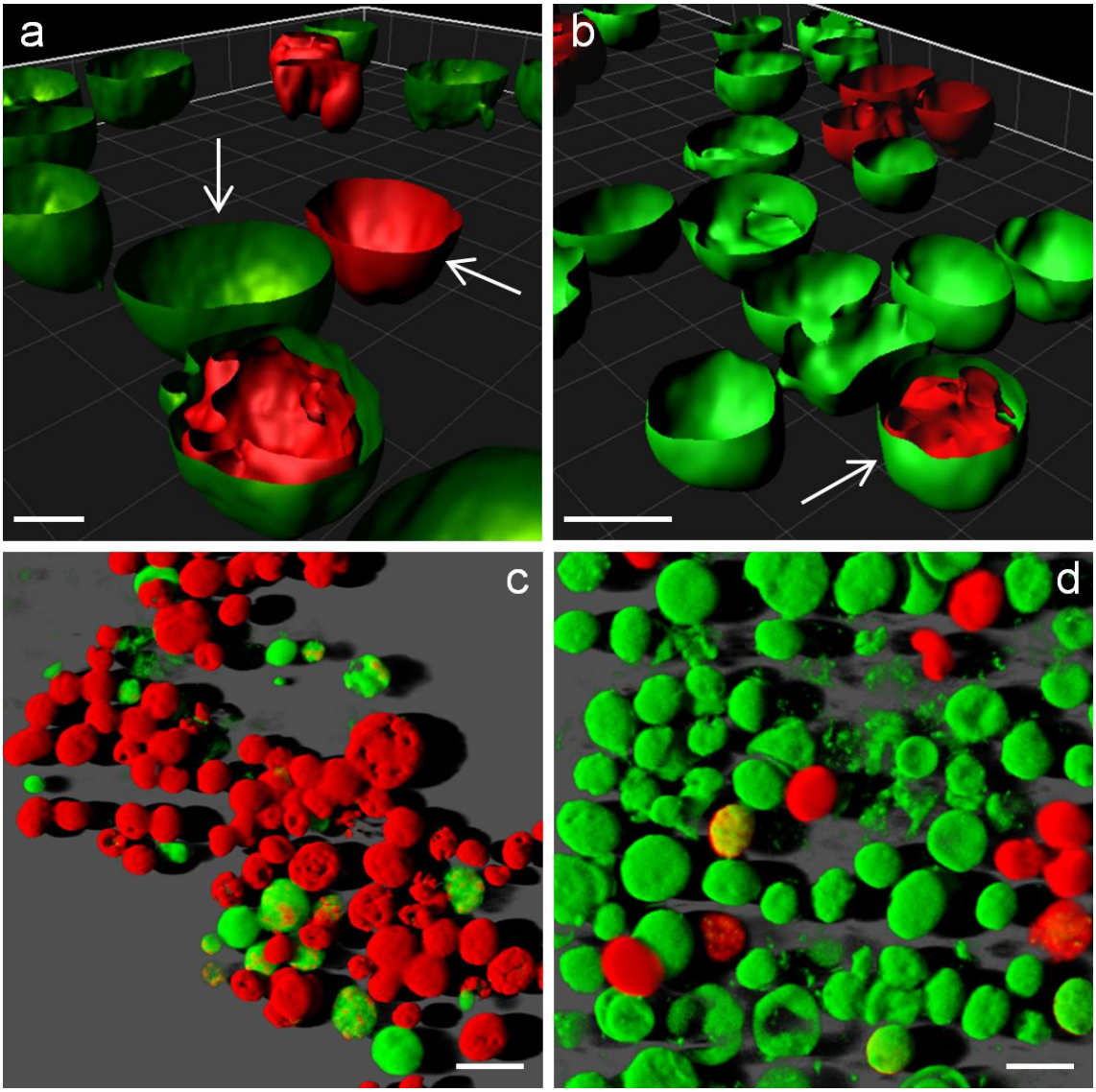

Figure 3.1.8. Red and green autofluorescence patterns observed for *Scenedesmus* sp. DE2009. 3D reconstructions of microalga cells at 75 g NaCl L^{-1} **(a)** and 100 g NaCl L^{-1} **(b)**. PAF and NPAF are indicated by arrows. Scale bars represent 5 μm. 3D easy projection for control culture **(c)** and 100 g NaCl L^{-1} **(d)**. Scale bars represent 10 μm.

REFERENCES

Al-Rubeai, M., Welzenbach, K., Lloyd, D.R., Emery, A.N. **(1997)** A rapid method for evaluation of cell number and viability by flow cytometry. *Cytotechnology*. 24, 161.

Antibus, D.E., Leff, L.G., Hall, B.L., Baeseman, J.L., Blackwood, C.B. **(2012)** Cultivable bacteria from ancient algal mats from the McMurdo Dry Valleys, Antarctica. *Extremophiles*. 16, 105-114.

Billi, D., Viaggiu, E., Cockell, C.S., Rabbow, E., Horneck, G., Onofri, S. **(2011)** Damage escape and repair in dried *Chroococcidiopsis* spp. from hot and cold deserts exposed to simulate space and Martian conditions. *Astrobiology*. 11, 65-73.

Büchel, C., Wilhelm, C. **(1993)** In vivo analysis of slow chlorophyll fluorescence induction kinetics in algae: progress, problems and perspectives. *Photochem. Photobiol.* 58, 137-148.

Buck, J. D. **(1979)** The plate count in aquatic microbiology, in: Costerton, J.W., Colwell, R.R. (Eds.), *Native aquatic bacteria: enumeration, activity, and ecology*. ASTM STP 695, Baltimore, pp. 19-28.

Burgos, A., Maldonado, J., de los Ríos, A., Solé, A., Esteve, I. **(2013)** Effect of copper and lead on two consortia of phototrophic microorganisms and their capacity to sequester metals. *Aquat. Toxicol.* 140-141, 324-336.

Cuadrado, D.G., Pan, J., Gómez, E.A., Maisano, L. **(2015)** Deformed microbial mat structures in a semiarid temperate coastal setting. *Sediment. Geol.* 325, 106-118.

de los Ríos, A., Ascaso, C., Wierzchos, J., Vicent, W.F., Quesada, A. **(2015)** Microstructure and cyanobacterial composition of microbial mats from the High Arctic. *Biodivers Conserv.* 24(4), 841-863.

Dorsey, J., Yentsch, C.M., Mayo, S., McKenna, C. **(1989)** Rapid analytical technique for the assessment of cell metabolic activity in marine microalgae. *Cytometry*. 10, 622-628.

Esteve, I., Ceballos, D., Martínez-Alonso, M., Gaju, N., Guerrero, R. **(1994)** Development of versicolored microbial mats: succession of microbial communities, in: Stal, L.J., Caumette, P. (Eds.), *Microbial mats: structure, development and environmental significance.* NATO ASI Series G: Ecological Sciences, Springer-Verlag, Berlin, Heidelberg, pp. 415-420.

Ferreira, V.S., Pinto, R.F., Sant'Anna, C. **(2016)** Low light intensity and nitrogen starvation modulate the chlorophyll content of *Scenedesmus dimorphus. J. Appl. Microbiol.* 120 (3), 661-70.

Garcia-Pichel, F., López-Cortés, A., Nübel, U. **(2001)** Phylogenetic and morphological diversity of cyanobacteria in soil desert crusts from Colorado plateau. *Appl. Environ. Microbiol.* 67 (4), 1902-1910.

Genty, B., Briantais, J.M., Baker, N.R. **(1989)** The relationship between the quantum yield of photosynthetic electron transport and quenching of chlorophyll fluorescence. *Biochim. Biophys. Acta.* 990, 87–92.

Green, S.J., Blackford, C., Bucki, P., Jahnke, L.L., Prufert-Bebbout, L. **(2008)** A salinity and sulfate manipulation of hypersaline microbial mats reveals stasis in the cyanobacterial community structure. *ISME J.* 2, 457-470.

Gregor, J., Maršálek, B. **(2004)** Freshwater phytoplankton quantification by chlorophyll *a*: a comparative study of in vitro, in vivo and in situ methods. *Water Res.* 38, 517-522.

Guerrero, R., Piqueras, M., Berlanga, M. **(2002)** Microbial mats and the search for minimal ecosystems. *Int. Microbiol.* 5, 177-188.

Hoffmann, D., Maldonado, J., Wojciechowski, M.F., Garcia-Pichel, F. **(2015)** Hydrogen export from intertidal cyanobacterial mats: sources, fluxes and the influence of community composition. *Environ. Microbiol.* 17(10), 3738-53.

Huot, Y., Babin, M. **(2011)** Overview of fluorescence protocols: theory, basic concepts and practice, in: Suggett, D.J., Prášil, O., Borowizka, M.A. (Eds.), *Chlorophyll a fluorescence in aquatic sciences: methods and applications*. Springer, Dordrecht, pp. 31-74.

Kroemer, G., Petit, P., Zamzami, N., Vayssière, J.L., Mignotte, B. **(1995)** The biochemistry of programmed cell death. *FASEB J.* 9, 1277-1287.

Lan, S., Wu, L., Zhang, D., Hu, C. **(2014)** Desiccation provides photosynthetic protection for crust cyanobacteria *Microcoleus vaginatus* from high temperature. *Physiol. Plant*. 152(2), 345-54.

Maldonado, J., de los Ríos, A., Esteve, I., Ascaso, C., Puyen, Z.M., Brambilla, C., Solé, A. **(2010b)** Sequestration and *in vivo* effect of lead on DE2009 microalga, using high-resolution microscopic techniques. *J. Hazard. Mater*. 183, 44-50.

Mehta, P., Jajoo, A., Mathur, S., Bharti, S. **(2010)** Chlorophyll *a* fluorescence study revealing effects of high salt stress on Photosystem II in wheat leaves. *Plant Physiol. Biochem*. 48, 16-20.

Millach, L., Solé, A., Esteve, I. **(2015)** Role of *Geitlerinema* sp. DE2011 and *Scenedesmus* sp. DE2009 as bioindicators and immobilizers of chromium in a contaminated natural environment. *Biomed Res. Int.* Vol. 2015, Article ID 519769, 11 pages.

Naganuma, T. **(1996)** Differential enumeration of intact and damaged marine planktonic bacteria based on cell membrane integrity. *J. Aquat. Ecosystem Health.* 5, 217-222.

Pal, S.W., Singh, N.K., Azam, K. **(2013)** Evaluation of relationship between light intensity (Lux) and growth of *Chaetoceros muelleri. Oceanography.* 1, 111.

Perkins, R.G., Oxborough, K., Hanlon, A.R.M., Underwood, G.J.C., Baker, N.R. **(2002)** Can chlorophyll fluorescence be used to estimate the rate of photosynthetic

electron transport within microphytobenthic biofilms? *Mar. Ecol. Prog. Ser.* 228, 47-56.

Pfennig, N., Trüpper, H.G. **(1992)** The family Chromatiaceae, in: Balows, A., Trüpper, H.G., Dworkin, M., Harder, W., Schleifer, K.H. (Eds.), *The Prokaryotes*, 2nd edn. Springer-Verlag, Berlin, pp. 3200-3221.

Pouneva, I. **(1997)** Evaluation of algal culture viability and physiological state by fluorescent microscopic methods. *Bulg. J. Plant Physiol.* 23(1-2), 67-76.

Rajeev, L., Nunes da Rocha, U., Klitgord, N., Luning, E.G., Fortney, J., Axen, S.D., et al., **(2013)** Dynamic cyanobacterial response to hydration and dehydration in a desert biological soil crust. *ISME J.* 7, 2178-2191.

Roldan, M., Thomas, F., Castel, S., Quesada, A., Hernandez-Marine, M. **(2004)** Noninvasive pigment identification in single cells from living phototrophic biofilms by confocal imaging spectrofluorometry. *Appl. Environ. Microbiol.* 70, 3745-3750.

Sato, M., Murata, Y., Mizusawa, M., Iwahashi, H., Oka, S. **(2004)** A simple and rapid dual-fluorescence viability assay for microalgae. *Microbiol. Cult. Coll.* 20, 53-59.

Schreiber, U. **(1998)** Chlorophyll fluorescence: new instruments for special applications, in: Garag, G. (Eds.), *Photosynthesis: Mechanisms and Effects*. Kluwer Academic Publishers, Dordrecht, Vol. V, pp. 4253-4258.

Solé, A., Diestra, E., Esteve, I. **(2009)** Confocal Laser Scanning Microscopy Image Analysis for Cyanobacterial Biomass Determined at Microscale Level in Different Microbial Mats. *Microb. Ecol.* 57, 649-656.

Tang, Y.Z., Dobbs, F.C. **(2007)** Green autofluorescence in dinoflagellates, diatoms and other microalgae and its implications for vital staining and morphological studies. *Appl. Environ. Microbiol.* 73(7), 2306-2313.

Veldhuis, M.J.W., Kraay, G.W., Timmermans, K.R. **(2001)** Cell death in phytoplankton: correlation between changes in membrane permeability, photosynthetic activity, pigmentation and growth. *Eur. J. Phycol.* 36, 167-177.

Wagenen, J.V., Holdt, S.L., Francisci, D.D., Valverde-Perez, B., Plósz, B.G., Angelidaki, I. **(2014)** Microplate-based method for high-throughput screening of microalgae growth potential. *Bioresour. Technol.* 169, 566-572.

Role of *Geitlerinema* sp. DE2011 and *Scenedesmus* sp. DE2009 as Bioindicators and Immobilizers of Chromium in a Contaminated Natural Environment

Laia Millach, Antonio Solé, and Isabel Esteve

Departament de Genètica i Microbiologia, Facultat de Biociències, Universitat Autònoma de Barcelona, Bellaterra, 08193, Barcelona, Spain.

ABSTRACT

The aim of this work was to study the potential of the two phototrophic microorganisms, both isolated from Ebro Delta microbial mats, to be used as bioindicators and immobilizers of chromium. The results obtained indicated that (i) the Minimum Metal Concentration (MMC) significantly affecting Chlorophyll *a* intensity in *Geitlerinema* sp. DE2011 and *Scenedesmus* sp. DE2009 was 0.25 μM and 0.75 μM respectively, these values being lower than those established by current legislation, and (ii) *Scenedesmus* sp. DE2009 was able to immobilize chromium externally in extracellular polymeric substances (EPS) and intracellularly in polyphosphate (PP) inclusions. Additionally, this microorganism maintained high viability, including at 500 μM. Based on these results, we postulate that *Geitlerinema* sp. DE2011 and *Scenedesmus* sp. DE2009 are good chromium-indicators of cytotoxicity and, further, that *Scenedesmus* sp. DE2009 plays an important role in immobilizing this metal in a contaminated natural environment.

INTRODUCTION

Metal contamination is a serious environmental problem that affects life forms and changes the natural microbiota of aquatic ecosystems. Currently, metals are released from natural and anthropogenic sources (e.g. industry, transport, fossil fuel combustion, the mining industry and agriculture) into natural aquatic environments (Nogales et al., 2011). These metals are accumulated in waters, sediments and biota, generating resistance in microorganisms that leads to environmental and public health problems. To study and predict the effects and removal of heavy metals on different ecosystems: nematode (Šalamún et al., 2014), plants (Chang et al., 2014) and algae (Magdaleno et al., 2014) among others, have been used. Cyanobacteria and algae are particularly very abundant in aquatic ecosystems, playing an important role in primary production in rivers and their deltas, where metals very often accumulate.

The Ebro River is 928 km long, flows from the north of the Iberian Peninsula to the Mediterranean Sea and drains an area of 85,000 km^2 approximately. The Ebro Delta, located at the outfall of the Ebro River, is the second most important wetland in Spain after Guadalquivir River marshes and the second of the Mediterranean area after the Camargue (France). The Ebro Delta is also considered, the third largest delta in the Mediterranean with a 320 km^2 triangular surface and it's located at the north-eastern coastline of the Iberian Peninsula (0°35'E–0°56'E; 40°33'N–40°47'N) (Guerrero et al., 2002). In 1983, some of the most outstanding natural areas of the delta were included in the Ebro Delta Natural Park (*Parc Natural del Delta de l'Ebre*) because of its ornithological importance, as well as for other geological, biological, economic and cultural aspects (Mañosa et al., 2001).

Microbial mats, developed in water-sediment interfaces, are formed by multilayered benthic microbial communities that are distributed along vertical micro-gradients of different physical-chemical parameters. These ecosystems are widely

distributed around the world in different extreme environments, such as lakes (Cole et al., 2014), marine waters (Hoffman et al., 2015) and cold waters (Antibus et al., 2012), among others. Ebro Delta microbial mats are formed by different microorganisms, principally cyanobacteria and microalgae are the most abundant prokaryotic bacteria located mainly in the upper layers of microbial mats (Esteve et al., 1994). These microbial mats receive waters and contaminants, including heavy metals dragged by the River Ebro into its estuary (delta). For this reason, in the last few years, our work group has isolated various microorganisms of this ecosystem and have developed several methods, in particular Confocal Laser Scanning Microscopy (CLSM), to determine their capacity to tolerate or resist metals, as well as to evaluate the effect of these *in vivo* both at cell and population level. These methods used for the *in vivo* study of phototrophic microorganisms have led to obtaining quantitative results more quickly. This is mainly due to the minimal necessary manipulation of the specimens, and as since these emit natural fluorescence, they do not require staining protocols. Furthermore, the majority of works have evaluated the effect of lead and copper toxicity in isolated microorganisms (Seder-Colomina et al., 2013) and the capacity of various microorganisms to uptake these metals extra- and/or intracellularly using Scanning Electron Microscopy (SEM) and Transmission Electron Microscopy (TEM), both coupled to an Energy Dispersive X-ray (SEM-EDX and TEM-EDX) (Maldonado et al., 2010b).

However, the role that microorganisms play in this same habitat on chromium detoxification is still unknown. Chromium can exist in the environment as Cr(III) or Cr(VI) (Rai et al., 1989; Gómez and Callao, 2006) and particularly, in the Cr(VI) form is extremely toxic, mutagenic and carcinogenic. In the environment, as occurs in Ebro Delta microbial mats, is introduced as the by-product of industries (Manahan, 2009) and phosphate fertilizers (Nziguheba and Smolders, 2008), being the reduction of Cr(VI) to Cr(III) an effective method of detoxification of Cr(VI) in highly contaminated habitats (Faisal and Hasnain, 2004; Sultan and Hasnain, 2007). Nevertheless, the

immobilization efficiency of Cr(III) is still unclear and different reports suggest that soluble organo-Cr(III) complexes are present in various chromate-reducing bacterial systems (Puzon et al., 2002; 2008). The permanence of soluble forms of Cr(III) causes a serious problem, since they can be re-oxidized to Cr(VI). It is for this reason there is great interest in studying the immobilization of Cr(III) in pilot-scale experiments (Cheng et al., 2010).

Nowadays, there is little information on this process in the natural environment, where the levels of contamination by chromium are very low, as in the River Ebro (< 2 μg L^{-1} Cr, according to data from the Ebro Hydrographic Association, in the last 10 years). In these cases, although the same probably occurs, the Cr(VI) is biotransformed to Cr(III), this can remain in ecosystems, immobilized or not, and could have a toxic effect on life forms. Likewise, very little is known about the role of indigenous microorganisms in these natural environments with low levels of chromium and also with a prolonged permanence of the metal in the ecosystem.

The aim of this work is to determine the role of *Geitlerinema* sp. DE2011 and *Scenedesmus* sp. DE2009, both isolated from Ebro Delta microbial mats, as bioindicators and immobilizers of chromium and, additionally, to analyze the effect of this metal on their biomass and cellular viability.

MATERIAL AND METHODS

Microorganisms and culture conditions

Geitlerinema sp. DE2011 (cyanobacterium) and *Scenedesmus* sp. DE2009 (microalga) were isolated from Ebro Delta microbial mats (Tarragona), Spain. Isolation and purification of the isolates were performed by dilution and plating of microbial mats samples. Isolated microorganisms were grown in liquid mineral Pfennig medium (Pfenning and Trüpper, 1992) in 100 mL flasks. Cultures were exposed and maintained at 27 °C in a growth chamber (Climas Grow 180, ClimasLab, Barcelona) under continuous illumination with a light intensity of 3.5 μE $m^{-2} s^{-1}$ for the cyanobacterium and 10 μE $m^{-2} s^{-1}$ for the microalga, provided by cold white fluorescence lights. These cultures were used as control in all the experiments performed.

Preparation of chromium stock solution

The stock solution of chromium was prepared by dissolving $Cr(NO_3)_3$ (Sigma-Aldrich, Bellefonte, PA, US) in deionized Milli-Q water at the concentration of 1 mM Cr(III) and sterilized by filtration in Millex-GP 0.2 μm filters (Millipore, USA). Working concentrations of Cr(III) were obtained by serial dilution. This solution was stored in the dark at 4 °C.

Pigment analysis of the strains using confocal laser scanning microscopy

The tolerance and the *in vivo* effect of chromium on cultures of *Geitlerinema* sp. DE2011 and *Scenedesmus* sp. DE2009 were determined by *λscan* function of CLSM (CLSM Leica TCS SP5; Leica Heidelberg, Germany). Moreover, in order to evaluate the effect of chromium on the biomass and viability of *Scenedesmus* sp. DE2009, a modification of the FLU-CLSM-IA (Fluorochrome-CLSM-Image Analysis) method described by Puyen et al., (2012a) was used.

λscan function

Cultures of *Geitlerinema* sp. DE2011 and *Scenedesmus* sp. DE2009 were contaminated at different $Cr(NO_3)_3$ concentrations: 0.025, 0.050, 0.1, 0.25, 0.50, 0.75, 1, 5 μM for the cyanobacterium DE2011 and 0.25, 0.50, 0.75, 1, 5, 10, 15 and 25 μM for the microalga DE2009. All experiments were performed for 9 days under the same conditions mentioned in Section 2.4.

Pigment analysis was realized by the *λscan* function of CLSM. This technique provides information on the state of the photosynthetic pigments of phototrophic microorganisms on the basis of the emission wavelength region and the fluorescence intensity emitted (autofluorescence). Each image sequence was obtained by scanning the same *xy* optical section throughout the visible spectrum. Images were acquired at the *z* position at which the fluorescence was maximal, and acquisition settings were constant throughout each experiment. The sample excitation was carried out with an Argon Laser at 488 nm (λexe 488) with a λ step size of 3 nm for an emission wavelength between 550 and 748 nm.

In order to measure the Mean Fluorescence Intensity (MFI) of the *xyλ* data sets, the Leica Confocal Software (Leica Microsystems CMS GmbH) was used. In these confocal images the pseudo-colour palette 4 was selected, where warm colours represented the maximum intensities and cold colours represented the low intensities of fluorescence. The regions-of-interest (ROIs) function of the software was used to measure the spectral signature. For each sample, 70 ROIs of 1 μm^2 taken from cells were analyzed.

This method allowed us to evaluate the physiological state of the phototrophic microorganisms at single-cell level, considering changes in the spectrum of Chlorophyll *a* (Chl *a*) used as a marker. For this purpose, the state of pigments was considered by

means of the Maximum Intensity Fluorescence (MIF) signal detected at: 661 nm (Chl *a*) for *Geitlerinema* sp. DE2011 and 685 nm for *Scenedesmus* sp. DE2009 (Chl *a*).

FLU-CLSM-IA modified method

To determine the effect of chromium on biomass and cellular viability of *Scenedesmus* sp. DE2009 cultures, experiments at different $Cr(NO_3)_3$ concentrations: 0.75, 25, 100, 200 and 500 µM were performed for a period of 9 days under the same conditions mentioned in Section 2.4 following a modification of the FLU-CLSM-IA method (Puyen et al., 2012a). This method combines the use of: specific fluorochrome, the CLSM microscope and the *ImageJ v1.48s* software.

In this study, *Scenedesmus* sp. DE2009 autofluorescence (emission at 616-695 nm) and SYTOX Green Nucleic Acid Stain fluorescence (emission at 520–580 nm; Invitrogen, Life Technologies) were used simultaneously as markers for live and dead cells, respectively, in a simple dual-fluorescence viability assay (Sato et al., 2004). Both, the red and green fluorescence signals, were captured separately in a *sequential scan* process in two channels from each same *xyz* optical section (Fig. 3.2.1a and 3.2.1c).

In order to differentiate between living and dead cells, red (living cells) and green (dead cells) pseudocolors were used and 20 red and green confocal images were acquired from every culture of *Scenedesmus* sp. DE2009 to determine the biomass and cellular viability at each Cr-concentration.

The CLSM images were transformed to binary images (black/white) applying fluorescence threshold values of 30 (red pixels) and 35 (green pixels) by means the *ImageJ v1.48s* software (Fig. 3.2.1b and 3.2.1d). To minimize the background detected in every pair of images a smoothing filter was used.

To obtain bio-volume values, the Voxel Counter plug-in was applied to these filtered images (Rasband, 2014). This specific application calculates the ratio between the thresholded voxels (red and green fluorescent voxel counts) to all voxels from every binary image analyzed. The bio-volume value (Volume Fraction) was finally multiplied by a conversion factor of 310 fgC μm^3 to convert it to biomass (Fry, 1990).

Ascertaining chromium immobilization through electronic microscopy techniques

With the aim of determining whether *Geitlerinema* sp. DE2011 and *Scenedesmus* sp. DE2009 could immobilize metals extra- and intracellularly, cells from cultures growing with and without chromium were analyzed by EDX coupled to SEM and TEM.

Scanning electron microscopy and energy dispersive X-ray analysis

Phototrophic microorganisms cultures were contaminated at different $Cr(NO_3)_3$ concentrations: 1, 5, 10, 25, 50, 100, 200 μM Cr(III) and incubated under the same conditions as mentioned above for a period of 9 days.

For SEM analysis, cultures were filtrated in Nucleopore™ polycarbonate membranes (Whatman, Ltd.) and then were fixed in 2.5% glutaraldehyde diluted in Millonig phosphate buffer (0.1 M pH 4) at 4 °C for 2 hours and washed four times in the same buffer, dehydrated in increasing concentrations of ethanol (30, 50, 70, 90 and 100 %) and dried by critical-point (CPD 030 Critical Point Drier, BAL-TEC GmbH D – 58579 Schalksmühle). Finally, samples were mounted on aluminium metal stubs and coated with a 5 μm gold layer (K550 Sputter Coater, Emitech, Ashford, UK) for better image contrast. A Zeiss EVO®MA 10 scanning electron microscope (Carl Zeiss NTS GmbH, Oberkochen, Germany) was used to view the images.

For EDX microanalysis, cells were homogenously distributed and filtered on polycarbonate membrane filters. These filters were fixed, dehydrated and dried by critical-point drying and then coated with gold. An EDX spectrophotometer Link Isis-200 (Oxford Instruments, Bucks, England) coupled to the microscope operating at 20 kV was used. Finally, EDX-SEM spectra from individual cells were obtained.

Transmission electron microscopy and energy dispersive X-ray analysis

TEM was used in order to observe the ultrastructure of the phototrophic microorganisms and TEM-EDX to assess whether *Geitlerinema* sp. DE2011 and *Scenedesmus* sp. DE2009 were able to bioaccumulate chromium intracellularly. So, cyanobacterium DE2011 and the microalga DE2009 were contaminated with 200 μM $Cr(NO_3)_3$ for a period of 9 days. Culture conditions were the same as described for SEM.

For TEM analysis, samples were fixed in 2.5% glutaraldehyde diluted in Millonig phosphate buffer (0.1 M pH 4) at 4 °C for 2 hours and washed four times (15 min) in the same buffer at 4 °C. Then samples were post-fixed in 1% OsO_4 at 4 °C for 2 hours, washed in the same buffer and centrifuged in order to obtain a pellet. They were then dehydrated in a graded series of acetone (50, 70, 90, 95 and 100 %) and embedded in Spurr's resin. Once the samples were included in the resin, ultrathin sections (70 nm), obtained with a Leica EM UC6 Ultramicrotome (Leica Microsystems, GmbH, Heidelberg, Germany), were mounted on carbon-coated titanium grids and stained with uranyl acetate and lead citrate. Samples were viewed in a Hitachi H-7000 transmission electron microscope (Hitachi Ltd., Tokyo, Japan).

For EDX microanalysis, sections of 200 nm thick were also stained with uranyl acetate and mounted on carbon-coated titanium grids. Samples were analyzed with an EDX spectrophotometer Link Isis-200 (Oxford Instruments, Bucks, England) coupled to a Jeol Jem-2011 (Jeol Ltd., Tokyo, Japan) operating at 20 kV. Finally, EDX-TEM spectra from individual cells were obtained.

Statistical analysis

Statistical analyzes were carried out by one-way analysis of variance (ANOVA) and Tukey and Bonferroni's comparison *post hoc* tests. Significant differences were accepted at $p < 0.05$. The analyzes were performed using IBM SPSS Statistics software (version 20.0 for Windows 7).

RESULTS AND DISCUSSION

Morphological characteristics of *Geitlerinema* sp. DE2011 and *Scenedesmus* sp. DE2009

The phototrophic microorganisms, isolated from Ebro Delta microbial mats, were identified as *Geitlerinema* sp. DE2011 (Burgos et al., 2013) and *Scenedesmus* sp. DE2009 (Maldonado et al., 2010b) by molecular biology methods. Both microorganisms are very abundant in Ebro Delta microbial mats and play an important role in the stabilization of deltaic sediments.

Geitlerinema sp. DE2011 is a cyanobacterium, which forms individual filaments, sometimes densely packed and surrounded by a sheath. Cells from filaments vary in size from 3.13 to 3.75 μm. On the other hand, *Scenedesmus* sp. DE2009 is a microalga, which like *Geitlerinema* sp. DE2011 forms a consortium with different heterotrophic bacteria. The microalga cells are spherical, with a diameter of 7-9 μm and its chloroplasts are distributed laterally in the cell.

Chromium tolerance in phototrophic microorganisms

In order to calculate the Minimum Metal Concentration (MMC) that significantly affects pigment intensity in *Geitlerinema* sp. DE2011 and *Scenedesmus* sp. DE2009, two experiments were performed. In the preliminary experiment, a wide range of chromium concentrations was assayed. Displacement of the fluorescence peak was observed only in *Geitlerinema* sp. DE2015 from 661 nm (MIF) towards to 670 nm, at maximum Cr-concentration assayed (5 μM fluorescence spectrum). In both cases, highly statistically significant differences ($P < 0.05$) were found between the control and all the concentration tested (Fig. 3.2.2a and 3.2.2b).

For this reason, a second experiment was carried out on *Geitlerinema* sp. DE2011 with lower doses from 25 nM to 0.75 μM Cr(III). The *xyz* optical sections of this microorganism, corresponding to the autofluorescence detected in control and contaminated cultures were shown in Figures 3.2.3a and 3.2.3b. The results indicated that the MMC of chromium (when compared with the control) that significantly ($P < 0.05$) affected the intensity of the pigment (Chl *a*) of *Geitlerinema* sp. DE2011 was 0.25 μM Cr. An analogous experiment to that mentioned above was performed with lower doses from 0.25 μM to 5 μM Cr(III) on cultures of *Scenedesmus* sp. DE2009. The autofluorescence detected in control and contaminated cultures was shown in Figures 3.2.4a and 3.2.4b. In this case, the MMC that significantly ($P < 0.05$) affected the intensity of the pigment in *Scenedesmus* sp. DE2009 was 0.75 μM Cr, and therefore, this microorganism was more tolerant to chromium than *Geitlerinema* sp. DE2011 (0.25 μM Cr).

On the other hand, the *λscan* plots graphs of both microorganisms indicated how the MIF peak (Chl *a*) decreased while the Cr-concentration increased following mainly the same pattern as the control culture (Fig. 3.2.3c and 3.2.4c). This results are in agreement with those obtained by different authors, which demonstrated in

Scenedesmus obliquus and *Nostoc muscorum* respectively, that metal stress results in direct inactivation of the photosystem II (PS II) reaction center and consequently, a decrease of chlorophyll *a* fluorescence intensity (F_{685}) (Mallick and Mohn, 2003; Prasad et al., 1991). Furthermore, other authors have demonstrated that in response to varying physical-chemical parameters, photosynthetic microorganisms undergo changes in their physiological characteristics, mainly changing the quality and concentration of their light-harvesting pigments (Roldán et al., 2014).

It is worth highlighting that the MMC values obtained were below the level permitted in continental surface waters (50 μg L^{-1} Cr) (in accordance with the Directive 2008/105/CE of the European Parliament and the Council on Environmental Quality Standards in the field of Water Policy, transposed into Spanish law "Real Decreto 60/2011, Anexo II"), which demonstrated that both microorganisms should be considered as good indicators of cytotoxicity.

Metal immobilization in phototrophic microorganisms

Cr-contaminated cultures of *Geitlerinema* sp. DE2011 were analyzed by SEM-EDX and chromium was not detected in the extracellular polymeric substances (EPS) (Fig. 3.2.3d, 3.2.3e and 3.2.3f). Nevertheless, in the contaminated samples of *Scenedesmus* sp. DE2009, the results confirmed that the microalga had the ability to sequester chromium in the EPS (Fig. 3.2.4d, 3.2.4e and 3.2.4f). Different parts of the filter were also tested as a control in all samples, to be sure that chromium was retained only in cells.

Both microorganisms have dense EPS envelopes, which explain the external uptake of heavy metals. Various authors have suggested that the overall negative charge of EPS may be essential for sequestering metal cations that are necessary for cell growth but present at low concentrations in their surroundings, and/or preventing the direct

contact between the cells and toxic heavy metals dispersed in the environment (Pereira et al., 2011). The functions of EPS in metal uptake are known, but other roles have been proposed for these polymers, such as protection against dehydration or UV radiation, biomineralization, phagocytosis and adhesion capacity to the surrounding substrate (De Philippis et al., 2003).

Although *Geitlerinema* sp. DE2011 gave a negative result for chromium uptake, in previous studies it has been shown that this cyanobacterium was able to capture lead and copper extracellularly (Burgos et al., 2013). These differences in metal immobilization were probably due to the fact that the same microorganism can capture distinct metals using different functional groups in the EPS. In accordance with studies carried out by Ozturk et al., (2014) an increase in uronic acid, glucuronic acid and galacturonic acid content was shown in the EPS of *Synechocystis* sp. BASO671 cultures contaminated by chromium. In addition, Çelekli et al., (2013) also confirmed that specific anionic groups played a significant role in the biosorption of Cd^{2+} by *Scenedesmus quadricauda* var. *longispina.*

On the other hand, TEM micrographs of the ultrathin sections of *Geitlerinema* sp. DE2011 and *Scenedesmus* sp. DE2009 growing at 200 μM Cr showed abundant high electrondense intracytoplasmic inclusions of different sizes in its cytoplasm identified as polyphosphate inclusions (PP) (Figs. 3.2.3h and 3.2.4h). In many cases, similar inclusions have been found when cells are grown in adverse culture conditions (Jensen and Sicko, 1974). Chromium was not detected internally in *Geitlerinema* sp. DE2011 or *Scenedesmus* sp. DE2009 in control cultures (Figs. 3.2.3g and 3.2.4g).

The results obtained through EDX analysis of the inclusions demonstrated that *Geitlerinema* sp. DE2011 did not have the capacity to accumulate chromium as no Cr peak was detected (Fig. 3.2.3i). In contrast to this, a significant Cr peak was detected in *Scenedesmus* sp. DE2009, demonstrating that this microorganism was able to

immobilize this metal internally in PP inclusions (Fig. 3.2.4i). These results agree with studies of Goldberg et al., (2001), which suggested that this kind of inclusions has a detoxifying effect and a large affinity by sequestering heavy metals. In general, algae seem to be more effective than cyanobacteria in capturing heavy metals (Zhou et al., 2012; Kováčik et al., 2015) and, as has been shown in this work, *Scenedesmus* sp. DE2009, due to its ability to capture chromium both extra and intra-cellularly, probably it plays an important role in chromium detoxification in Ebro delta microbial mats.

Effect of chromium on biomass and cellular viability of *Scenedesmus* sp. DE2009

For this objective, previously, the red and green fluorescent voxels counts were measured as mentioned in Section 2.7.1. The red voxels (living cells) ranged from 162097 ± 9220 (control experiment) to 143390 ± 6638 (at 500 μM) and the green voxels (dead cells) varied from 23450 ± 1822 (control experiment) to 32113 ± 2277 (at 500 μM). The conversion of this data into biomass values made it possible to observe that the live biomass slightly decreased from 47.92 ± 2.73 mgC cm^{-3} in the control culture to 42.39 ± 1.96 mgC cm^{-3} at 500 μM Cr.

The changes in viability were shown in Figure 3.2.5. These results were expressed as the percentages (%) of living cells and dead cells for each contaminated culture. These values showed low significant differences ($P < 0.05$) for all of them compared to the control culture, which indicated a slight effect of the metal in the viability of *Scenedesmus* sp. DE2009. However, there were no significant differences ($P < 0.05$) between the various concentrations tested, with the percentage of viable cells in all the Cr-concentrations tested remaining stable.

Thus, on comparing the growth of *Scenedesmus* sp. DE2009 in control culture and the maximum tested concentration (500 μM), it was observed that in the control experiment living cells represented 87.19 % and dead cells 12.81 %, and in the

contaminated culture living cells represented 81.61 % and dead cells 18.39 % (Fig. 3.2.5). These results confirmed that a high level of viability of the microalga is maintained, even at the highest concentration of chromium tested.

CONCLUSIONS

The results obtained in this paper lead to the conclusion that, *Scenedesmus* sp. DE2009 is more tolerant to chromium than *Geitlerinema* sp. DE2011 and that both microorganisms could be considered as good indicators of chromium toxicity in low contaminated natural ecosystems. On the other hand, *Scenedesmus* sp. DE2009 maintains an elevated biomass and viability at high Cr-concentrations and also has the ability to capture chromium extracellularly in EPS and intracellularly in PP inclusions, which demonstrates its capacity to immobilize this metal.

ACKNOWLEDGEMENTS

This research was supported by the following grants: DGICYT (CGL2008-01891/BOS) and the UAB postgraduate scholarship to Laia Millach. We express our acknowledgment to the staff of the *Servei de Microscòpia* for technical assistance with the confocal and electron microscopes and the *Servei de Llengües* both at the Universitat Autònoma de Barcelona. We also thank Eneko Mitxelena for his support on images digital processing and Cristina Sosa for her help in this work.

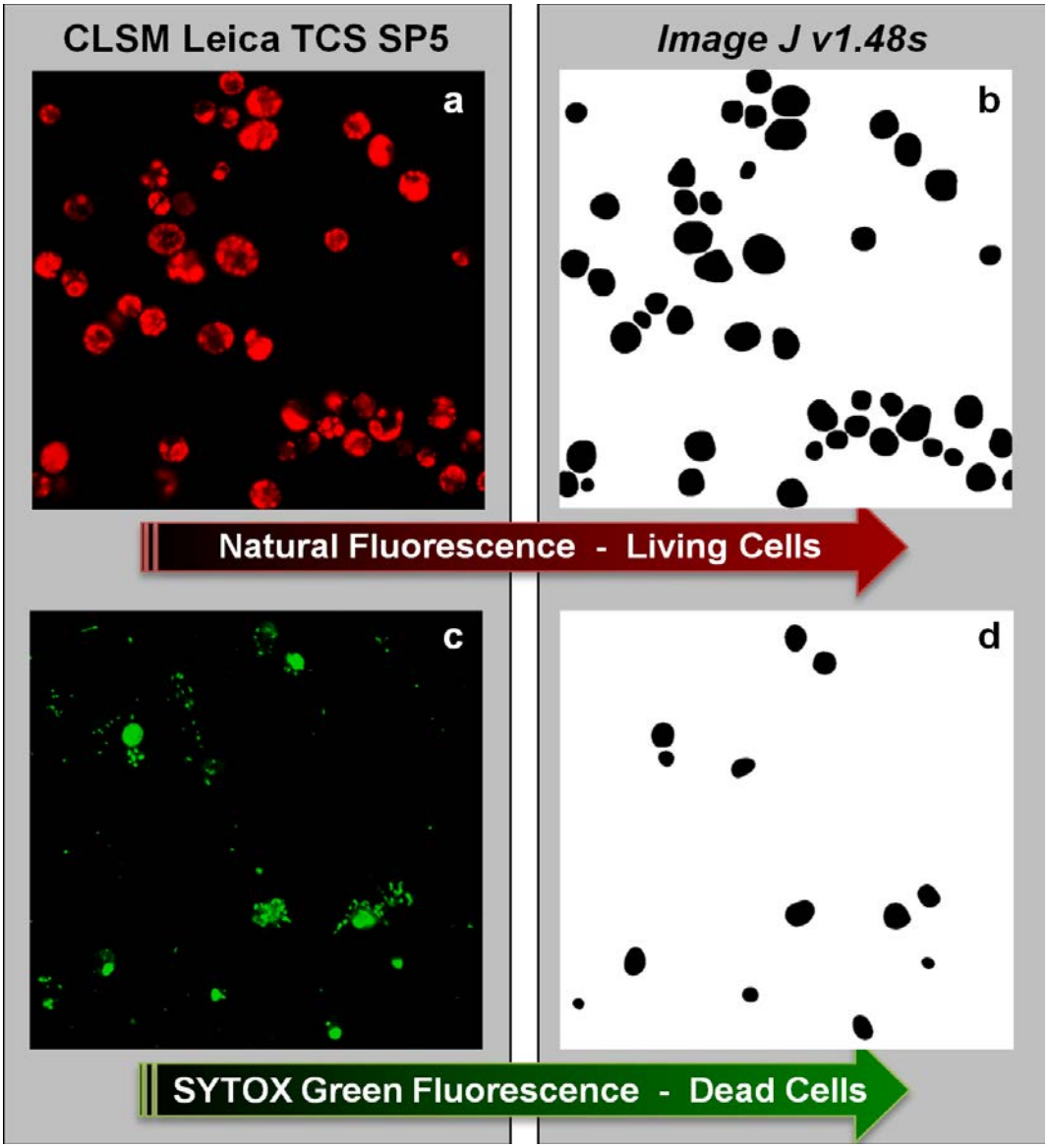

Figure 3.2.1. xyz CLSM optical sections **(a)** and **(b)** and their corresponding binary images of live **(b)** and dead **(d)** *Scenedesmus* sp. DE2009 cells analyzed using the modified FLU-CLSM-IA method.

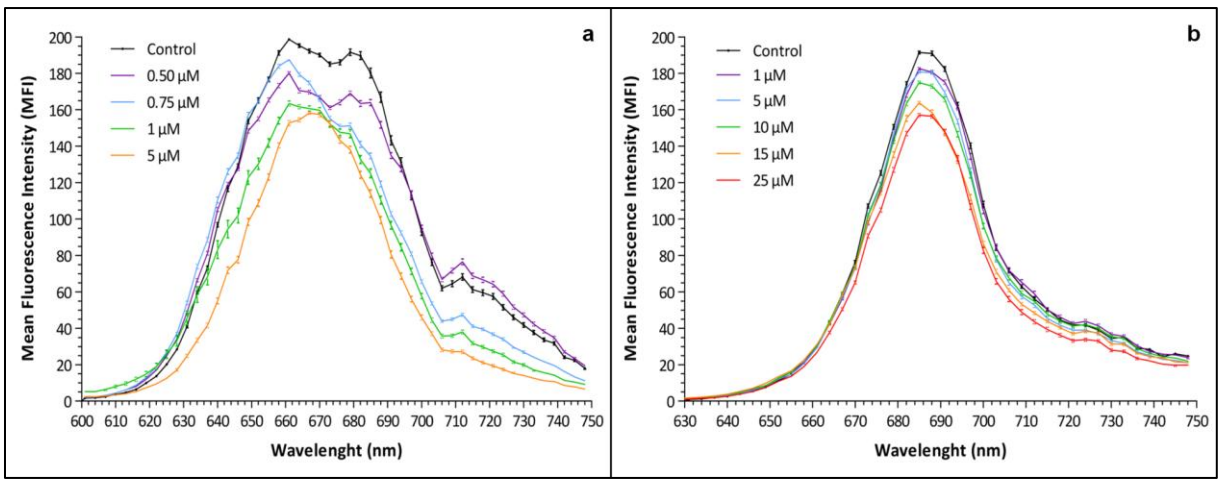

Figure 3.2.2. *λscan* plots of *Geitlerinema* sp. DE2011 **(a)** and *Scenedesmus* sp. DE2009 **(b)** contaminated with a wide range of chromium concentrations.

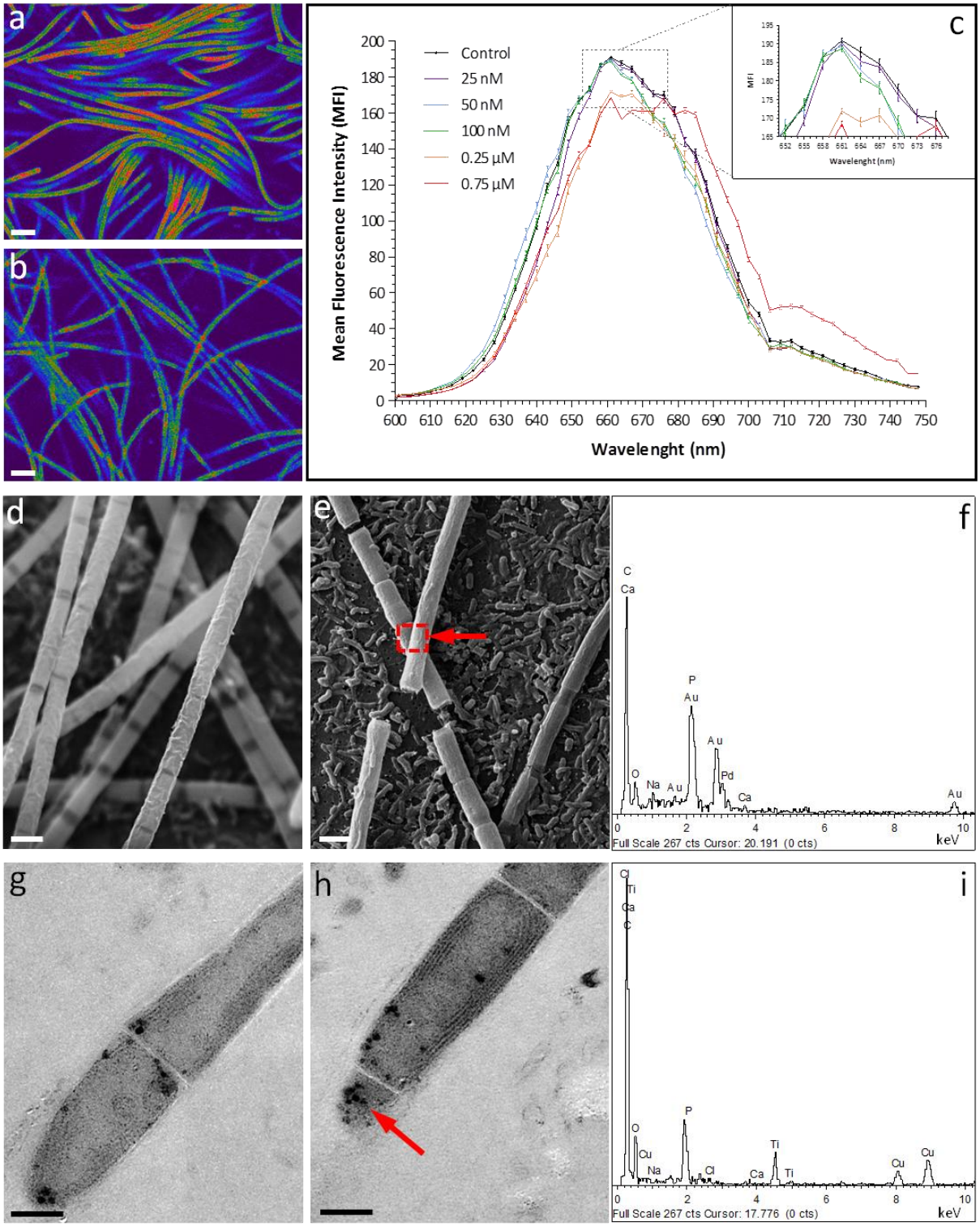

Figure 3.2.3. CLSM images of control **(a)** and chromium contaminated **(b)** cultures of *Geitlerinema* sp. DE2011 (Scale bars represent 10 μm) and *λscan* plot **(c)**. SEM images of control **(d)** and 200 μM chromium contaminated **(e)** cultures. Scale bars represent 2 μm. Contaminated EDX spectrum **(f)**. TEM images of control **(g)** and 200 μM chromium contaminated **(h)** cultures. Scale bars represent 1 μm. Contaminated EDX spectrum **(i)**.

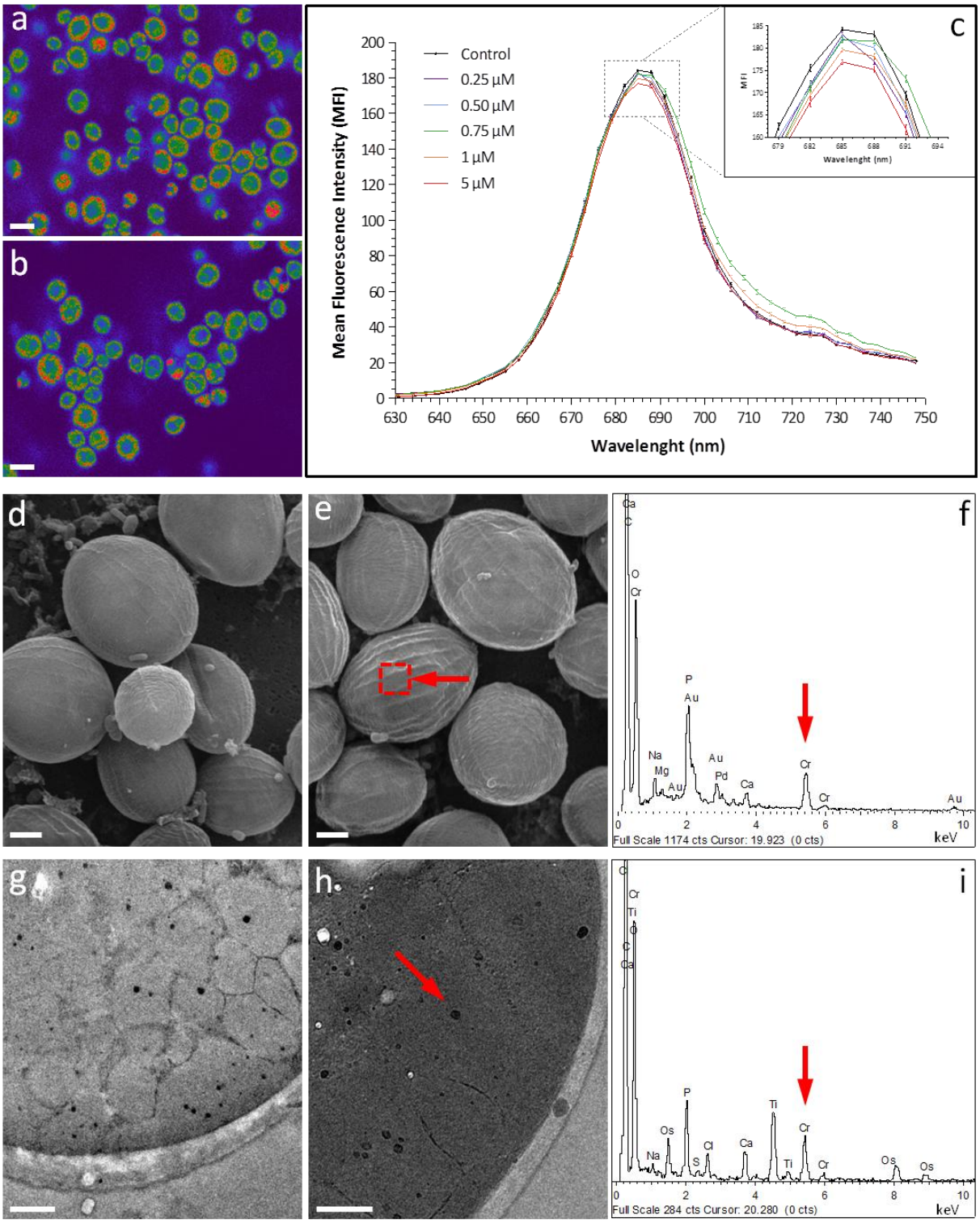

Figure 3.2.4. CLSM images of control **(a)** and chromium contaminated **(b)** cultures of *Scenedesmus* sp. DE2009 (Scale bars represent 10 *µ*m) and *λscan* plot **(c)**. SEM images of control **(d)** and 200 *µ*M chromium contaminated **(e)** cultures. Scale bars represent 2 *µ*m. Contaminated EDX spectrum **(f)**. Arrow indicates the main Cr peak at 5.4 keV. TEM images of control **(g)** and 200 *µ*M chromium contaminated **(h)** cultures. Scale bars represent 1 *µ*m. Contaminated EDX spectrum **(i)**. Cr peaks are indicated by arrows.

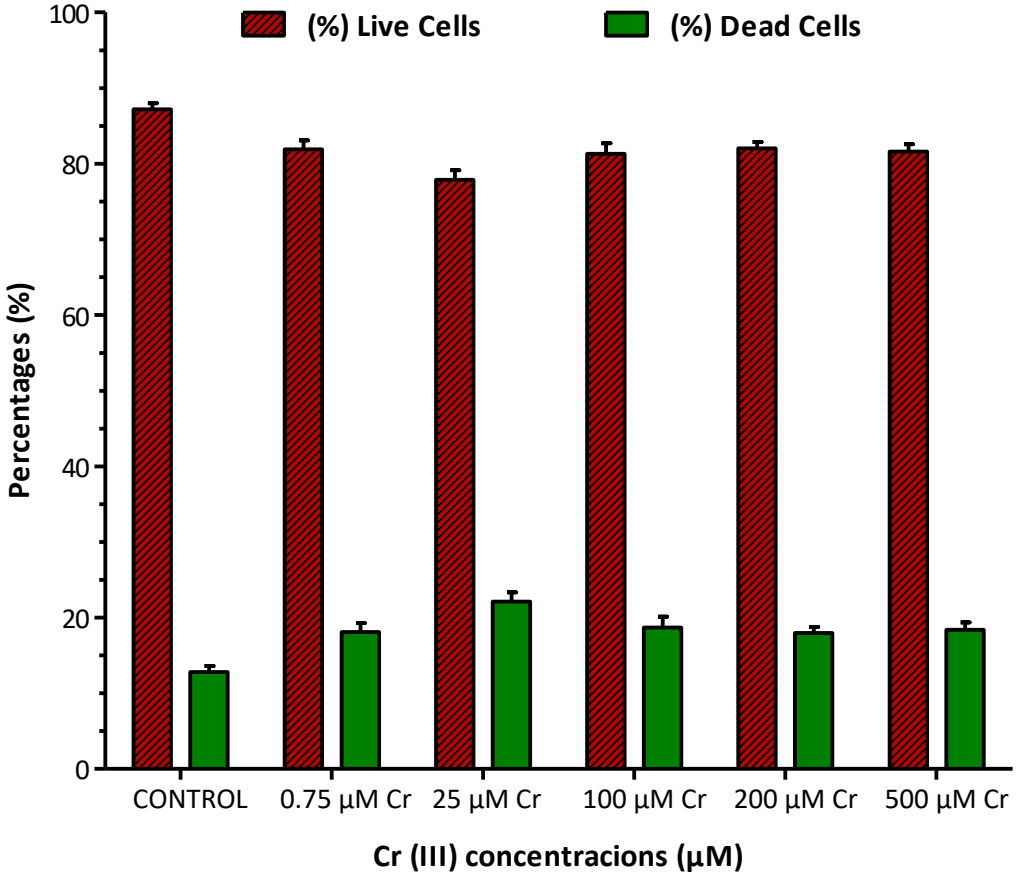

Figure 3.2.5. Percentages of live and dead *Scenedesmus* sp. DE2009 cells at different Cr(III) concentrations. The bars indicate the Standard Error of Means (S.E.M.).

REFERENCES

Antibus, D.E., Leff, L.G., Hall, B.L., Baeseman, J.L., Blackwood, C.B. **(2012)** Cultivable bacteria from ancient algal mats from the McMurdo Dry Valleys, Antarctica. *Extremophiles.* 16, 105-114.

Burgos, A., Maldonado, J., de Los Rios, A., Solé, A., Esteve, I. **(2013)** Effect of copper and lead on two consortia of phototrophic microorganisms and their capacity to sequester metals. *Aquat. Toxicol.* 140-141, 324-336.

Chang, F.C., Ko, C.H., Tsai, M.J., Wang, Y.N., Chung, C.Y. **(2014)** Phytoremediation of heavy metals contaminated soil by *Jatropha curcas. Ecotoxicology.* 23, 1969-1978.

Cheng, Y., Yan, F., Huang, F., Chu, W., Pan, D., Chen, Z., Zheng, J., Yu, M., Lin, Z., Wu, Z. **(2010)** Bioremediation of Cr(IV) and immobilization as Cr(III) by *Ochrobactrum anthropi. Environ. Sci. Technol.* 44, 6357-6363.

Cole, J.K., Hutchison, J.R., Renslow, R.S., Kim, Y.M., Chrisler, W.B., Engelmann, H.E., Dohnalkova, A.C., Hu, D., Metz, T.O., Fredrickson, J.K., Lindemann, S.R. **(2014)** Phototrophic biofilm assembly in microbial-mat-derived unicyanobacterial consortia: model systems for the study of autotroph-heterotroph interactions. *Front. Microbiol.* 5, 109.

Çelekli, A., Kapı, M., Bozkurt, H. **(2013)** Effect of cadmium on biomass, pigmentation, malondialdehyde, and proline of *Scenedesmus quadricauda* var. *longispina. Bull. Environ. Contam. Toxicol.* 91, 571-576.

De Philippis, R., Vincenzini, M. **(2003)** Outermost polysaccharidic investments of cyanobacteria: nature, significance and possible applications. *Recent. Res. Dev. Microbiology.* 7, 13-22.

Esteve, I., Ceballos, D., Martínez-Alonso, M., Gaju, N., Guerrero, R. **(1994)** Development of versicolored microbial mats: succession of microbial communites, in: Stal L.J. and Caumette P. (Eds.), *Microbial mats: structure, development and*

environmental significance. NATO ASI Series G: Ecological Sciences, Springer-Verlag, Berlin, Heidelberg, pp. 4165–4420.

Faisal, M., Hasnain, S. **(2004)** Comparative study of Cr(VI) uptake and reduction in industrial effluent by *Ochrobactrum intermedium* and *Brevibacterium* sp. *Biotechnol. Lett.* 26, 1623-1628.

Fry, J.C. **(1990)** Direct methods and biomass estimation. *Method Microbiol.* 22, 41-85.

Goldberg, J., González, H., Jensen, T.E., Corpe, W.A. **(2001)** Quantitative analysis of the elemental composition and the mass of bacterial polyphosphate bodies using STEM EDX. *Microbios.* 106, 177-188.

Gómez, V., Callao, M.P. **(2006)** Chromium determination and speciation since 2000. *Trends Analyt. Chem.* 25, 1006-1015.

Guerrero, R., Piqueras, M., Berlanga, M. **(2002)** Microbial mats and the search for minimal ecosystems. *Int. Microbiol.* 5, 177-188.

Hoffmann, D., Maldonado, J., Wojciechowski, M.F., Garcia-Pichel, F. **(2015)** Hydrogen export from intertidal cyanobacterial mats: sources, fluxes and the influence of community composition. *Environ. Microbiol.* 17(10), 3738-3753.

Jensen, T.E., Sicko, L.M. **(1974)** Phosphate metabolism in blue-green algae. I. Fine structure of the "polyphosphate overplus" phenomenon in *Plectonema boryanum*. *Can. J. Microbiol.* 20, 1235-1239.

Kováčik, J., Babula, P., Hedbavny, J., Kryštofová, O., Provaznik, I. **(2015)** Physiology and methodology of chromium toxicity using alga *Scenedesmus quadricauda* as model object. *Chemosphere.* 120, 23-30.

Magdaleno, A., Vélez, C.G., Wenzel, M.T., Tell, G. **(2014)** Effects of cadmium, copper and zinc on growth of four isolated algae from a highly polluted Argentina river. *Bull. Environ. Contam. Toxicol.* 92, 202-207.

Maldonado, J., de los Rios, A., Esteve, I., Ascaso, C., Puyen, Z.M., Brambilla, C., Solé, A. **(2010b)** Sequestration and *in vivo* effect of lead on DE2009 microalga, using high-resolution microscopic techniques. *J. Hazard. Mater*. 183, 44-50.

Mallick, N., Mohn, F.H. **(2003)** Use of chlorophyll fluorescence in metal-stress research: a case study with the green microalga *Scenedesmus*. *Ecotoxicol. Environ. Saf.* 55, 64-69.

Manahan, S.E. **(2009)** Environmental chemistry, 9th ed.; CRC Press LLC, Taylor and Francis Group, USA.

Mañosa, S., Mateo, R., Guitart, R. **(2001)** A review of the effects of agricultural and industrial contamination on the Ebro Delta biota and wildlife. *Environ. Monit. Assess*. 71, 187-205.

Nogales, B., Lanfranconi, M.P., Piña-Villalonga, J.M., Bosch, R. **(2011)** Anthropogenic perturbations in marine microbial communities. *FEMS Microbiol. Rev*. 35, 275-298.

Nziguheba, G., Smolders, E. **(2008)** Inputs of trace elements in agricultural soils via phosphate fertilizers in European countries. *Sci. Total Environ.* 390, 53-57.

Ozturk, S., Aslim, B., Suludere, Z., Tan, S. **(2014)** Metal removal of cyanobacterial exopolysaccharides by uronic acid content and monosaccharide composition. *Carbohydr. Polym.* 101, 265-271.

Pereira, S., Micheletti, E., Zille, A., Santos, A., Moradas-Ferreira, P., Tamagnini, P., De Philippis, R. **(2011)** Using extracellular polymeric substances (EPS)-producing cyanobacteria for the bioremediation of heavy metals: do cations compete for the EPS functional groups and also accumulate inside the cell? *Microbiol.* 157, 451-458.

Pfennig, N., Trüpper, H.G. **(1992)** The family Chromatiaceae, in: Balows, A., Trüpper, H.G., Dworkin, M., Harder, W., Schleifer, K.H. (Eds.), *The Prokaryotes*, 2nd edn. Springer-Verlag, Berlin, pp. 3200-3221.

Prasad, S.M., Singh, J.B., Rai, L.C., Kumar, H.D. **(1991)** Metal-induced inhibition of photosynthetic electron transport chain of the cyanobacterium *Nostoc muscorum*. *FEMS Microbiol. Lett.* 82, 95-100.

Puyen, Z.M., Villagrasa, E., Maldonado, J., Diestra, E., Esteve, I., Solé, A. **(2012a)** Viability and biomass of *Micrococcus luteus* DE2008 at different salinity concentrations determined by specific fluorochromes and CLSM-image analysis. *Curr. Microbiol.* 64, 75-80.

Puzon, G. J., Petersen, J. N., Roberts, A. G., Kramer, D. M., Xun, L. **(2002)** A bacterial flavin reductase system reduces chromate to a soluble chromium (III)-$NAD^{(+)}$ complex. *Biochem. Biophys. Res. Commun.* 294, 76–81.

Puzon, G. J., Tokala, R. K., Zhang, H., Yonge, D., Peyton, B. M., Xun, L. **(2008)** Mobility and recalcitrance of organo-chromium(III) complexes. *Chemosphere.* 70, 2054-2059.

Rai, D., Eary, L.E., Zachara, J.M. **(1989)** Environmental chemistry of chromium. *Sci. Total Environ.* 86, 15-23.

Rasband, W.S. **(2014)** ImageJ. US National Institutes of Health, Bethesda, MD, USA. http://imagej.nih.gov/ij

Roldán, M., Ascaso, C., Wierzchos, J. **(2014)** Fluorescent fingerprints of endolithic phototrophic cyanobacteria living within halite rocks in the Atacama Desert. *Appl. Environ. Microbiol.* 80, 2998-3006.

Šalamún, P., Kucanová, E., Brázová, T., Miklisová, D., Renčo, M., Hanzelová, V. **(2014)** Diversity and food web structure of nematode communities under high soil salinity and alkaline pH. *Ecotoxicology.* 23, 1367-1376.

Sato, M., Murata, Y., Mizusawa, M., Iwahashi, H., Oka, S. **(2004)** A simple and rapid dual-fluorescence viability assay for microalgae. *Microbiol. Cult. Coll.* 20, 53-59.

Seder-Colomina, M., Burgos, A., Maldonado, J., Solé, A., Esteve I. **(2013)** The effect of copper on different phototrophic microorganisms determined in vivo and at cellular level by confocal laser microscopy. *Ecotoxicology.* 22, 199-205.

Sultan, S., Hasnain, S. **(2007)** Reduction of toxic hexavalent chromium by *Ochrobactrum intermedium* strain SDCr-5 stimulated by heavy metals. *Bioresour. Technol.* 98, 340-344.

Zhou, G.J., Peng, F.Q., Zhang, L.J., Ying, G.G. **(2012)** Biosorption of zinc and copper from aqueous solutions by two freshwater green microalgae *Chlorella pyrenoidosa* and *Scenedesmus obliquus*. *Environ. Sci. Pollut. Res.* 19, 2918-2929.

Combined CLSM Techniques for Rapid Assessment of the Effect and Cell Viability of Phototrophic Microorganisms under Metal Stress

Laia Millach, Antonio Solé, and Isabel Esteve

Departament de Genètica i Microbiologia, Facultat de Biociències,
Universitat Autònoma de Barcelona, Bellaterra, 08193, Barcelona, Spain.

ABSTRACT

In natural habitats, mainly in microbial mats, the dominant populations of phototrophic microorganisms are exposed to metals over a long period of time. Distinct methods have been used to evaluate the toxic effect of metals on the preservation of these ecosystems; however, most of these techniques are difficult to apply in phototrophic microorganism since they form consortia with other heterotrophic bacteria as they grow, and also because they are difficult to obtain in axenic cultures.

We recently published an innovative and rapid evaluation method using Confocal Laser Scanning Microscopy (CLSM) and Dual Laser (CLSM-DL). This allows us to clearly differentiate two types of autofluorescence signatures linked to living and dead cells. Additionally, a pigment analysis using CLSM-λscan function was performed to determine separate and combined metal effect and the IC_{50} values in individual cells. In this paper, we apply all of these *in vivo* methodologies for the first time in order to analyze the physiological state and viability of *Scenedesmus* sp. DE2009 consortium on metal-stress conditions at single-cell level.

SHORT COMMUNICATION

Metals are released from natural and anthropogenic sources, being agriculture and industry the most potential contributors of this kind of pollution (Roane et al., 2009). Because of its toxicity, and persistence for several decades in aquatic environment, metals have become a serious environmental problem mainly in coastal zones (Kamala-Kannan et al., 2008). The Ebro delta, located at the north-eastern coastline of the Iberian Peninsula, is the second most important wetland in Spain with a 320 km^2 of surface. This ecosystem is rich in microbial mats which developed in water-sediment interfaces, and are formed by multilayered benthic microbial communities that are distributed along vertical micro-gradients of several physical-chemical parameters. Among microorganisms living in microbial mats, cyanobacteria and algae are the most dominant and located mainly in the upper green layers, where they play a major role in primary production and stabilization of deltaic sediments (Esteve et al., 1994).

One of the most significant difficulties in directly assessing the impact of metals on photosynthetic populations from natural environments is that these populations form consortia with heterotrophic bacteria and/or either do not grow or else do so sparsely in solid media. Furthermore, most of the conventional techniques used to determine the toxicity and viability of phototrophic microorganisms in metal-stress conditions require counting plate or specific stains and, more importantly still, provide information at the population level and not at the cellular level. To avoid this problem, we recently published a new, fast, non-invasive and *in vivo* method based on Confocal Laser Scanning Microscopy (CSLM) and a *sequential scan* using a Dual Laser (CLSM-DL) that allows clearly distinguish living cells from dead ones, overlapping and separately, without the need of either prior staining or additional use of image treating software.

In this present study, the CLSM-DL method has been applied for the first time, combined with the CLSM-*λscan* function, a technique that analyzes the physiological state of photosynthetic pigments using Chlorophyll *a* (Chl *a)* as a biomarker. The objectives of this study were to apply both techniques for assessing the separate and combined effect of different metals on photosynthetic pigments and cell viability at single-cell level. In addition, this study is complemented by the set up of an IC_{50} parameter also based on pigment analysis in individual cells as an alternative and sensitive toxicity test for metal pollutants with any phototrophic microorganisms.

For this work, *Scenedesmus* sp. DE2009, a very abundant microalga in Ebro delta microbial mats (Tarragona, Spain), was selected as a model because it grows with difficulty in a solid medium, forms a consortium with heterotrophic bacteria and is sensitive to environmental pollution. The isolated *Scenedesmus* sp. DE2009 was grown in mineral Pfennig medium (Pfennig and Trüpper, 1992) at 27 ºC under continuous illumination of 6 μE m^{-2} s^{-1}. Cells in exponential growth phase were used as the inocula for experiments. Control experiments for each test were performed in the absence of metals.

For toxicity studies, lead (Pb^{2+}), copper (Cu^{2+}) and chromium (Cr^{3+}) were selected because, although they are usually present at low concentration in Ebro delta microbial mats, they are very toxic pollutants. On the one hand, the metal concentrations were selected based on (i) the Minimum Metal Concentration (MMC) values obtained in previous works (Seder-Colomina et al., 2013, Millach et al., 2015) and (ii) the level permitted in continental surface waters (7.2 μg Pb^{2+} L^{-1}, 22-40 μg Cu^{2+} L^{-1}, and 50 μg Cr^{3+} L^{-1}; in accordance with the Spanish law "Real Decreto 817/2015, Annex IV & V"). Bearing the above in mind, *Scenedesmus* sp. DE2009 cultures were contaminated at fixed doses of 0.1 μM Pb^{2+}, 0.1 μM Cu^{2+} and 0.75 μM Cr^{3+} to assess how the presence of multiple metals both separately (Pb^{2+}, Cu^{2+} and Cr^{3+}) and in combination (Pb^{2+}–Cu^{2+}, Pb^{2+}–Cr^{3+}, Cu^{2+}– Cr^{3+} and Pb^{2+}–Cu^{2+}–Cr^{3+}) may alter photosynthetic pigments and

viability by exposing the microalga cells for 9 days. On the other hand, various concentrations of metals individually (from 0.1 µM to 25 mM Pb^{2+}; from 0.1 µM to 25 mM Cu^{2+}; from 0.75 µM to 25 mM Cr^{3+}) and in combination (from 0.1-0.1-0.75 µM to 1-1-7.5 mM Pb^{2+}- Cu^{2+}- Cr^{3+}) were prepared for the dose-response curves to evaluate the effectiveness of a metal in inhibiting the Chlorophyll *a* fluorescence (biomarker) at cell level, until pigment fluorescence intensity signal was not detected. This was done to determine the IC_{50}: the inhibitor concentration that provokes a response half way between the maximal (Top) response and the maximally inhibited (Bottom). The downward sloping dose curves follow a symmetrical sigmoidal shape and the IC_{50} data were calculated using a three parameter logistic model (GraphPad Prism, version 5.02 for Windows, CA, USA).

Pigment analysis was realized by the *λscan* function of Leica TCS-SP5 CLSM (Leica Microsystems Heidelberg GmbH, Mannheim, Germany). This rapid technique shows the complete spectral distribution of the fluorescence signals emitted by photosynthetic pigments of phototrophic microorganisms. Statistically changes in the emission spectrum of Chl *a* at 688 nm, used as a biomarker, was considered to evaluate the state of pigments by means of the Maximum Intensity Fluorescence (MIF) (Burnat et al., 2010). Additionally, in this work, the MIF obtained from each metal concentration was selected as an endpoint to plot the sigmoidal curves and calculate the IC_{50} values.

Furthermore, a viability assay was performed applying the novel CLSM-DL method described by Millach et al., (2017). This technique allows the capturing of various and specific wavelengths within the spectrum simultaneously and to differentiate clearly two types of autofluorescence signals at single-cell level: photosynthetic pigment autofluorescence signal (PAF) used to identify living cells and non-photosynthetic autofluorescence signal (NPAF) used to detect dead cells. Finally, one-way ANOVA followed by Tukey and Bonferroni's multiple comparison tests were

performed using SPSS 20.0 (IBM, Portsmouth, UK) for all statistical analyzes. Significant differences were accepted at $P < 0.05$.

The emission spectral profiles recorded for *Scenedesmus* sp. DE2009 indicated a high intensity emission peaks at 688 nm. The differences were statistically significant ($P < 0.05$) between the control and all the metal blends tested (Fig. 3.3.1a). The results obtained by CLSM-*λscan* function demonstrated that the highest MIFs correspond to single metal solutions and these decreased slightly as compared to the control cells following the order: $Pb^{2+} > Cr^{3+} > Cu^{2+}$. In this study, the lowest concentration (LOEC) of Pb^{2+} tested with significant effect ($P < 0.05$) on pigments relative to control was lower (0.1 μM Pb^{2+}) than that assayed by Burgos et al., (2013) (0.1 mM Pb^{2+}), decreasing by an order of magnitude. Nevertheless, *Scenedesmus* sp. DE2009 is highly resistant and tolerant to Pb^{2+}. Similarly, Shanab et al., (2012) reported that Pb^{2+} concentrations up to 10 mg L^{-1} (48.26 μM Pb^{2+}) increased chlorophyll concentration in cultures of *Pseudochlorococcym typicym* and *Scenedesmus quadricauda.* On the contrary, a decrease in the MIF in response to varying metals mixtures was observed, being the combinations with Cu^{2+} the most toxic and no statistically significant differences ($P < 0.05$) were found between them, using the Tukey and Bonferroni comparison test. An *xyz* optical section corresponding to PAF detected in the microalga growing in tri-metallic solution is shown in Fig. 3.3.1b.

The viability results showed high percentage of living microalga cells in single, bi and tri-metallic combination, which indicated a negligible effect of the metal mixtures at these low concentrations (Fig. 3.3.2a). In cultures contaminated with a single metal, *Scenedesmus* sp. DE2009 was more resistant to Pb^{2+} followed by Cr^{3+} and Cu^{2+}. However, the percentage of living cells decreased in multimetal combinations with Cu^{2+}, hence the presence of this metal negatively affected microalga growth. Specifically, a reduction of 4.68 % (Pb^{2+}–Cu^{2+}) and 5.83 % (Pb^{2+}–Cu^{2+}–Cr^{3+}) versus Pb^{2+} and 3.08 % (Cu^{2+}–Cr^{3+}), and 5.01 % (Pb^{2+}–Cu^{2+}–Cr^{3+}) versus Cr^{3+} was observed compared to the single metal test.

In contrast, Cu^{2+} effect on viable cells was not much influenced by Pb^{2+} and Cr^{3+} in binary and tri-metallic combination, since no statistically significant differences ($P < 0.05$) were found between them. These results suggest that, even at low concentration of 0.1 μM Cu^{2+}, the effect of copper is very harmful for living microorganisms. Similar results were obtained in different studies of copper toxicity on microalgae, where the LOEC values after 72-h exposure was 5.8 μg Cu^{2+} L^{-1} (0.091 μM Cu^{2+}) for a consortium of *Nitzschia closterium* (Levy et al., 2007) and 0.09 μM Cu^{2+} for *Chlorella* sp. (Franklin et al., 2002). It can therefore be observed in the *xyz* optical sections of unpolluted culture (Fig. 3.3.2b) and for each metal mixture (Fig. 3.3.2c – 3.3.2f) that the percentage of living cells decreased in multimetal combinations with Cu^{2+}, whereas the presence of Pb^{2+} and Cr^{3+} in binary and ternary mixtures did not have such a considerable effect.

To determine the IC_{50} parameter as an alternative method from dose-response curves, a pigment analysis by CLSM-*λscan* was carried out for Pb^{2+}, Cr^{3+}, Cu^{2+} ions and its tri-metallic solution (Fig. 3.3.3). The emission spectral profiles recorded for *Scenedesmus* sp. DE2009 showed a maximum fluorescence peak at 688 nm for control cultures and the lowest metal doses assayed. To contrast this, the microalga fluorescence intensity signal decreased with increasing concentration of each metal, attaining minimal inhibition (no pigment fluorescence signal) at 25 mM for Pb^{2+}, 25 mM for Cr^{3+}, 5 mM for Cu^{2+} and 1-1-7.5 mM in the combination of Pb^{2+}-Cr^{3+}-Cu^{2+}. In some cases, a displacement of the MIF peak from 688 towards 676 was observed (Fig. 3.3.3b).

The concentration-response curves for Pb^{2+}, Cr^{3+} and Cu^{2+} ions versus its tri-metallic mixture are shown in Fig. 3.3.4. The IC_{50} values obtained for *Scenedesmus* sp. DE2009 polluted with a single metal were 0.328 ± 0.016 mM for Cu^{2+}, 2.343 ± 0.162 mM for Cr^{3+} and 6.427 ± 0.529 mM for Pb^{2+} and in this case, it was again confirmed that Cu^{2+} was the most toxic metal followed by Cr^{3+} and Pb^{2+}. Comparing the results obtained by other authors, *Scenedesmus* sp. DE2009 was slightly more sensitive to copper than others microalgae such as *Euglena gracilis* (0.54 ± 0.26 mM Cu^{2+}) (Willeman, 2002) or

Tetraselmis suecica (0.63 ± 0.06 mM Cu^{2+}) (Millán de Kuhn et al., 2006), respectively. Different parameters derived from the effect-dose curves are given in Table 3.3.1. The best fit was obtained for Cu^{2+} (R^2 = 0.9879). In general, the interactive effect between single metal exposure and tri-metallic solution (IC_{50} ratio) was found to be synergistic, thus highlighting the fact that single Pb^{2+} was 36.52 times less toxic than in tri-metallic combination. This indicates that mixture-toxicity experiments may reflect the actual pollution of ecosystems in a more realistic way than experiments in which toxicant are tested individually (Spurgeon et al., 1994).

In conclusion, the practical application of distinct CLSM-methodologies simultaneously and in a same sample, using Chl *a* fluorescence as a biomarker, allows a swift diagnosis of the effect of stress pollution and of viability at cell level. At permitted concentrations of metal, viability remains high, whilst at the highest levels a reduction is observed. This demonstrates that the CLSM-DL method could be used as a reliable and sensitive viability assay for potential pollutants with phototrophic microorganisms. It is worth highlighting that these techniques are carried out *in vivo* and without any type of sample manipulation; this is highly important in undertaking ecological studies *in situ*. The assayed methods have a broad range of future perspectives since they allow differentiating the physiological state of distinct phototrophic microorganisms in complex samples within a natural environment, avoiding the heterotrophic community.

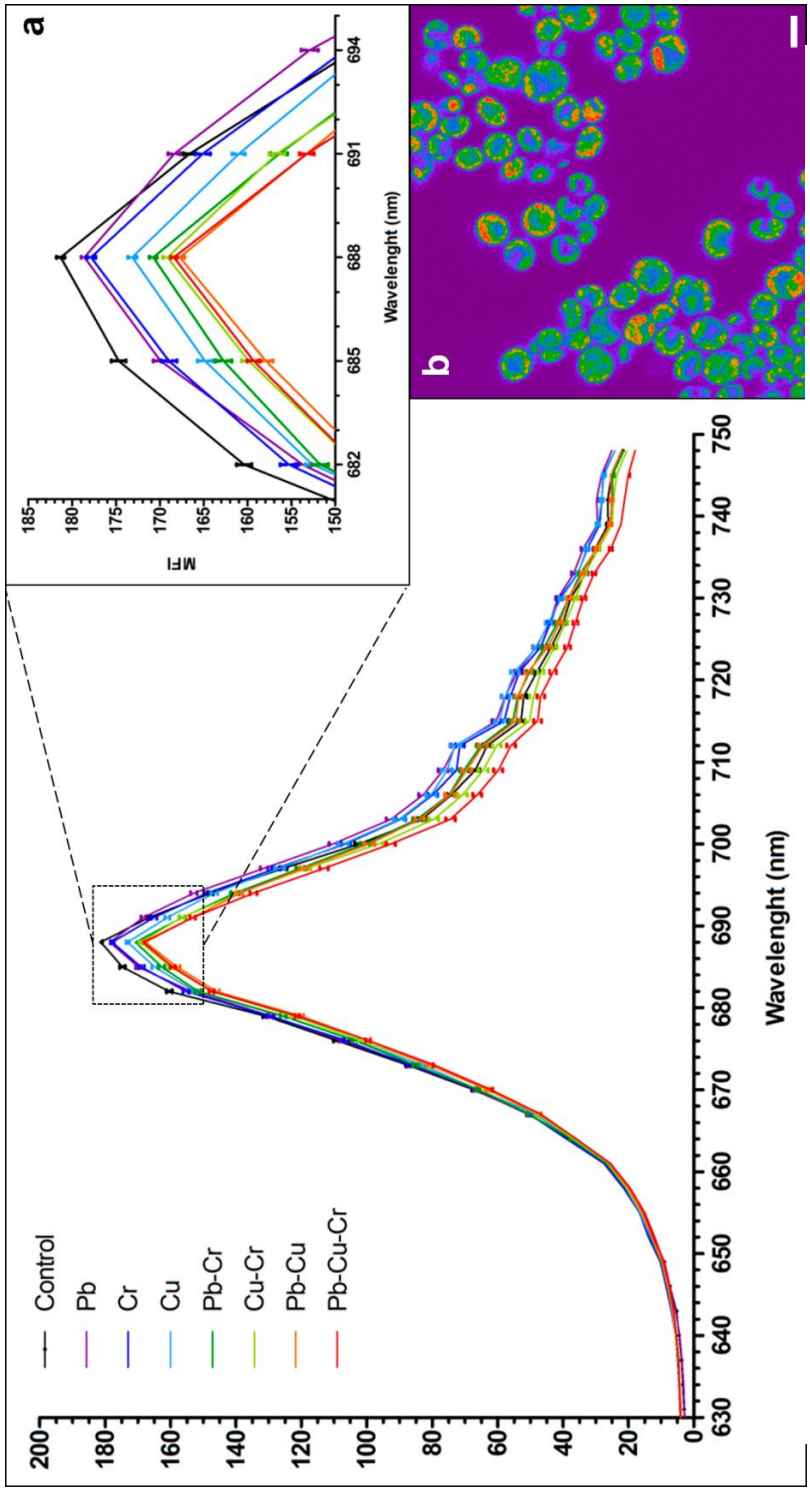

Figure 3.3.1. *λscan* plots of *Scenedesmus* sp. DE2009 cultures polluted with different mixture of metals. Detail of the emission peak at 688 nm for chlorophyll *a*, used as biomarker **(a)**. 2D plots represent the mean fluorescence intensity spectra ± SE: emission wavelength, *x* axis; MFI, *y* axis. CLSM image of microalga sp. DE2009 culture exposed to a mixture of three metals **(b)**. Scale bars represent 10 *μ*m.

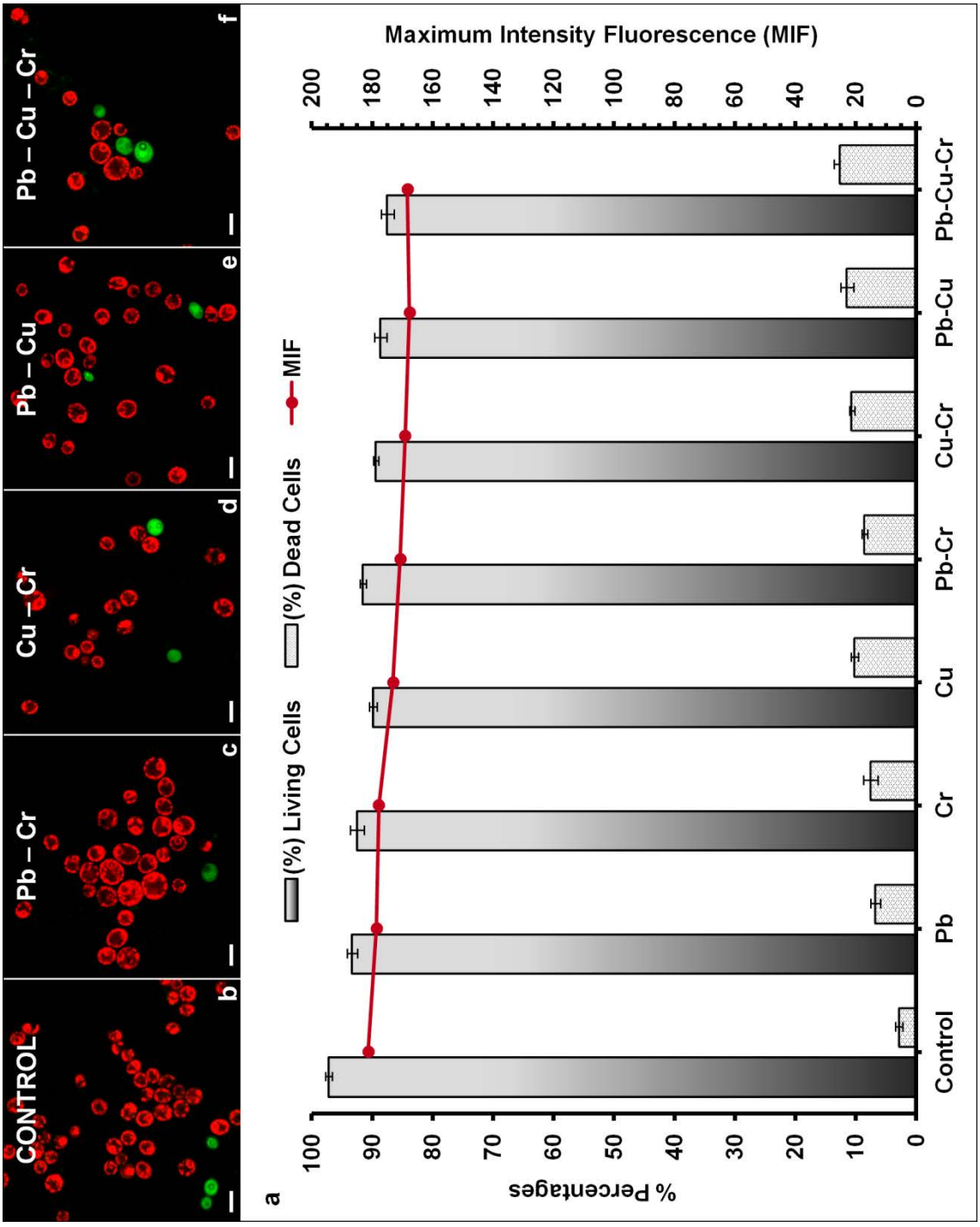

Figure 3.3.2. MIF and relative abundance of living and dead *Scenedesmus* sp. DE2009 cells at distinct metal combinations **(a)** (expressed as a percentage). The bars indicate the standard error of the mean. CLSM image of unpolluted microalga culture **(b)**. Summa projection of both autofluorescence signals recorded for *Scenedesmus* sp. DE2009 grown with Pb^{2+}–Cr^{3+} **(c)**, Cu^{2+}–Cr^{3+} **(d)**, Pb^{2+}–Cu^{2+} **(e)** and Pb^{2+}–Cu^{2+}–Cr^{3+} **(f)**. Scale bars represent 10 μm.

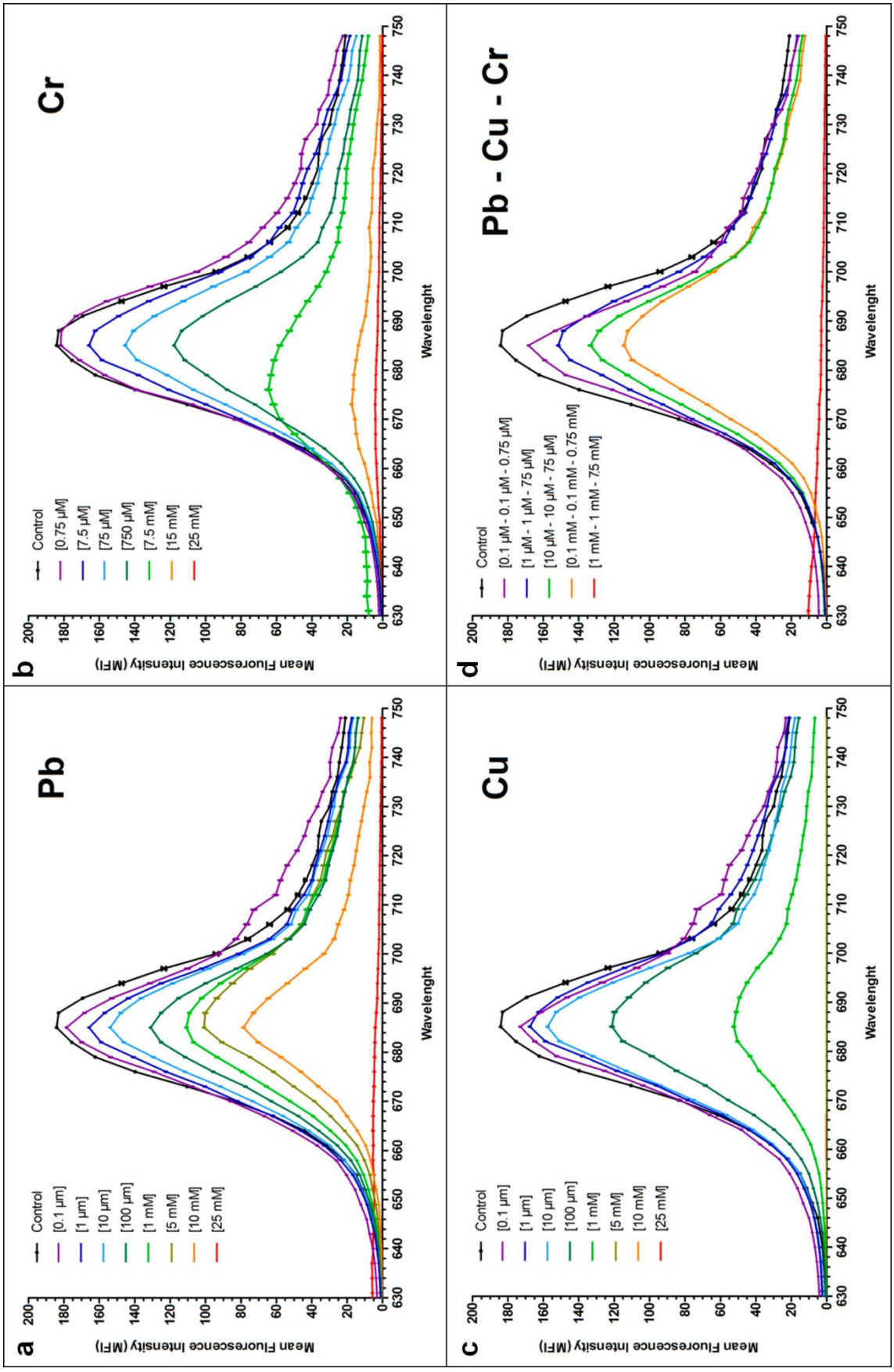

Figure 3.3.3. *λscan* plots of *Scenedesmus* sp. DE2009 cultures polluted with different concentrations of Pb^{2+} **(a)**, Cr^{3+} **(b)**, Cu^{2+} **(c)** its tri-metallic mixture **(d)**. 2D plots represent the mean fluorescence intensity spectra ± SE: emission wavelength, *x* axis; MFI, *y* axis.

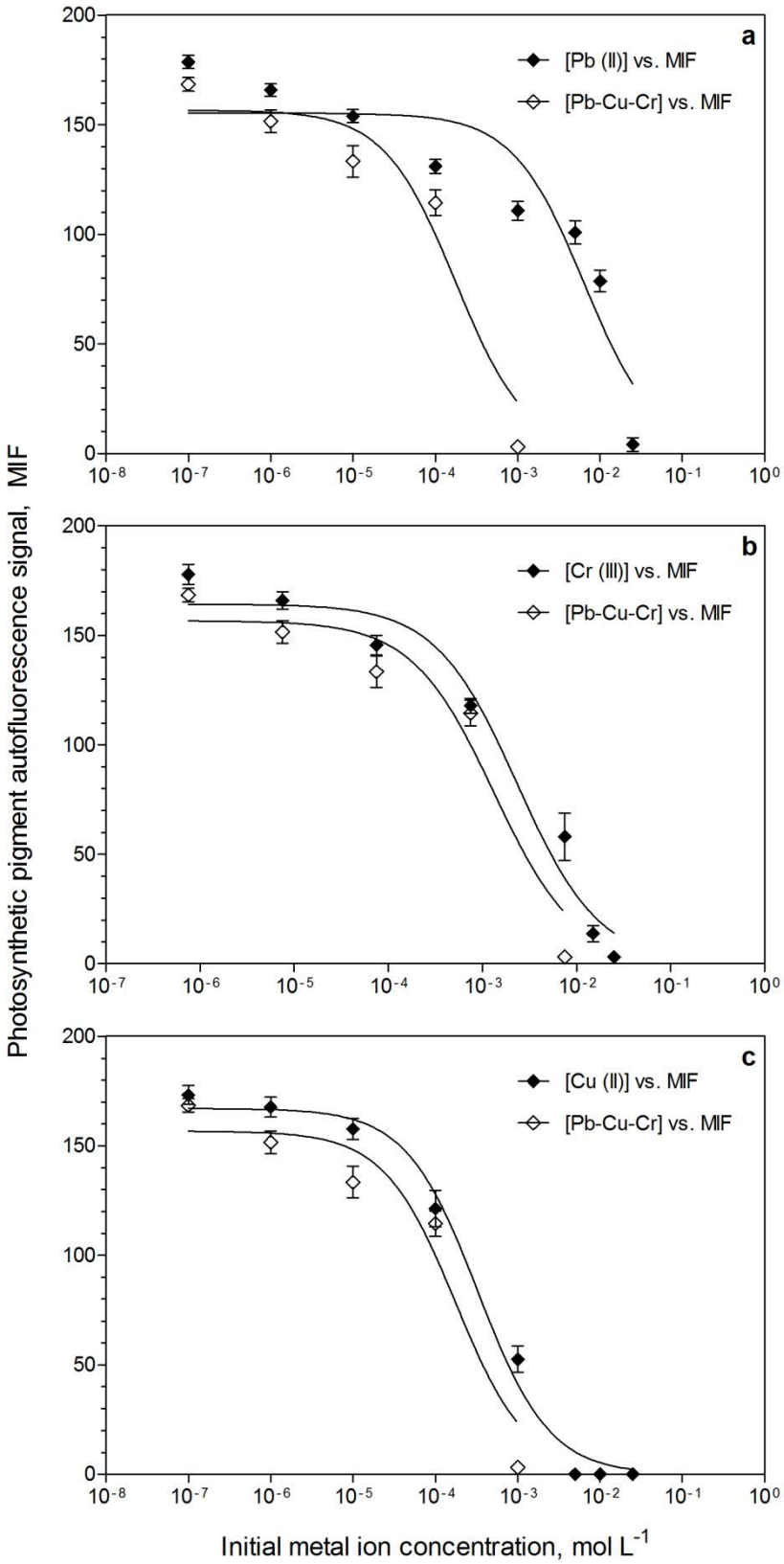

Figure 3.3.4. Dose response curves for the effect of lead **(a)**, chromium **(b)** and copper **(c)** (black rhombus) and tri-metallic combination (white rhombus) on photosynthetic pigments of *Scenedesmus* sp. DE2009 for 9 days. The figure shows the experimental data and the fitted curves (represented by solid line). The X axis plots the logarithm of the initial metal concentration (mol L^{-1}) and the Y axis plots response (MIF). The bars represent the standard deviation of the mean.

Table 3.3.1. Toxicity parameters for *Scenedesmus* sp. DE2009 polluted with a single metal (Pb^{2+}, Cu^{2+} and $Cr3^{+}$) and a tri-metallic solution. Values obtained by the three parameter logistic model.

Metal	IC50 (mol L^{-1})	95% Confidence Intervals, (mol L^{-1})	R square	IC50 Ratio	MIF_{IC50}	CLSM-DL	
						Living cells	*Dead cells*
Pb	0.006427	0.005919 to 0.006977	0.8628	36.5171	77.6	53.74%	46.26%
Cr	0.002343	0.002187 to 0.002510	0.9629	1.7750	82.1	52.85%	47.15%
Cu	0.0003277	0.0003125 to 0.0003436	0.9879	1.8619	83.5	52.76%	47.24%
Pb-Cr-Cu	0.0001760[a] / 0.001320[b]	0.0001603 to 0.0001934[a] / 0.001202 to 0.001450[b]	0.9345	1	78.3	50.38%	49.62%

Results obtained from Pb^{2+}, Cu^{2+} **(a)** and Cr^{3+} **(b)** concentrations considering the MMC values.

REFERENCE

Burgos, A., Maldonado, J., de los Ríos, A., Solé, A., Esteve, I. **(2013)** Effect of copper and lead on two consortia of phototrophic microorganisms and their capacity to sequester metals. *Aquat. Toxicol.* 140(141), 324-336.

Burnat, M., Diestra, E., Esteve, I., Solé, A. **(2010)** Confocal laser scanning microscopy coupled to a spectrofluorometric detector as a rapid tool for determining the *in vivo* effect of metals on phototrophic bacteria. *Bull. Environ. Contam. Toxicol.* 84, 55-60.

Esteve, I., Ceballos, D., Martínez-Alonso, M., Gaju, N., Guerrero, R. **(1994)** Development of versicolored microbial mats: succession of microbial communites, in: Stal L.J. and Caumette P. (Eds.), *Microbial mats: structure, development and environmental significance*. NATO ASI Series G: Ecological Sciences, Springer-Verlag, Berlin, Heidelberg, pp. 4165–4420.

Franklin, N.M., Stauber, J.L., Lim, R.P., Petocz, P. **(2002)** Toxicity of metal mixtures to a tropical freshwater alga (*Chlorella* sp.): the effect of interactions between copper, cadmium, and zinc on metal cell binding and uptake. *Environ. Toxicol. Chem.* 21(11), 2412-2422.

Kamala-Kannan, S., Dass Batvari, B.P., Lee, K.J., Kanna, N., Krishnamoorthy, R., Shanti, K., Jayaprakash, M. **(2008)** Assessment of heavy metals (Cd, Cr and Pb) in water, sediment and seaweed (*Ulva lactuca*) in the Pulicat Lake, South East India. *Chemosphere.* 71, 1233-1240.

Levy, J.L., Stauber, J.L., Jolley, D.F. **(2007)** Sensitivity of marine microalgae to copper: The effect of biotic factors on copper adsorption and toxicity. *Sci. Total Environ.* 387, 141-154.

Millach, L., Solé, A., Esteve, I. **(2015)** Role of *Geitlerinema* sp. DE2011 and *Scenedesmus* sp. DE2009 as bioindicators and immobilizers of chromium in a contaminated natural environment. *Biomed Res. Int.* Vol. 2015, Article ID 519769, 11 pages.

Millach, L., Obiol, A., Solé. A., Esteve, I. **(2017)** A novel method to analyze *in vivo* the physiological state and cell viability of phototrophic microorganisms by confocal laser scanning microscopy using a dual laser. *J. Microsc.* doi:10.1111/jmi.12586.

Millán de Kuhn, R., Streb, C., Breiter, R., Richter, P., Neeβe, T., Häder, D.-P. **(2006)** Screening for unicellular algae as possible bioassay organisms for monitoring marine water samples. *Water Res.* 40, 2695-2703.

Pfennig, N., Trüpper, H.G. **(1992)** The family Chromatiaceae, in: Balows, A., Trüpper, H.G., Dworkin, M., Harder, W., Schleifer, K.H. (Eds.), *The Prokaryotes*, 2nd edn. Springer-Verlag, Berlin, pp. 3200-3221.

Roane, T.M., Rensing, C., Pepper, I.L., Maier, R.M. **(2009)** Microorganisms and Metal Pollutants, in: *Environmental Microbiology*. Elsevier Inc., pp. 421-441. doi: 10.1016/B978-0-12-370519-8.00021-3.

Seder-Colomina, M., Burgos, A., Maldonado, J., Solé, A., Esteve I. **(2013)** The effect of copper on different phototrophic microorganisms determined *in vivo* and at cellular level by confocal laser microscopy. *Ecotoxicology*. 22, 199-205.

Shanab, S., Essa, A., Shalaby, E. **(2012)** Bioremoval capacity of three heavy metals by some microalgae species (Egyptian Isolates). *Plant Sing. Behav.* 7(3), 1-8.

Spurgeon, D.J., Hopkin, S.P. and Jones, D.T. **(1994)** Effects of cadmium, copper, lead and zinc on growth, reproduction and survival of the earthworm *Eisenia fetida* (Savigny): assessing the environmental impact of point source metal contamination in terrestrial ecosystems. *Environ. Pollut.* 84, 123-130.

Willemann, R. L. **(2002)** Development of an application of the ECOTOX System in the Estuarine Zone of the Baía da Babitonga, SC, Brazil, Diplom, Friedrich-Alexander Universität, Erlangen-Nürnberg, pp. 1-72.